Drivers of benthic oxygen flux in coastal shelf sea environments

Ellis, Rebecca

Award date:
2022

Awarding institution:
University of Bath

DRIVERS OF BENTHIC OXYGEN FLUX IN COASTAL SHELF SEA ENVIRONMENTS

Rebecca Ellis

A Thesis Submitted for the Degree of Doctor of Philosophy

Department of Architecture and Civil Engineering

University of Bath

August 2021

Abstract

Dissolved oxygen concentrations in the coastal ocean are controlled by a combination of physical and biogeochemical processes. Physical processes include turbulence, advection, and diffusion, biogeochemical processes include respiration, and photosynthesis. However, the influence of these processes on oxygen dynamics within coastal shelf sea environments are not fully understood. The main objective of this research was to develop new methodologies to enable measurements of in situ oxygen dynamics using the Eddy Correlation (EC) method in a dynamic shelf sea environment.

EC data were collected to determine oxygen flux within two study sites L4 and Cawsands within the Western Channel Observatory (WCO). The first study provided further validation of the EC technique within a challenging environment by comparing EC measurements with the well-established microprofiler technique measurements. This study also provided an initial assessment of flux drivers within a seagrass habitat. The second study deployed the EC over a five-month field campaign. During this campaign other parameters were also collected such as: acoustic velocity data to estimate the contribution of the tide, conductivity, temperature and depth sensors, sediment composition and nutrient analysis. These complementary parameters aided assessment and understanding of drivers in relation to oxygen flux within the L4 study findings.

A comparison of the relatively unstudied EC technique was made against a microprofiler, which measures diffusive point flux. Oxygen flux data between microprofiler and EC correlated during dark periods however did not during light periods. The EC captured photosynthetic drivers of oxygen flux during light periods. This validated the EC in a seagrass environment and demonstrated the microprofiler did not measure some key processes as it cannot capture all fluxes during photosynthetic periods.

Previous studies have improved EC processing techniques and have reported the magnitudes of the fluxes at varying sites. However, little is known about benthic oxygen flux drivers, especially within coastal shelf sea environments, yet they have substantial ecological and economic importance. This study (Chapter 4) demonstrated that it is possible to gain insight into the controlling oxygen dynamics at the seabed by analysing the various tidal influences. Contribution of surface versus internal tides was assessed in relation to fluxes. While surface tides were shown to be the primary driver, there was a significant contribution driven by

internal tides. During the weak stratification period there was a contribution from internal tides and it is suspected that as the summer progresses the internal tidal contribution would increase, becoming a stronger driver of flux.

Building on this preliminary study, oxygen fluxes over five months were assessed by evaluating all major drivers of benthic oxygen flux at the L4 study site. The EC technique, which measures total turbulent oxygen flux, along with accompanying instruments was used to document and assess drivers of benthic oxygen uptake over the five-month field campaign at L4. Drivers such as nutrients, temperature, the dumping of dredged spoils and chlorophyll concentration were assessed. Flux correlated weakly with flow velocity over the five-month sampling campaign. Furthermore, without sediment analysis and settling chambers at the specific location of where the EC fluxes were measured, the contribution of dredge material, plankton bloom and nutrients have on benthic oxygen flux cannot be conclusively quantified.

A lack of data capturing nutrients within the sediment and ADCP data throughout the five-month sampling campaign at L4 meant that a complete quantification of the drivers of oxygen flux at this site was not achievable. A more complete picture could be obtained if a microprofiler (measuring diffusive flux) and benthic chambers (measuring sediment oxygen uptake) were deployed alongside the EC as well as settling chambers and sediment nutrient analysis. Nonetheless, this study has made advances in EC processing and has provided a first insight into tidal and oxygen dynamics at a historical research station. The work presented has provided further validation of the EC technique and processing methods within a challenging environment by comparing EC and microprofiler measurements. Furthermore, this study has provided the first insight into water column oxygen budgets, with a particular focus on the influence of benthic oxygen flux drivers, in this shelf sea environment.

Acknowledgements

Firstly, I would like to express my sincere gratitude to my supervisors Dr Danielle Wain, Dr. Chris Blenkinsopp, Dr. Lee Bryant, and Dr. Tom Bell for their support during my Ph.D. My supervisory team has provided me continuous support, patience and motivation. I am indebted to them for all the support given to me from field work advice, to learning MATLAB and improving my writing skills. In addition to my supervisory team, I would like to express my profound gratitude to my fellow students at Plymouth Marine Laboratory (Kevin Purves, Saskia Ruhl, Becca Shellock, and Andrew Landels) and University of Bath (Steve Davey, Vesna Raicic, Emily Slavin, Anna Chaliasou, and Freddy Mevoli) for providing me with continuous support and encouragement throughout the past three years. I have been very fortunate to have such friendly and sociable office mates. I would also like to express my deepest gratitude to the technicians at the UOB as well as the boat crew and skippers of RV Quest for deploying my delicate and complicated equipment through challenging conditions. I am also grateful to the NERC studentship for the financial support given to me to conduct this research. Last but not least, I would like to thank my family for their support and patience, in particular Tess for providing me with comfort during stressful times.

Contents

Table of Figures

List of Tables

Chapter 1

1. Introduction

1.1 Background

Oxygen plays a critical role in maintaining the health of shelf sea environments. Shelf seas are vital for supporting ecological habitats and industry including fishing, oil, shipping, aquaculture, tourism, recreation, and waste disposal (Lindeboom, 2002). These anthropogenic pressures have contributed to changes in the health of shelf sea ecosystems and can create or exacerbate oxygen minimum zones (Breitburg et al., 2018). As such, these areas are becoming more prevalent and threaten habitats within shelf sea waters (Greenwood et al., 2010). This thesis will investigate oxygen transfer across the benthic boundary layer (BBL) within two shelf sea habitats, the L4 monitoring station and a seagrass bed at Cawsands. Both sites lie within the Western Channel Observatory (WCO) off the coast of Plymouth, UK.

Oxygen levels are controlled by multiple interlinked drivers which fall into three categories: physical, chemical, and biological (Table 1.1). Yet, the influence of these processes on oxygen dynamics within coastal shelf sea environments is frequently overlooked in the assessment of oxygen budgets. This chapter focuses particularly on in situ measurements of oxygen flux which are currently lacking within permeable shelf sea environments. Aquatic permeable sediment habitats include seagrass, sandy/muddy sediment, mangrove, kelp forest, soft coral and many more.

Table 1.1: Drivers of to the oxygen within oceanic environments

Physical	**Chemical**	**Biological**
Advection/Diffusion	Oxygen demand	Photosynthesis / Respiration / Decomposition
Turbulence	Nutrients	Bioturbation

All physical, chemical, and biological processes are linked and are influenced by anthropogenic impacts such as pollution from land run off and coastal activities (tourism and fishing) as well as climate change. These anthropogenic impacts are a motive, within this thesis, to examine drivers of coastal habitats, as well as providing a critical analysis of the measurement techniques used to quantify their impact on key benthic habitats.

1.2 Why coastal habitats are important?

Within aquatic environments, the concentration of dissolved oxygen is an important parameter for ecological health as oxygen is a crucial element for all forms of life. Oxygen is sensitive to complex drivers on both local and global scales and can therefore be used as a proxy to identify changes in ecological health. As detailed above, oxygen levels are controlled by a range of physical, chemical and biological drivers. These processes are particularly variable along the continental shelf as it is shallower compared to the rest of the ocean, allowing for stratification and light penetration through a larger portion of the water column. This can have significant impact on water quality and ecological health in marine environments.

The continental shelf comprises of only 7% of the world's ocean and yet contains 15% of the ocean's ecology; it is also of great economic importance to the United Kingdom (National Oceanography Centre, 2016). Globally, this region is critical to oil and gas extraction, shipping, telecom, fisheries as well as aquaculture, raw material extraction and renewable energy generation (National Oceanography Centre, 2016). Coastal environments, in particular shelf seas provide a range of food supply services which are vital for the ever-increasing human population, with over 1.2 billion people relying on shelf sea protein production from coastal regions (Badjeck et al., 2010). Pauly et al., (2002) estimates 90% of global fish catches are taken from shelf seas. Furthermore, shelf sea regions are typically densely populated (around 40% of the world's population live within 100 km of the ocean). Consequently, they are home to substantial human development and activity: industrial, agricultural, residential, tourism, which puts substantial pressure on the coastal environment. Continual monitoring and management of coastal environments is therefore critical to preserve these services (Sharples et al., 2019).

Within shelf sea environments a key component of overall system metabolism and nutrient cycling is benthic metabolism (McGlathery et al., 2007). Where the seafloor lies within the photic zone seagrass, mangroves, algae, reef systems and many other coastal habitats form

critical marine ecosystems, which are all characterized by high levels of productivity and ecosystem diversity (Wilkinson, 2012; Harrison and Booth, 2007). The metabolism of these primary producers and associated communities acts as a vital carbon and nutrient sink in shallow coastal systems (Hume et al., 2011). Hence, pollution and climate change may have a profound effect on these areas (Brodie et al., 2015; Huettel et al., 2000). Whilst it is established that anthropogenic activities are contributing significantly to detrimental oxygen loss in all parts of global biogeochemical cycles, resulting in reduced ecosystem health and poor water quality in aquatic systems (Vitousek et al., 1997; Matson et al., 1997; Camargo et al., 2006), coastal drivers of oxygen dynamics are not well documented and are the primary focus of this research.

1.3 Coastal oxygen dynamics

1.3.1 Oxygen biogeochemical cycle

The biogeochemical cycle is the continuous movement of oxygen and water between the atmosphere and earth surface, regulating many aspects of the earth's natural processes, from the climate to controlling the ecological function of aquatic systems. This cycle is also vital in the circulation of nutrients and sediment in and out of aquatic ecosystems. Anthropogenic impacts such as pollution, coastal activities (fishing, tourism etc.) can cause substantial changes to oxygen drivers, hence impacting a variety of ecosystems.

The global oxygen biogeochemical cycle incorporates three main zones: the atmosphere, biosphere, and lithosphere (Schlesinger et al., 2013). Oxygen moves through these zones via processes such as photolysis, weathering, and respiration/photosynthesis (Connell, 2005) as depicted in Figure 1.1. In the ocean, physical processes such as turbulent mixing, drive atmospheric oxygen from the water surface to bottom waters (Kanwisher et al., 1963). This physical method of mixing oxygen within the water column of water bodies can be reduced by stratification, which occurs during certain times of year, when surface water temperature differs from bottom water temperatures (Stanley et al., 1992). Stratification leads to a reduction of oxygen transfer to bottom waters by mixing (the transport of oxygen in bottom waters is discussed further in Chapter 2, Section 2.1) and can subsequently lead to hypoxic conditions (low levels of oxygen) (Diaz et al., 1995; Breitburg et al., 2018). One of the primary

biogeochemical factors leading to oxygen depletion in stratified waters are seasonal algal blooms (Glibert et al., 2018).

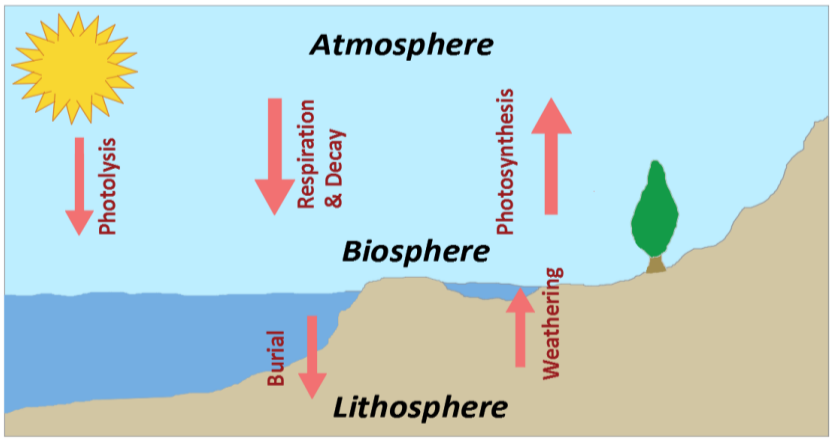

Figure 1.1: Illustration of the oxygen cycle. Oxygen is transported between the three main zones: 1, Atmosphere 2, Biosphere 3, Lithosphere.

Figure 1.1 illustrates the main zones of the oxygen cycle:

1. Atmosphere: oxygen is released through photolysis as ultraviolet rays break down oxygen -bearing molecules.
2. Biosphere: Respiration or decay (e.g., algal decay, senescence) can deplete oxygen in the atmosphere due to metabolic processes, releasing CO_2 (Tappan et al., 1968; Shmeis et al 2018). Photosynthesis is the process which feeds oxygen back into the atmosphere.
3. Lithosphere: oxygen is taken from the biosphere by biochemical processes, e.g., via calcifying organisms as calcium carbonate shells are created. Oxygen is then transferred to the lithosphere as the organisms die and their shells are buried by benthic sediments, eventually being incorporated into the bedrock. Weathering allows the oxygen to be re-released into the atmosphere and biosphere as bedrock becomes subjected to corrosion and chemical reactions (e.g., the formation of metal oxides), as well as plant and animal extractions (Copper, 1992). Diffusive transfer is a component of oxygen transfer within the lithosphere. This physical process is a key driver investigated in this thesis.

There are also many other processes and drivers impacting the movement of oxygen from the lithosphere to the biosphere or/and atmosphere and vice versa such as, metabolic processes (benthic respiration) and transport processes, comprising of bio-diffusion and advection, that lead to oxygen consumption. As oxygen in the oceans has already decreased by 2% since 1960 due to anthropogenic activities (Resplandy, 2018), understanding these mechanisms which lead to the increase and depletion of oxygen in the environment, is critical to prevent harmful

consequences, such as hypoxia or oxygen minimum zones within aquatic systems (Diaz et al., 2008; Altieri and Diaz et al., 2019).

Drivers of oxygen cycling are interconnected, as oxygen molecules are constantly stored and recycled through physical, chemical, and biological processes. A change in the cycle can lead to impacts on a variety of natural processes. For example, leaching of nitrogen and phosphorous (major components of fertiliser used in agriculture) from the biosphere can rapidly alter organisms in the hydrosphere. Therefore, measurement of oxygen transfer from all drivers is vital in understanding the complexity of a habitat. This thesis focuses on shelf sea environments which are increasingly under threat from anthropogenic activities.

1.3.2 Anthropogenic impacts on coastal oxygen dynamics.

Coastal environmental management requires an understanding of oxygen dynamics and key drivers within ecosystems. This is especially true when considering the effects of climate change and nutrient loading. Increased temperatures (decreasing oxygen solubility levels) will lead to altered concentrations of oxygen levels in coastal waters (Breitburg et al., 2018). Increased temperatures will also lead to changes in the intensity of stratification, reducing the supply of oxygen to bottom waters (Keeling et al., 2010; Pena et al., 2010). Furthermore, climate change may also increase the frequency and intensity of storms which will alter stratification gradients, further impacting oxygenation rates of bottom waters (Rabalais et al., 2010). In addition, higher water temperatures will change organism metabolic and respiratory rates, increasing biological oxygen demand within benthos (Conley et al., 2009). This impact can be exacerbated by an increase in nutrient loading.

As anthropogenic activities, such as farming and land use have accelerated over the last half-century, the associated nutrient loading has created higher rates of primary production in coastal environments. This increased supply of organic matter (OM) to coastal benthic sediments induces higher respiration rates, which impacts bottom water oxygenation. Studies have shown an increased number of coastal environments that have been affected by nutrient supplies from heightened anthropogenic land activities, leading to more coastal zones which are prone to hypoxia (Diaz and Rosenberg, 2008; Diaz, 2001; Zhang et al., 2010). Measurement, monitoring and understanding of the oxygen biogeochemical cycle and nutrient loading within coastal systems will aid management efforts (Meire et al., 2012).

This thesis aims to uncover key oxygen drivers within two coastal environments which are potentially vulnerable to anthropogenic impacts. To enable deeper insight into the potential physical, chemical, and biological oxygen drivers within coastal habitats, these drivers are further discussed in Sections 1.4, 1.5 and 1.6 below. It is important to note these drivers are interlinked even though they are discussed individually.

1.4 Physical drivers of oxygen in aquatic habitats

Physical drivers assessed within this section are diffusion, advection, and turbulence. Molecular diffusion is a key mechanism for transporting oxygen across the sediment-water interface (SWI) in coastal environments (Lin et al., 2011). The SWI is the boundary layer between the sediment and overlying water. Diffusion is defined as the movement of a substance from an area of high concentration to an area of low concentration. In this thesis, diffusion relates to the imbalance of oxygen concentration in the benthos and overlying water. Turbulence is the irregular motion of gas or fluids leading to vertical currents and eddies transferring masses across boundary layers, such as water/sediment (increasing mixing). Turbulence can directly impact the rate of diffusion. This is caused as bottom water velocities increase and more turbulence is generated, the oxygen gradient between the water column and sediment will increase, and the thickness of the diffusive boundary (DBL) layer changes due to turbulent energy. Advection is the is horizontal or lateral transfer of mass. In the case of this thesis, advection relates to currents within waterbodies, transferring water from colder/oxygen rich regions to shallower environments.

Oceanic currents drive oxygen rich water to shelf sea zones thereafter, horizonal turbulence transfers oxygen to bottom waters, increasing the oxygen gradient near the benthic boundary. This results in molecular diffusion driving oxygen into the sediment. A reduction in turbulence/mixing, for example due to a thermocline, would result in oxygen transfer reducing/depleting in the bottom waters leading to an increased oxygen gradient. Hypoxia (no oxygen) can result in sediment within an environment where mixing is significantly reduced. Tidally driven turbulence has direct implications on bottom boundary dynamics, influencing pore water circulation and biogeochemical processes affecting oxygen dynamics including molecular diffusion, nutrient exchange and biological oxygen demand (Huettel et al., 2014; McGinnis et al., 2014).

Advective fluxes of oxygen and carbon solutes between the water column and sediment are tightly coupled with sediment surface topography and porosity/permeability (Marchant et al., 2016; Wiberg et al., 1994). This coupling allows for a dynamic reaction scheme for biogeochemical processes to occur, which is more commonly found in muddy cohesive sediments typical for aquatic systems (Webb and Theodor, 1968).

1.5 Chemical drivers of oxygen in aquatic habitats

Chemical drivers are interlinked with physical (advection, turbulence) and biological (diffusion, biological oxygen demand) processes. Oxygen demand could be considered a biological driver as organisms consume oxygen. However, in this section it is discussed as a chemical driver. This is due to nutrient loading changing oxygen concentration being a focus within this thesis.

Shelf seas play a crucial role in the global cycling of nutrients and carbon. It has been estimated that ocean carbon cycling drives 30% of marine primary production, 30% of inorganic carbon burial and 80% of organic carbon burial (Smith et al., 1993; Koziorowska et al.,2018). Due to anthropogenic activities, shelf seas have become a net sink for carbon dioxide compared to a net source in pre-industrial times. For these reasons shelf sea environments play a disproportionately vital role in nutrient and carbon cycling compared to their geographical area.

Nutrients are essential in maintaining ecological diversity and biomass however, an excess amount can lead to increased biological oxygen demand which may result in hypoxia. Coastal environments are impacted by riverine and land run-off which is a main contributor to high levels of nutrients and sediments in shelf sea waters. The amount of nutrients and debris from run-off into shelf sea environments is strongly subject to human management of catchment areas. Oxygen demand can be increased due to the enhanced nutrient loading from sources such as wastewater release, dumping of dredged material and agricultural runoff. The EU Water Framework Directive has been implemented to mitigate against eutrophication which can lead to hypoxia and harmful algal blooms which cause toxicity and has been an issue in the North Sea, Baltic Sea and eastern English Channel (Lancelot et al. 1987, Riegman et al. 1992, Schoemann et al. 2005).

Xie et al., (2015) conducted a study at the site (L4) described in this thesis (detailed in Section 1.11.1). This study assessed phytoplankton community structures and how they were affected by the increasing temperatures and nutrients. Results were derived from a 14-year timeseries

and illustrated that Dinoflagellate and Coccolithophorid biomass exhibited a positive correlation with temperature. This study concluded that Dinoflagellate blooms correlated with increased temperatures and high river runoff during summer months. Plankton blooms were shown to increase during stratification at the site however, no correlation between nutrient input and phytoplankton biomass was recorded (Xie et al., 2015). This study is particularly relevant as this site has experienced a succession of temperature events (cooling and heating) with a 1 ^{o}C increase in sea surface temperature for a decade in the 1990s. This caused a change in the abundance of phytoplankton with a decrease in diatoms/ Phaeocystis sp. and an increase in Dinoflagellates and Coccolithophorids between 1992 and 2007. Furthermore, an earlier study by Rees et al., (2009) documented higher than average chlorophyll-a levels at the same site in 2007. This was caused by increased river run-off creating higher nutrient loads into surrounding coastal waters. These results are particularly notable as annual rainfall and temperatures are predicted to change in the UK according to climate change models. Yet, further investigations are required to determine the relationship between nutrients and plankton blooms at this site.

As anthropogenic pressures on shelf sea waters increase, drivers such as temperature and nutrient loading become more prevalent. These drivers lead to plankton blooms which increase the biological oxygen demand within a habitat, in some environments this can result in hypoxia. To build a greater insight into this system, biological drivers (photosynthesis/respiration) are to be further discussed in Section 1.6.

1.6 Biological drivers of oxygen in aquatic habitats

In addition to physical and chemical processes driving oxygen between the sediment and the overlying water, ecological drivers such as photosynthesis, respiration, decomposition, and bioturbation can influence oxygen transport (Jørgensen and Revsbech, 1985). Plankton within oceanic systems play a crucial role in circulating oxygen locally through these ecological drivers. The nitrogen cycle, which is a chemical driver (nutrients), is a fundamental component in plankton blooms which drive biological responses (photosynthesis, respiration and decomposition). This biological and chemical response is interlinked.

Similar to oxygen, nitrogen cycles through the earth's biosphere, and is essential for life. The nitrogen cycle largely governs the earth's biogeochemistry through biological nitrogen fixation

from the atmosphere to marine and terrestrial ecosystems. Important processes in the nitrogen cycle include fixation, ammonification, nitrification, and denitrification.

Nitrification

In this process, the ammonia is converted into nitrate by the presence of bacteria in the soil. Nitrites are formed by the oxidation of Ammonia with the help of Nitrosomonas bacterium species. Later, the produced nitrites are converted into nitrates by Nitrobacter. This conversion is very important as ammonia gas is toxic for plants.

The reaction involved in the process of Nitrification is as follows:

$$2NH_4^+ + 3O_2 \rightarrow 2NO_2^- + 4H^+ + 2H2O$$

$$2NO_2– + O_2 \rightarrow 2NO_3^-$$

Assimilation

Primary producers – plants take in the nitrogen compounds from the soil with the help of their roots, which are available in the form of ammonia, nitrite ions, nitrate ions or ammonium ions and are used in the formation of the plant and animal proteins.

Ammonification

When plants or animals die, the nitrogen present in the organic matter is released back into the soil. The decomposers, namely bacteria or fungi present in the soil, convert the organic matter back into ammonium. This process of decomposition produces ammonia, which is further used for other biological processes.

Denitrification

Denitrification is the process in which the nitrogen compounds makes their way back into the atmosphere by converting nitrate (NO_3^-) into gaseous nitrogen (N). This is the final stage of the nitrogen cycle and occurs in the absence of oxygen. Denitrification is carried out by the denitrifying bacterial species- Clostridium and Pseudomonas, which will process nitrate to gain oxygen and gives out free nitrogen gas as a by-product.

Micro-organisms convert fixed nitrogen into oxidized compounds such as amino acids. Finally, microbial denitrification within sediments, soils and marine waters returns molecular nitrogen (N_2) to the atmosphere. N_2 consists of two nitrogen atoms covalently bonded to one another and unlike carbon it cannot be directly fixed by autotrophs/complex organisms. Nevertheless, nitrogen fixation bacteria such as prokaryotes can fix nitrogen molecules from the atmosphere to create ammonia (NH_3) which is accessible to complex organisms. As these complex organisms decompose, bacteria break down the organism to NH_3, nitrites (NO_2) and nitrates (NO^{-3}).

During algal blooms, nitrogen has been shown to be a primary regulator of phytoplankton growth. An increase in phytoplankton growth can increase the respiration, photosynthesis, and decomposition within a system. This increase leads to varying levels of oxygen consumption and production within the water column and sediment. Suspended matter particulate (SPM) /marine snow deposit in the benthic zone, creating a nitrogen store and has been shown to impact bioturbation and bio-irrigation rates (Toussaint et al., 2021). Bioturbation and bio-irrigation are two of the primary ecologically driven transport types for oxygen across the SWI (Ziebis et al., 1996; Muyzer, 2016). Bioturbation is the reworking of sediments by organisms (Jørgensen and Revsbech, 1985). Bio-irrigation is a process by which benthic organisms flush their burrows with the overlying water (Kristensen et al., 2012); this is a critical control on the biogeochemistry of the oceans due to the transport of dissolved substances between the pore water and the overlying sediment (Ford and Hancock, 1999). Bio-irrigation also involves particle reworking and ventilation as a result of benthic macro-invertebrates which burrow, feed, defecate, and respire in the sediment (Middelburg and Levin, 2009; Kristensen et al., 2014) (Figure 1.2).

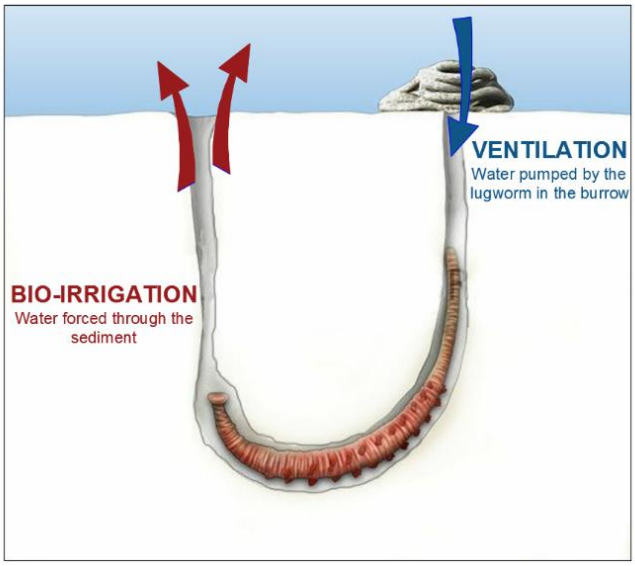

Figure 1.2: Image modified from Delefosse et al. (2015). A diagram showing the burrow with ventilation and bio-irrigation indicated by arrows. Arrows represent direction of ventilation (right) and bio-irrigation (left).

A study by Queirós et al., (2015) at the Western Channel Observatory (WCO), (the study site used in this thesis, details in Section 1.11.1) found that plankton phenology impacted bioturbation rates seasonally. Increases in bioturbation activity/depth followed peaks of spring blooms and decreased during winter months. It was found that more than 40% of the phytoplankton mass during the spring bloom reached the benthos. Therefore, during this study plankton was the major source of OM to the seabed but a similar trend was not detected in the surface water. A possible explanation may be that the water required for the benthic cores within the laboratory was filtered, this excluded the largest fraction of the bloom biomass. Similarly, Zhang et al., (2015) found plankton bloom OM could reach the benthos in a few days within both shallow and deep sites at the WCO.

Temperature is another key driver of varying bioturbation rate throughout seasonal cycles (Bernard et al., 2019). Energy is required for cellular function, impacting metabolic rates of ectotherms. Changes in temperature are associated with shifts in microorganism mobility and foraging rates. Querios et al., (2015) found food availability variations altered the structure of benthic communities, however a lag existed in the response time of this driver.

The uncertainties within these studies highlight the need for a long-term and multi-disciplinary approach to uncovering the benthic-pelagic seasonal dynamics, especially at the WCO. This site is an area of conservation and a special protected area, with scientific records spanning for over 20 years. However, minimal work has been conducted on the seasonal benthic-pelagic dynamics within this site. This is due to environmental variability complicating and masking

physical, chemical, and biological drivers within this ecosystem. To address this issue two representative habitats within a shelf sea environment were chosen in this study to determine oxygen drivers using in situ measuring techniques.

1.7 Key aquatic habitats within shelf sea environments

Many continental shelf habitats are characterized by permeable sediment (Emery, 1968). Permeability is a measure of how easily water can pass through material. The importance of the sediments permeability allows substances (water) to flow easily through the sediment, thereby allowing supply circulation of substances (e.g., oxygen) within the sediment. As water can flow more easily through permeable sediment, it plays a role in the rate that oxygen is transferred by physical, chemical, and biological drivers. Permeable, sandy sediments are located within areas where there are a combination of processes occurring which influence oxygen dynamics, including primary production, mixing, influences from land use, and strong linkage between water column and sediment interactions (Huettel et al., 2014).

Seagrass meadows and sandy/muddy sediment habitats are examined within this thesis. Sections 1.7.1 and 1.7.2 investigate and discuss oxygen dynamics within these critical habitats. Seagrass meadows represent a habitat which can produce oxygen mainly through photosynthesis during daylight, whereas the semi-permeable sandy sediment habitat represents a site which consumes oxygen through molecular diffusion, biological oxygen demand, advection, turbulence etc.

1.7.1 Seagrass

Seagrass habitats are important to understand as they provide vital breeding and nursery grounds for many species (Nurse et al., 2001). Previous studies (Orth et al., 1984; Orth et al., 2006; O'Brien et al., 2018; Duarte et al., 2018) have investigated the productivity of seagrass, as well as physiological and ecosystem diversity within these beds. However, Fourqurean et al. (2012) noted that there are a lack of studies which investigate benthic oxygen dynamics within seagrass beds. Berg et al., (2019) also discusses how seagrass dynamic metabolisms are not fully understood. This work is vital as the benthos holds two thirds of the carbon stored within a seagrass habitat (Kennedy et al., 2009). Kondoy, (2017) estimated that seagrass is capable of storing 83,000 metric tons of carbon per km^2. This is possible because seagrass beds

are affected by multiple benthic oxygen flux drivers, including photosynthesis/respiration, generation of turbulence/mixing as well as seagrass mortality which affects oxygen and carbon cycling (Hume et al., 2011).

Benthic metabolism is a key component of overall nutrient cycling within the photic zone. Seagrass and algae are benthic autotrophs which are carbon and nutrient sinks. These habitats also influence bacterial processes within sediment which include anaerobic ammonium oxidation, nitrification-denitrification and mineralization and are performed by small groups of autotrophic bacteria. Seagrass beds are ecologically important carbon stores and are becoming increasingly under threat due to climate change and rising pollution levels (Erwin, 2009).

Within seagrass meadows CO_2 and oxygen concentrations are driven by plant metabolism and are strongly correlated with each other (Hendriks et al. 2014; Pacella et al. 2018). Previous studies have found water column variabilities in oxygen and pCO_2 concentration in seagrass meadows at tidal and diel time scales (Ruesink et al., 2015; Berg et al., 2019), as well as seasonal variations (Duarte et al. 2013a; Waldbusser and Salisbury 2014; Berg et al., 2019). Mazarrasa et al. (2015), Howard et al. (2018) and Saderne et al. (2019) have indicated that dissolution and calcium carbonate precipitation can affect CO_2 fluxes. Due to the variety of influences from external inputs such as coastal upwelling, and nutrients from rivers, a large range of benthic metabolism rates within the similar habitats such as seagrass are reported within literature. There is considerable uncertainty regarding metabolism rates, this may be due to deficiencies in the available measurement techniques rather than real variation. In addition, uncertainties in the role of inorganic carbon processing in relation to carbon sequestration exist (Berg et al., 2019). Conventional methods used to determine metabolisms within seagrass environments have included mass balance models (Kaldy et al., 2002) and direct oxygen flux measurements (laboratory incubations of sediment cores and in situ chambers).

Berg et al., (2009) documented seagrass metabolism rates at various timescales using an in situ, non-invasive method. The study found night-day cycles drove oxygen concentrations in the water column, concluding that future seagrass meadows may not benefit from future ocean conditions (increase in CO_2 concentrations). However, this study did not address other stressors such as temperature and pH but did emphasise the need for in-situ studies of natural drivers which influence seagrass metabolism.

Methods described in these studies (Kaldy et al., 2002; Berg et al., 2019; Ruesink et al., 2015) all have limitations such as not replicating the natural hydrodynamic forcing, incorrect lighting and disturbance to cores. Much of the literature has stated a requirement for an in-situ technique which captures metabolism rates that causes minimal disturbance to light, hydrodynamic and temperature levels. This is particularly relevant as oxygen dynamics within seagrass meadows are governed by multiple drivers (hydrodynamic, photic, and nutrient).

Due to the dynamic biogeochemical and hydrodynamic processes that occur within seagrass beds, quantifying oxygen flux drivers is not trivial. Therefore, a combination of oxygen flux measurement tools is required to quantify the various drivers of the total oxygen flux (photosynthesis, respiration, diffusion and bioirrigation). To date, only few studies have used a combination of oxygen flux measurement tools (Reimers et al., 2012; Berg et al., 2013; McGinnis et al 2014). Therefore, a study within this thesis was conducted at a seagrass bed using two in situ oxygen flux measuring techniques (Section 1.11.1 for description of study site, Cawsands).

1.7.2 Semi-permeable sandy/muddy sediment

A dynamic and exposed coastal shelf site containing semi-permeable sandy/muddy sediments is investigated within this thesis (study site L4). Studies examining oxygen dynamics, have been undertaken in a variety of substrate types, including marine and freshwater muddy sediments (Berg et al., 2003; Brand et al., 2008; McGinnis et al., 2008), seagrass (Berg and Huettel, 2008; Reimers et al., 2012; Berg et al., 2013), deep ocean sediments (Berg et al., 2009), rock surfaces (Glud et al., 2010), oyster beds (Reidenbach et al., 2013), coral reefs (Long et al., 2013; Cathalot et al., 2015; Rovelli et al., 2015), seagrass meadows (Hume et al., 2011; Rheuban et al., 2014; Long et al., 2015; Long et al., 2015a), vertical cliffs (Glud et al., 2010), and down-facing sea-ice surfaces (Long et al., 2012). However, only a few have been performed in sandy/muddy shelf benthic environments (similar to the L4 study site) (McGinnis et al., 2014, Reimers et al., 2012, Attard et al., 2015).

As discussed in Section 1.3.2 increases in anthropogenic impacts on these habitats are becoming more prominent due to an excess of phosphorus and nitrogen, causing enhanced algal growth (Paerl et al., 2016). As the plankton eventually die and settle on the seafloor, aerobic bacteria feed on and decompose this OM, thereby consuming oxygen in the process (Altieri, 2018). Due to this excess nourishment source within the benthos, quantities of bacteria

increase, allowing for an even larger than average uptake of dissolved oxygen. This is just one of the main contributing factors which influence oxygen benthic flux measurements in sandy environments and is further investigated within this thesis. Varying sandy sediment types will change the chemical oxygen demand within the benthos, thus impacting benthic oxygen demand (Attard et al., 2019).

The combination of hydrodynamics and biology control the temporal and spatial movement of oxygen through sediment (Hicks et al., 2016). Understanding the oxygen dynamics in sandy sediment environments and their role in biogeochemical cycling is crucial as these environments constitute up to 70% of the benthic habitats of the world's shelf seas (Glud, 2008). Greenwood et al. (2010) argue oxygen levels within shelf seas are declining, and it is vital to understand why this is occurring. An important way to predict future impacts to our coastal environments is to understand the influences and interactions of oxygen water/sediment dynamics within permeable sediments (Santos et al., 2012). A better understanding of the interaction between drivers will contribute to the modelling of benthic oxygen fluxes as thus far, little work on benthic oxygen dynamics in sandy shelf sea environments has been carried out.

1.8 Measurement of oxygen flux

Transfer of oxygen across the BBL is a key component in the oxygen cycle within shelf sea environments as discussed above. As a result, a number of different measurement techniques have been developed to quantify this process.

Traditional techniques for measuring benthic oxygen flux include microprofilers (Revsbech et al., 1981) and benthic chamber/cores techniques (Huettel et al., 1992; Jönsson et al., 1991). The aquatic EC technique has been developed more recently in 2003 (Berg et al., 2003), and is still considered an understudied technique. These three measuring techniques measure different components of oxygen flux: diffusive oxygen uptake, benthic oxygen uptake and total turbulent oxygen flux, respectively. An overview of each technique is provided in Sections 1.8. Each technique has associated advantages and disadvantages therefore, using a combination of techniques can be beneficial as they complement one another to build a comprehensive picture of oxygen dynamics within a benthic ecosystem. The microprofiler and EC were selected within this thesis primarily because they are less invasive and enable measurement at higher temporal resolution (Table 1.2).

Table 1.2 An overview of advantages and disadvantages for each measuring technique. More detail on each factor is further discussed within each correlating section.

Consideration	**Advantages**			**Disadvantages**		
	EC	**Microprofiler**	**Benthic Chamber**	**EC**	**Microprofiler**	**Benthic Chamber/core**
What is measured?	Total flux (Berg et al., 2003).	Diffusive flux (Bryant et al., 2010)	Biological oxygen uptake rate		Underestimates total flux (Bryant et al., 2010)	Underestimates total flux (McGinnis et al., 2014)
Instrument robustness			Robust	Fragile	Fragile	
Invasive/non-invasive measurements	Non-invasive (does not disrupt pore water				Invasive (does disrupt pore water) (Bryant et al., 2011)	Invasive (does disrupt pore water) (berg et al., 2003)
		Established processing technique (Bryant et al., 2010)	Established processing technique (Hume et al., 2011)	Complicated processing of data (Lorrai et al., 2010)		
	Continuous measuring and fast response (Berg et al., 2003)	Fast responsive oxygen sensor			Taking flux over a 50min period in time (Bryant et al., 2011)	Taking a snapshot (Berg et al., 2003)
			Inexpensive	Expensive	Expensive	
	In situ	In situ				Ex situ (cores)/ in situ (chambers) but isolates environmental parameters (Berg et al., 2003)
	Diverse range of environments (Berg et al 2003; McGinnis et al., 2011; Rheuban et al., 2014; Chipman et al 2016)				Only permeable sediment (Reimers et al., 1987; Larsen et al 2019)	Only permeable sediment (cores) (Precht et al., 2004; Turner et al., 2010) variety of environments (chambers) (Kemp et al., 1980; Calhoun et al., 2017)

1.8.1 Chamber/core technique

Two very similar container (chamber and core) techniques are used to measure benthic oxygen uptake by measuring oxygen depletion in the overlaying water of the sediment over time within a sealed control volume. The core method recovers sediment cores of ~5 to 10 cm in diameter from the chosen environment (Rabouille et al., 2009). These cores are kept in an environment similar to the in situ conditions (temperature, light, etc.) within a laboratory upon recovery of these cores. Oxygen flux is calculated by measuring the rate of concentration change in the overlying water of the core. An alternate technique utilizes an in-situ chamber of ~30 cm in diameter which isolates a section of bottom water and overlaying water from the surroundings (Davies et al., 1995; Berg et al., 2003). Chambers are often equipped with autonomous recording dissolved oxygen, temperature and salinity sensors. Both techniques typically use controlled mixing to replicate current velocity of water column (Berg et al., 2003).

These techniques are commonly used to estimate bioturbation and bioirrigation (Riisgård and Banta, 1998; Rabouille et al., 2009). These studies have mainly focused on assessing the circulation of substances (including oxygen) via suspension feeders rather than to fully estimate the oxygen flux within an environment. A study by Volkenborn et al. (2007) measured bio-irrigation in permeable sediments. This study illustrated how large burrowing macrofauna can influence hydrodynamics within sediments, though it was unable to determine the full effect of bioirrigation on the seafloor (Volkenborn et al., 2007).

Several challenges arise when using these techniques in an energetic shelf sea environment. Studies (Riisgård and Banta, 1998; Glud et al., 1999; Valdemarsen et al., 2011; Kristensen et al., 2012) have made it evident that the chamber and core techniques isolate driving factors (advection, wave, tidal flows, etc.). Laboratory-based incubations of intact sediment cores from coastal environments consistently underestimate the fluxes from in situ incubations of larger benthic chambers, often by a factor of 2 or 3 (Archer, 1992; Glud et al., 1998, 2003). For correct faunal representation it is highly recommended to use relatively large core samplers or benthic chambers, the problem of using small enclosures increases with increasing natural heterogeneity and the average size of macrofauna specimens contributing to the benthic exchange rate. These techniques also tend to represent bioturbation and bioirrigation caused by meiofauna well, but underestimate bioturbation and bioirrigation rates caused by macrofauna (Berg et al., 2003). Glud et al., (1999, 2003) compared several oxygen uptake rates within the

same sediment and found oxygen uptake to differ by orders of magnitudes due to the size of the chamber/cores. A larger surface area would allow larger fauna to recirculate the sediment changing the rate of oxygen consumption. Therefore, chambers/cores often do not account for macrofauna sediment oxygen consumption rates as they are often not captured within the footprint of the chamber area.

These issues are also demonstrated when comparing studies (Glud et al.,1998, 1999, 2003) which measured oxygen uptake using either in situ chambers or cores in the same benthic area. It has been found that there are significant differences in oxygen uptake rates between and within techniques. These differences are attributed to the artificial stirring rates within chamber/cores which differ from the naturally occurring flow patterns (tidal, advection, wave) (Bryant et al., 2010). These issues may elucidate why certain studies (Huettel and Webster 2001; Reimers et al., 2001), in environments where hydrodynamics is a primary driver of oxygen uptake have not used chamber/core techniques.

Oxygen uptake can be influenced by ecological factors such as bioirrigation and bioturbation. Measuring these processes can be beneficial to assess benthic oxygen uptake using chamber techniques. Even though bioirrigation studies may not establish a full picture of bioirrigation events on the sea floor, these laboratory studies can demonstrate the effect of bioturbating organisms on the SWI processes, as well as determining benthic infauna characteristics (Volkenborn et al., 2007). Less invasive in situ measurements such as the EC technique can provide flux estimates based on a larger footprint whereas microprofile measurements can facilitate a in situ single-point-based flux analysis.

1.8.2 Measurement of benthic oxygen flux in situ

Each method of oxygen flux measurement has its strengths and limitations, as detailed in Table 1.2, all provide some insight into the transfer of oxygen across the sediment-water interface. Methods selected within this thesis worked by capturing timeseries data in situ (EC and Microprofiler) which differentiates them from the coring methods which are laboratory based.

Oxygen transfer to the sediment and sediment oxygen consumption processes can be physically limited by the function of sediment oxygen uptake (Glud et al., 2009). Oxygen dynamics in aquatic systems can be characterized by measuring the sediment oxygen uptake rate (JO_2); this critical parameter can be quantified by resolving the vertical distribution of oxygen at the

sediment water interface (microprofile) or by measuring total oxygen uptake by methods such as EC (Wetzel 2001; Glud 2008). Measurements of oxygen fluxes via microprofiles (diffusive uptake) and EC (total uptake) will be a foundation of this project.

Principles of the microprofiler technique

Sediment oxygen uptake rate JO_2 is calculated using Ficks Law. Fick's first law of diffusion is used to calculate the diffusive flux JO_2 (Tyrrell et al., 1964):

$$JO_2 = \varphi D \frac{\delta c}{\delta z} \quad [1.1]$$

where *J* is the diffusive oxygen flux in mmol $m^{-2}d^{-1}$, φ is the porosity, $\frac{\delta C}{\delta z}$ is the oxygen gradient across the DBL and D is the temperature diffusion coefficient.

One of the most established technique used to measure oxygen dynamics in situ is microprofiling (Revsbech, 1983, Jørgensen et al., 1985). This measurement of diffusive oxygen flux using a microprofiler allows for the characterisation of the oxygen dynamics from the water to the sediment in aquatic systems (Wetzel, 2001). The microprofiler technique has been used to develop a deeper knowledge of how multiple processes dictate the structure of the SWI (Fabricius et al., 2014; Fabricius et al., 2016). The microprofiler technique quantifies sediment oxygen uptake flux by observing the vertical distribution of oxygen concentration at the SWI (Revsbech, 1983). The diffusive oxygen exchange is calculated by measuring a vertical profile of oxygen concentration, then calculating the oxygen concentration gradient across the DBL, point by point, via a microsensor profile (Figure 1.3). Equation 1.1 is subsequently used to estimate diffusive oxygen flux.

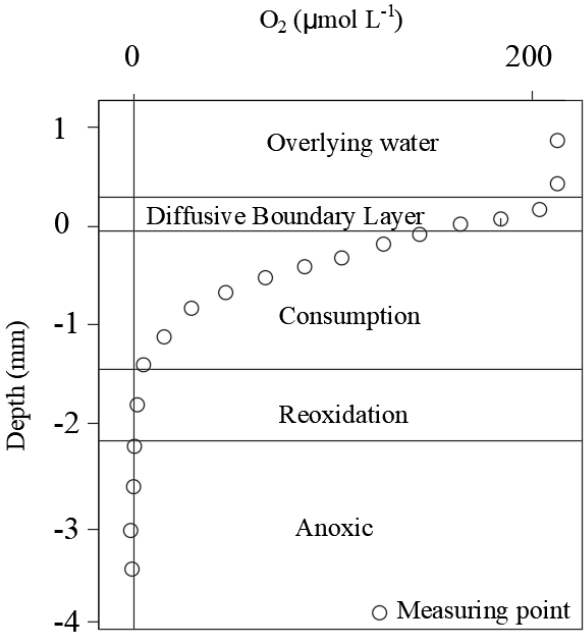

Figure 1.3: An oxygen microprofile indicating the various oxygen boundaries within sediment.

Diffusive flux is dictated by the consumption/production rates within sediments, the thickness of the DBL and hydrodynamics (Boudreau and Marinelli, 1994). The thickness of the DBL layer changes due to hydrodynamics (dissipation of turbulent energy). For example, as shear velocities increase, the DBL becomes thinner, allowing for a higher diffusive oxygen flux rate (Mann and Lazier, 2013).

The microprofiler technique has been used to measure diffusive oxygen flux within lakes (Schwefel et al., 2017; Edwards et al., 2005; Adams et al., 1982; Bierlein et al., 2017) and marine environments (Jørgensen et al., 1985; Reimers et al., 1987; Sulu-Gambari et al., 2016; Larsen et al., 2019), as well as to monitor benthic oxygen concentrations in artificial water bodies (Larsen et al., 2019; Bierlein et al., 2017). The advancement of autonomous (i.e., independently powered) microprofilers has allowed for deployments in deep lakes (Schwefel et al., 2018), oligotrophic deep-sea sediments (Donis et al., 2015) and deep-ocean margins (Glud et al., 2009). It is clear from these studies, which have reported substantial loss of data due to breakage of the fragile glass Clark-type oxygen microelectrode sensor, that there is a need for technological advancement to create a more robust system. An early study (Klimant et al., 1995) examined fibre-optic oxygen microsensors which are more robust; however, relatively few studies have implemented these new sensors (Attard et al., 2018) nor have any comparative in situ studies (between glass oxygen and optic sensors) been undertaken. Another related disadvantage of the microprofiler technique is that it can only sample within permeable

sediment, limiting the environments in which the technique can be deployed. The microprofiler technique also only measures diffusive component of flux rather than total flux (Bryant et al., 2011), and it is slightly invasive as it measures the same point repeatedly (Bryant et al., 2010).

However, the microprofiler technique has been shown to be a valuable monitoring tool for the remediation of contaminated permeable sediments. This is especially important as there is a need to assess ecosystem health within environments which are vital for ecology (e.g., seagrass beds) and are sensitive to anthropogenic activities. Studies by Liu et al. (2017) and Bonaglia et al. (2019) both used the microprofiler technique to assess pollutants in urban river sediments in relation to aeration. Another study by Wang et al. (2016) assessed oxygen consumption rates in sediments within the polluted Fuyang River, China. Studies by Wang et al., (2016) and Liu et al. (2017) concluded from oxygen profiles that sediment oxygen consumption rates were strongly affected (increased oxygen consumption) by the addition of organic matter (OM). The input of OM changed the oxygen gradient within the sediment in turn, increasing oxygen flux into the sediment. However, the microprofiler only measures point diffusive oxygen flux (rather than total flux), and is invasive, which may alter results therefore, the use of the other techniques (EC and chambers/ core incubations) in combination with the microprofiler technique would be beneficial in documenting and understanding the full oxygen flux dynamics within a certain environment.

Background of the Eddy Correlation technique

The EC method is a relatively recent technique which has been established for measuring total turbulent oxygen flux; this method is based on atmospheric EC which was established over 30 years ago in micrometeorology and has been adapted to aquatic systems by Berg et al. (2003). The EC method has been used for many years within the field of agricultural sciences for areas of yield research, agricultural carbon sequestration, bio-fuel investigation and crop management, as well as other areas (Burba, 2013; Chang, 2017; Sankey et al., 2018; Alberto et al., 2018; Maguire, 2018). The EC method provides measurements of gas emissions and consumption rates. It is now the most common method for measuring fluxes between land and air and is emerging as a dominant technique for aquatic environments (Baldocchi, 2003; Berg et al., 2003; McGinnis et al., 2008; Reimers et al., 2012; Reimers et al., 2016).

As discussed in Section 1.3 the open shelves of the ocean contain highly dynamic environments, creating challenges and limitations for continuous oxygen flux measurements. The aquatic EC technique (Berg et al., 2003; Reimers et al., 2016) is a method to measure

oxygen fluxes between the overlying water and benthic sediments. However, minimal work has been conducted in exposed areas such as coastal shelf sea environments (McGinnis et al., 2014). The EC method has many advantages over traditional in situ chamber and microprofiler techniques, such as minimal disturbance of natural hydrodynamics, ambient light, and sediment (Berg and Huettel, 2008; Lorrai et al., 2010; Reimers et al., 2012). The EC system is non-invasive, and samples at high resolutions (64 Hz, typically at 10 cm to 30 cm above the sediment). However, disadvantages, such as the cost combined with the fragile nature of the instrument, as well as complicated data analysis (i.e., various assumptions required for data filtering) deters many users from deploying the instrument in challenging and complex environments (Lorrai et al., 2010; Reimers et al., 2012).

The aquatic EC technique was founded on the idea of observing turbulent eddies transporting oxygen to the upper benthic layers where it is consumed (Figure 1.4) (Berg et al., 2003). Turbulent flux is measured by fast response microsensors (e.g., oxygen microsensors, although the technique is also possible with temperature and hydrogen sulphide sensors) paired with a velocimeter (e.g., Acoustic Doppler Velocimeter; ADV) to obtain simultaneous oxygen concentration (c) and vertical velocity measurements (w). As the EC method resolves turbulent scalar fluctuations, measured values are separated into their mean ($\overline{w}$, $\overline{c}$) and fluctuating components (w', c') (Berg et al., 2003). When vertical velocity fluctuations (w') are directed downwards (upwards) and oxygen fluctuations (c') are above (below) average this indicates oxygen is transported into (out of) the sediment (Figure 1.4) (Berg et al., 2003).

Measurements are averaged over a timescale longer than turbulent fluctuations (Figure 1.4A and B), over which time the time-averaged vertical velocity, $\overline{w}$ is assumed to equal zero (Equation 1.2 and 1.3). Vertical oxygen flux JO_2 is calculated in Equations 1.2 and 1.3:

$$w'(t) = w(t) - \overline{w}(t);\ c'(t) = c(t) - \bar{c}(t) \quad [1.2]$$

$$JO_2 = \overline{w'c'} \quad [1.3]$$

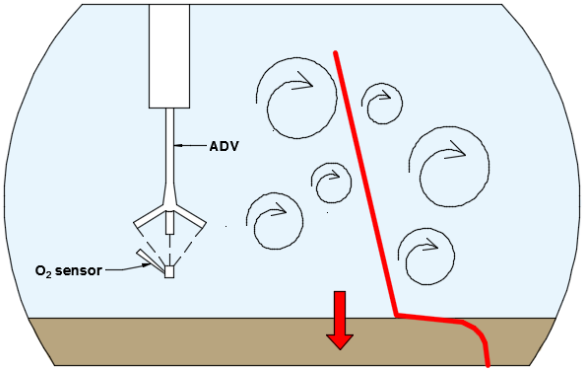

Figure 1.4A: Demonstrating the EC technique, indicating the position of the ADV in relation to the oxygen sensor. A focal point 12 cm below the ADV where the oxygen sensor sits, creating a 1 cm^2 measurement area. To the right of the diagram the turbulent transport in the water column is shown with an uptake of oxygen in the sediment (Berg, 2019).

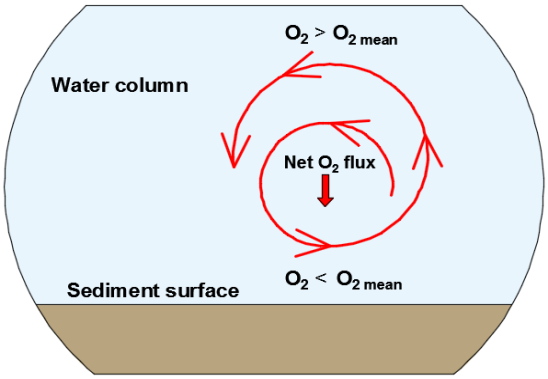

Figure 1.4B: Demonstrating the oxygen consumption in the upper sediment layers; turbulent eddy mixing bringing oxygen into the sediment surface (Berg et al., 2003). Diagram edited from Berg et al, (2019).

The method assumes homogenous conditions with steady horizontal flows and minimally varying oxygen concentrations (Lorrai et al., 2010). As this is rarely the case in real flows, heterogeneity can be corrected by the use of analysis tools, e.g., size of window length and specific detrending tools. Holtappel et al. (2015) have shown that heterogeneity induces substantial error in flux estimations. This error can be reduced by lowering the height of the measuring volume from substrate; however, this reduces the size of the EC measurement area, or 'footprint' (Berg et al., 2007) which may underrepresent the flux of the habitat in question.

As mentioned briefly above, aspects of the technique are known to be more challenging to apply than the traditional methods (chambers/cores and microprofiler), nevertheless, the EC method has some significant advantages (Pilegaard, 2001). In contrast to traditional techniques, the EC technique is non-invasive; therefore, the measurement of oxygen flux is not restricted to permeable sediments. Studies to date have used the EC technique within a variety of hard bottom environments (Glud et al., 2010) such as sea ice (Long et al., 2012) and coral (Rovelli et al., 2015). The EC technique also measures oxygen flux over a footprint (>50 m elliptical area, upstream of the EC system), (Berg et al., 2007) which provides a better representation of benthic flux within a habitat compared to the other techniques (e.g. chamber/core and microprofiler) which only measure at one point. In order for the EC technique to measure total flux (fluxes at all frequencies), a fast response glass type microelectrode oxygen sensor is used, which can sample continuously at 64 Hz and has a tip diameter of (100 μm). Many studies (Reimers et al., 2012; McGinnis et al., 2014; Reimers et al., 2016; Reimers et al., 2016A) report

loss of data during deployment as debris breaks these fragile sensors. Few in situ studies (Long et al., 2015; Reimers et al., 2016; Berg et al., 2016) have replaced the glass oxygen microelectrode with a robust optical oxygen sensor. These optic sensors have a larger measuring diameter and slower response time. Chipman et al. (2012) undertook a comparative EC study between a glass microelectrode and optic sensor and found negligible difference between readings. However, this study was within shallow water with minimal hydrodynamical drivers (waves, advection, tidal flows) (Chipman et al., 2012). To date, the optic sensor has not been compared with the glass microelectrode in a variety of in situ environments (waves, advection, tidal flows, etc.) to assess performance in reading oxygen flux levels.

A further deterrent for using the EC technique is the complex processing and interpretation of the data (Holtappel et al., 2015). Studies have found variations in oxygen flux when different processing tools were applied (Lorrai et al., 2010; Reimers et al., 2012). The inappropriate choice of processing tool can lead to a misrepresentation of oxygen flux within the environment. For this reason, some EC studies (Kuwae et al., 2006; Lorrai et al., 2010) have focused on establishing the EC data processing methods in a variety of environments rather than discussing the drivers of oxygen flux in those environments. However, research is still required to further establish a robust EC data processing methods in a variety of environments.

McGinnis et al. (2008) undertook an in-depth analysis of the importance of defining an appropriate time-averaging window when applying Equation 1.3. This study emphasised as the importance of this time-averaging window, demonstrating when the time-averaging is too long, artefacts such a sensor drift and environmental changes (flow changes) are included. However, when the averaging window is too short all flux frequencies would not be captured (McGinnis et al., 2008). Ongoing development and advancement have also been made on despiking, phase-shifting (Lorrai et al., 2010), rotation (Lorke et al., 2013) and detrending (Reimers et al., 2012) of the data. Reimers et al. (2016) also examined the added complexity of wave interference on processing EC data. Reimers et al. (2012) and Lorrai et al. (2010) advised and discussed the most suitable detrending method (running mean, frequency filter, block averaging or linear detrend) for a specific environment. Volaric et al. (2018) suggests the use of a combination of detrending methods, changing the method depending on the state of tide.

These studies have increased our understanding of handling and processing datasets and has led to the development of software such as SOHFEA (McGinnis et al., 2014) which enables

flux to be calculated. However, manual processing of data is still required to understand how different processing methods affect the results, particularly when applied to complex and understudied environments such as shelf seas.

To date only two studies have been conducted in challenging shelf sea environments (offshore, > 25 m depth): the North Sea (Tommeliten) (McGinnis et al., 2014) and off the coast of Oregon (Reimers et al., 2012; McCann-Grosvenor et al., 2014; Reimers et al., 2016).

McGinnis et al. (2014) examined benthic oxygen exchange in permeable sediment within the North Sea (~75 m depth). This study used a model which linked bottom boundary layer turbulence with pore water exchange and in situ data to discuss tidally driven turbulence in relation to benthic oxygen flux rates. This study found median oxygen flux rates of ~10 mmol m^{-2} d^{-1}. These rates also followed tidal trends as predicted by modelling. A combination of biogeochemical and hydrodynamic (wave, internal waves/tides) water-column measurements coupled with SWI dynamics were not conducted at this North Sea site. Such an investigation would have provided further understanding of the biogeochemical and ecological processes within this dynamic and ecologically important system.

A separate study of the Oregon inner shelf examined how oxygen upwelling (hypoxia effects) as well as waves and currents impact benthic oxygen fluxes (McCann-Grosvenor et al., 2014). This study site has been key for the investigation of wave interference in relation to processing of EC data (Reimers et al., 2016). Reimers et al. (2012) and (2016) found a need for more oxygen flux measurements to be taken in permeable coastal shelf sea environments to further develop the EC technique in these environments. The studies found mean oxygen flux levels of ~6 mmol m^{-2} d^{-1} throughout their field campaign, with wave interface creating variations in the velocity and oxygen components. The flux at this study site was found to be driven mainly by strong currents and large waves. Water column measurements of these hydrodynamic components have not been conducted. Therefore, there is still a need to assess and document further drivers dictating oxygen dynamics, in turn this will aid the identification of changes in shelf sea ecosystem health from anthropogenic influences.

In both study sites (L4 and Cawsands), fishing was documented as the only direct prevalent anthropogenic factor. Therefore, a study site closer to the shoreline which is affected by land use would be more appropriate to assess and monitor how anthropogenic factors affect benthic oxygen fluxes.

The lack of studies within coastal shelf sea environments may be due to difficulties associated with the EC technique. These include cost implications of sensitive and expensive sensors which are at risk in coastal shelf sea hydrodynamically harsh conditions, as well as uncertainties in flux values due to velocity artefacts, especially when wave contributions are present (Reimers et al., 2016). The increase in study site environments, in combination with the continual advancement of technology and improvement in processing of data will enable a greater insight into the scope of the EC method. This will also enable the possibility of the EC technique to become an intricate part of a routine monitoring system.

1.8.3 Combination of oxygen flux techniques

To date, few studies (Berg et al., 2009; Reimers et al., 2012; Attard et al., 2015; Reimers et al., 2016) have simultaneously used a combination of measuring techniques, (core /chamber incubations, microprofiler and EC). Berg et al., (2009) and Donis et al., (2015) emphasised the need to validate the newer EC method using the traditional methods.

Attard et al. (2015) assessed benthic oxygen uptake rates using chambers and the EC technique within Maerl beds. The EC measured total benthic flux rates of $\approx$ -13 mmol m^{-2} d^{-1} and chamber incubations measured oxygen consumption rates of $\approx$-24 mmol m^{-2} d^{-1}. As these results where within the same order of magnitude, this chamber experiment validated the EC flux values (Attard et al., 2015). Reimers et al. (2016) used both the microprofiler and EC techniques to determine benthic respiration rates, as well as benthic oxygen flux at a site on the Oregon Shelf. The study was able to document a comprehensive overview of temporal and spatial variabilities within the study site (Reimers et al., 2016). However, further studies are still required to validate the EC technique using traditional techniques in a variety of environments.

Traditional techniques (chamber incubations/cores and microprofiler) as well as the EC technique in regard to measuring oxygen dynamics all have their merits and disadvantages, as previously stated, including: cost, accessibility, ability to control the environment in mesocosms, disturbance to surrounding environment, measurement of both sediment and water interfaces, and limitations in the range of measurements taken. Using a combination of techniques to measure oxygen dynamics on the seafloor will create a comprehensive data set of a particular environment.

1.9 Gaps in knowledge

To date only two in situ (non-invasive) EC oxygen flux studies have been conducted in shelf sea environments (Reimers et al., 2016 and McGinnis et al., 2008). These two studies conducted a series of microprofile and EC field campaigns within shelf sea environments similar to those examined within this thesis. The environment addressed in this thesis was more challenging than the two study sites described in Reimers et al., (2016) and McGinnis et al., (2008) due to complex topographical features, creating internal tidal dynamics, justifying a new examination of processing methods further developed in this thesis. The work of Reimers et al., (2016) and McGinnis et al., (2008) investigated drivers of oxygen flux which included tidal flows, upwelling, and varying sediment topography, and discussed various methods to calculate benthic oxygen flux. However, they, together with the wider literature detailing oxygen fluxes measured by the EC technique, do not address all oxygen flux drivers and potentially important factors such as varying topographic features, temperature and nutrient levels remain unstudied. This is particularly relevant for the complex and energetic shelf sea environment studied in this thesis which required modified data collection and data processing methods to obtain valid data. The work presented in this thesis makes progress towards filling the research gaps identified in the preceding literature review, providing new information about oxygen transfer and giving confidence that the EC method for measuring benthic oxygen fluxes is a key tool for better understanding of these critical environments.

1.10 Aims and objectives

This study aims to examine benthic flux drivers within two coastal shelf sea environments off the coast of Plymouth, UK (L4 and Cawsands), with particular focus on seasonal variations of organic OM (spring and summer), hydrodynamics and the corresponding oxygen measurements within marine benthic regions. This thesis also aims to progress towards assessing and quantifying the drivers of diurnal benthic oxygen fluxes in shallow-water permeable seagrass sediments using a combined EC and microprofiler technique. With regard to water-column oxygen dynamics and oxygen budgets, this study is focused on; 1) validation of the EC technique in a complex shelf sea environment using a well-established oxygen flux measurement technique (microprofiler); 2) assessment of hydrodynamic drivers on benthic oxygen fluxes; and 3) the influence of drivers such as plankton blooms/dumping of dredged

spoils on benthic oxygen flux, linked to historical water column data at a shelf sea location over a five-month field campaign. To achieve these aims, three primary objectives were defined:

Hypothesis 1: The EC technique is a valid technique to establish oxygen flux within a shelf sea environment and it outperforms the traditional microprofiler technique.

Objective 1: Validate and assess the eddy correlation technique by comparing with the traditional microprofiler method within a seagrass meadow**.**

- Develop novel processing method to cope with the complexity of the shelf sea environment
- Compare the impact of point measurements from a microprofiler with those from the footprint measurements of the EC.
- Evaluate the validity of the EC to determine oxygen flux during both, light and dark conditions.
- Assess how hydrodynamics impact EC measurements within the seagrass habitat.

Hypothesis 2: Oxygen flux is primarily driven by hydrodynamics and is modulated by various other drivers at the L4 long-term coastal marine monitoring station

Objective 2: Assess how a variety of drivers influence benthic oxygen dynamics at a long-term coastal marine monitoring station over a five-month sampling campaign.

- Assess the influence of surface and internal tides on benthic oxygen flux at L4
- Assess the role of dumping of dredging spoils, temperature, nutrients and algal blooms in driving benthic oxygen fluxes, over a five-month sampling period.

By assessing in situ oxygen dynamics, this thesis aims to improve understanding of seasonality in benthic-pelagic processes in a coastal environment. Results from this thesis will fill a gap in the existing historical (50+ year) dataset to provide the first insight of marine oxygen cycling and benthic oxygen drivers at this site. The methodology used to achieve theses aims and objectives is outlined in Section 1.11. Further detail of the methods is found in Chapter 2.

1.11 Description of studies

The methodology illustrates two field campaigns, 1) A week-long field campaign at a seagrass meadow, at a study site named Cawsands. 2) A five-month field campaign at a sandy/muddy semi-permeable site, named L4 at the WCO. This section outlines the study site, the

instrumentation used at both sites, details the study sites and discusses post-processing. Further detailed description of methods for both campaigns is found in Chapter 2.

1.11.1 Study site

This study was performed within the WCO which is operated by Plymouth Marine Laboratory (PML) and the Marine Biological Association (Smyth et al., 2010). The WCO provides one of the most comprehensive living documents of coastal and open shelf ecosystems in the world. Because of this, the WCO is recognized internationally as a marine biodiversity reference site. This scientific sampling effort records a wide range of marine conditions in and around Plymouth Sound waters (including special areas of conservation and special protected areas), with records spanning for over 20 years (Western Channel Observatory, 2016). The data also feeds into international Earth observation initiatives and is used around the world for informing environmental management policies and regulations (Western Channel Observatory, 2016). While the WCO is more readily recognized for its automated buoys (L4 and E1) the WCO also operates across a cluster of sites in and around Plymouth Sound such as Cawsands. PML conducts on-going benthic surveys as part of the WCO. These studies provide an ecological time-series, created to capture the temporal and spatial variability in marine ecosystems (Smyth et al., 2015).

Cawsands

To characterise benthic oxygen dynamics within a seagrass meadow, a study site Cawsands (50.3312° N, 4.2020° W) was selected due to the varying exposure levels including tidal influences, primary production and anthropogenic influences e.g., pollution and boating activities. This assessment will provide the first steps into evaluating oxygen dynamics at this site.

Cawsands Bay (Figure 1.5) is situated on the Rame Peninsula (Area Outstanding Nature Beauty) and incorporates the twin villages Cawsands and Kingsand, overlooking Plymouth Sound. This site is also vital for local tourism economy, fishing and ecology (seagrass meadow). The bay is an east-facing sandy and shingle beach (Smyth et al., 2015). Cawsand Bay has a maximum depth of 15 m with an average tidal range of 4.6 m (Figure 1.5). The study site represents a shallow seagrass habitat with permeable sandy sediment which is sheltered from south westerly prevailing winds.

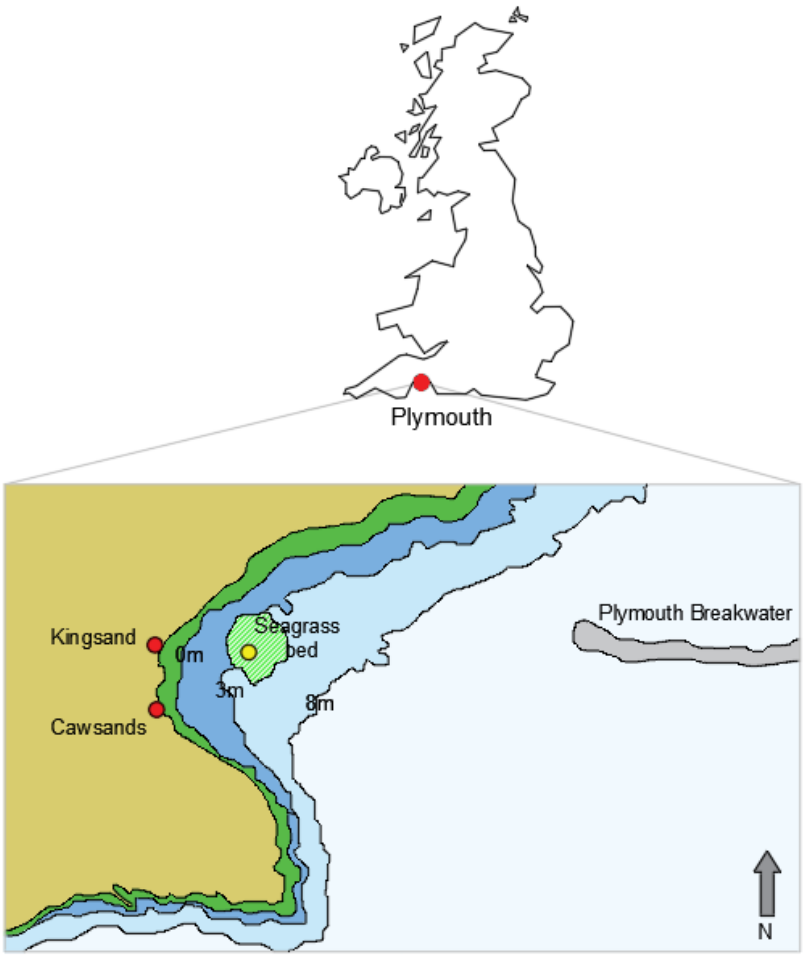

Figure 1.5: The location of the Cawsands study site, GPS: N500 20.017, W 0040 11.8523, the EC and microprofiler instrumentation were set up at location marked by the yellow circle. Numbers indicate minimum Chart Datum. The brown colour represents land, green represents the intertidal area and the varying shades of blue indicate changing water depths. The seagrass bed is indicated by light green hash.

L4

The site chosen for this study lies within the Western Channel Observatory (WCO), Plymouth, UK at the L4 buoy (50°15.0'N; 4°13.0'W), 22 km from the shore and is operated by PML and the Marine biological Association (Figure 1.6). The L4 site has many environmental and anthropological influences affecting water quality, sediment characteristics, and ecosystem health (Smyth et al., 2015). L4 is subject to two algal bloom events annually, one in May/June and the other in August/September (Groom et al., 2009; Smyth et al., 2009; Widdicombe et al., 2010; Xie et al., 2015). The site is located close to Plymouth Sound, a busy area where boating takes place (shipping, recreational and naval), as well as regular dredging within the harbour and dumping of this material (Smyth et al., 2015). The area is also affected by freshwater influences from three major river systems (Tamer, Plym and Yealm). Agricultural land surrounding the area feeds OM and nitrates into the river systems, which flows into Plymouth Sound harbour, especially during and following periods of rain (Smyth et al., 2009). Therefore, this dynamic site has many varying influences throughout an annual cycle that may have significant influence on sediment-water oxygen fluxes.

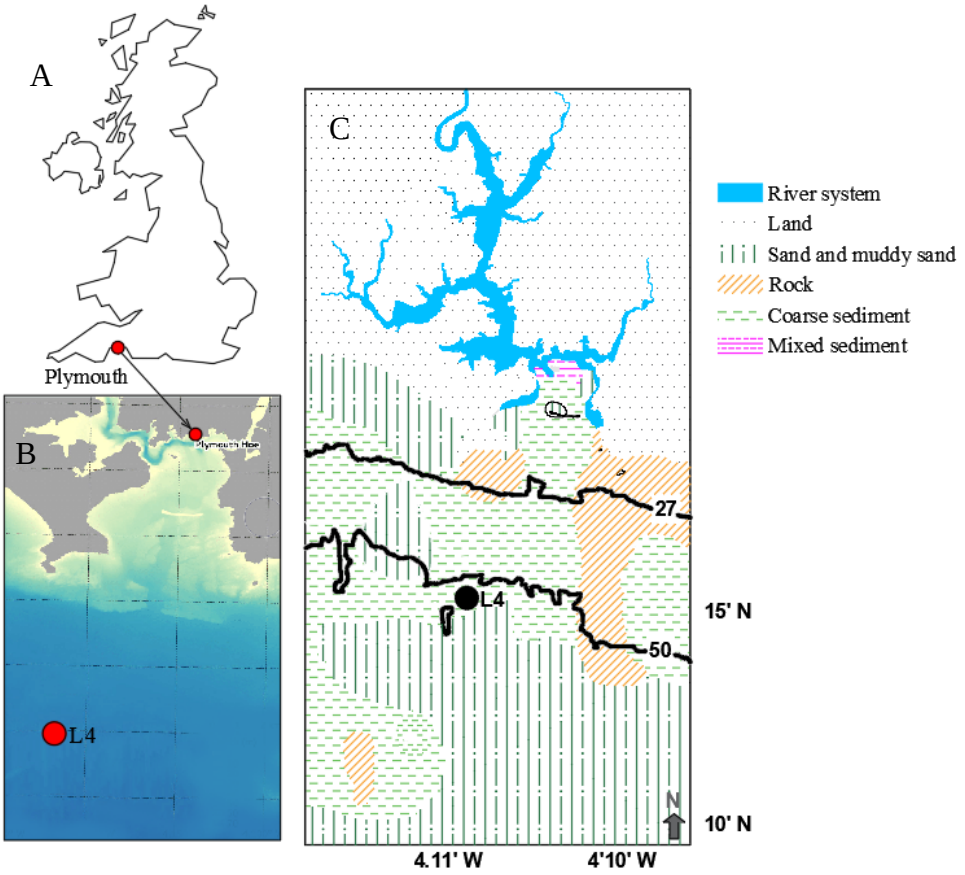

Figure 1.6: A) Schematic of the United Kingdom, indicating Plymouth, the study site. B) L4 location in relation to Plymouth, image edited from Queirós et al. (2019). C) The L4 site is 22 km from the coast of Plymouth at a minimum depth of 50 m, chart datum. Sediment types are indicated and two shelfs are indicated by solid black lines, numbers are the minimum depth. The EC and ADCP were deployed at position 50'15.095N 004'13.016W which was 20 m north of the L4 monitoring buoy. Data obtained curtesy of PML/Tom Bell.

Historic sampling at L4

As part of the ongoing data collection at L4, Conductivity Temperature Depth profiler (CTD) data is collected weekly along with hourly surface data from an active automated buoy at a depth of around 1.5 m (Smyth et al., 2009; Smyth et al., 2015).

The site has historical importance as nutrient chemistry and taxonomic monitoring dates from 1923 (Jordan, 1998; Atkins, 1923). It has been a test centre for attaining in-depth knowledge in complex marine and atmospheric fields (Smyth et al., 2009).

Topography and hydrodynamics at L4

The site exhibits topographic features which influence the tidal dynamics in the area. The sediment surrounding the site is spatially heterogeneous and changes throughout the season due to input of OM. Sediment at the site varies from silty to coarse sand. Historically, plankton blooms occur within the euphotic zone in late May/June and again in late August however, the

timing of these blooms' changes depending on water column mixing events and temperature (stratification of water column) (White et al., 2015).

Dumping of dredged material at L4

Riverine detritus is periodically dredged from Plymouth harbour to facilitate large vessel movements. This material is dumped offshore, however in 2017 the dumping ground was relocated to the region of L4. A disposal campaign of 10.3 kt occurred between 22nd May and 2nd June, with maximum disposal activity occurring between 30th May and 1st June (Smyth, 2017). A monitoring campaign was conducted by PML to assess the effect of releasing this dredged material on the surrounding areas. On the 30th May 2017 they found turbidity levels from 0.5 to 5 mg l^{-1} and SPM, which affected water quality (Bolam et al., 2018; Smyth, 2017). These turbidity levels fluctuated due to tidal modulations, however, consistently high values (> 5 mg L^{-1}) were seen until 15th June (Smyth, 2017). During this time both heavy rainfall and neap tides occurred. Low current velocities associated with neap tides would have been less effective in dispersing the dredged detritus material offshore, and the rainfall leading to riverine inflow would have added OM as well as nutrients into the marine system (Smyth, 2017).

Echo sounder data (immediately after dumping of dredged spoils) indicated some lighter fragments of the dredged material remained in the surface layers, whereas most of the dredged material descended rapidly below 30 m (Smyth, 2017). Continuous turbidity and sediment measurements conducted at L4 by PML confirmed that the addition of this dredged material was significant in magnitude in this environment when compared to natural levels historically (Bolam et al., 2018).

Plankton blooms at L4

Plankton blooms at L4 comprise of various plankton groups, including coccolithophores, cyanobacteria and dinoflagellates (Widdicombe et al., 2010; Tait et al., 2015). Once a plankton bloom is established, zooplankton will feed on the phytoplankton. Any remaining phytoplankton which has not been consumed eventually sinks to the seafloor, where senescence of the dead plankton takes place (O'Boyle et al., 2016). The degradation of this OM by bacteria leads to oxygen depletion within the sediment (Middelburg, 2019).

Data published by PML report plankton levels in 2017 (Tarran, 2019). Coccolithophore levels in particular, were found to be <100 organisms per ml during the peak of the season (April – September). In contrast, the autumn bloom was associated with a tenfold increase in plankton

abundance, with Cryptophytes peaking in October with an abundance of >1000 organisms per mL, with the bloom being concentrated at 10 m. PML reported that Phaeocystis spp., had normal levels of bloom in the upper levels of the water column (Tarran, 2019). However, PML predict that unlike other years the standard accumulation of cells in benthic waters and eventual senescence within the seabed were less than in other years. 2017 was an atypical year for plankton bloom events, which may become more common in future years, as chlorophyll levels at this site are becoming lower on average (Tarran, 2019).

1.11.2 Field campaign

The first field campaign (Cawsands) utilised a microprofiler and EC setup which were deployed for 41-hours to obtain high-resolution SWI profiles and total oxygen flux data within Cawsands bay. The second field campaign was conducted using an EC lander and an ADCP. A Conductivity Temperature Depth (CTD) profiler cast was taken as part of the long-term time series at L4. Due to loss of equipment during the subsequent deployments ADCP measurements were only collected in May.

1.11.3 Equipment and data processing

Equipment and data processing are outlined in this section however, a comprehensive theory and description are provided in Chapter 2 (methodology).

Microprofiler set up

The microprofiler was equipped with oxygen and temperature microsensors. Both microsensors had 100 μm tips and fast response times (90% in < 8 ms). A single sediment-water profile duration was 50 minutes. The oxygen microsensor was lowered vertically through the BBL and DBL (Figure 1.7). Measurements were obtained at small vertical increments over the lowest 10 cm above the bed and into the sediment.

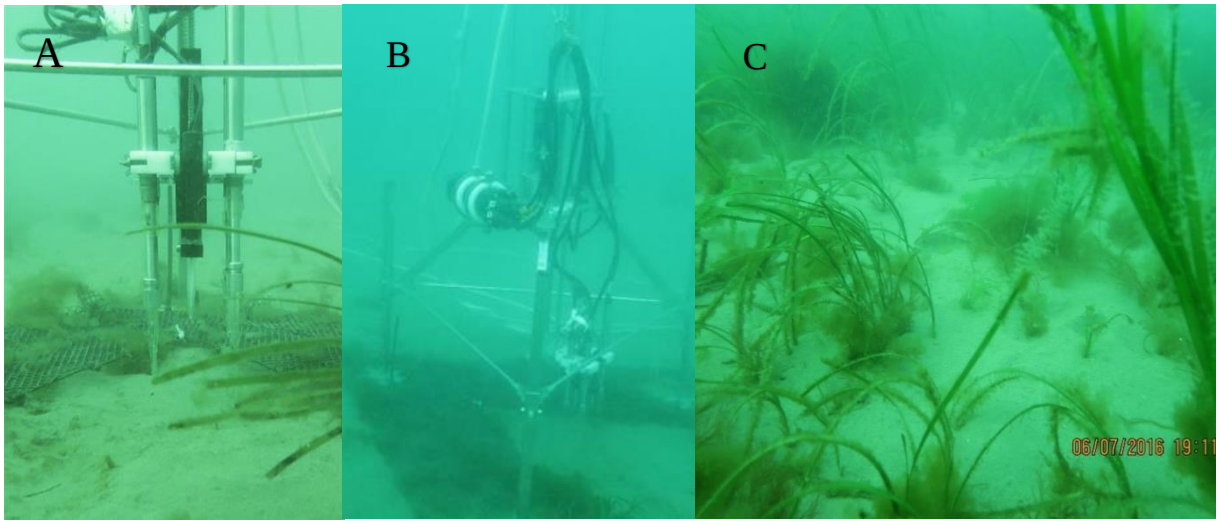

Figure 1.7: A) Oxygen and temperature microprofiler sensors in situ, B) Full microprofiler instrumentation in situ including sensors, cables and motor, C) The surroundings of the microprofiler (seagrass meadow).

Microprofiler data processing

The sediment oxygen uptake rate and the DBL thickness were calculated using the water-side direct method (Bryant et al., 2010) applied to oxygen profiles. Diffusive oxygen uptake was calculated using Fick's first law of diffusion, Equation 1.1, (Rasmussen and Jørgensen 1992). Further detail of microprofile processing is outlined in Chapter 2.

Eddy Correlation system set-up

The EC consists of an ADV paired with a fast-response Clark-type oxygen microsensor. Both instruments were sampled continuously at 64 Hz. An oxygen optode was mounted on the EC frame to calibrate the microprofiler oxygen sensor (during the Cawsands campaign) and EC oxygen sensor, and to provide independent oxygen concentration data within the BBL. The EC instrumentation was mounted on a tripod frame and was autonomous.

Eddy correlation data processing

In order to process EC oxygen flux values, data obtained from the various sensors (ADV, microelectrode and optode) must first be processed. The oxygen microelectrode was calibrated against optode data. Both, velocity and oxygen data were despiked and downsampled to 8 Hz. The data were divided into 15-minute windows as described in McGinnis et al. (2008). Thereafter, a linear detrend and a timelag was applied to every window. EC oxygen flux was calculated using Equation 1.3 (section 1.8.2). A detailed description of data processing is outlined in Chapter 2.

To determine the length and width of the EC footprint, methods stated in Berg et al. (2007) were used. The EC system measures oxygen flux over an elliptical footprint which extends from the EC system upstream, the size of which is dependent on the sediment surface roughness, friction velocity and the height of the measurement volume over the sediment (Berg et al., 2007). The orientation of the major axes of the ellipse is always in the horizontal direction (Figure 1.8).

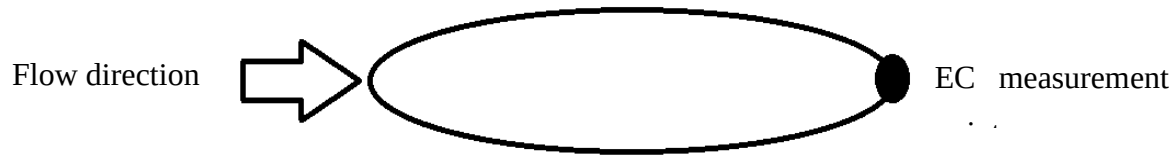

Figure 1.8: Typical shape of EC footprint. The filled circle mark is the measurement point and the arrow indicate the flow direction. The footprint forms upstream of the EC measurement point.

Supporting equipment set-up

To aid interpretation of in situ EC data various readings (temperature, oxygen and nutrient) throughout the water column were obtained. A CTD profiler, (Seabird SBE 19+) was equipped with a transmissometer, a Chelsea Photosynthetically Active Radiation (PAR) sensor, a fluorometer and an oxygen and temperature optode, as well as a 24-carousel rosette for water column samples (Smyth, 2019). The CTD was deployed to obtain measurements of oxygen, chlorophyll, nutrients, and temperature throughout the water column. CTD casts were conducted weekly at L4 during the field campaign. Core samples were collected at L4 and Cawsands to examine sediment oxygen uptake rates however, due to unforeseen circumstances this data was discarded.

To obtain current velocities throughout the water column an ADCP was mounted on a trawl resistant bottom type mount. ADCP data were only collected during the May deployment due to unforeseen circumstances.

Chapter 2

2. Methods

2.1 Introduction

There are many points to be considered when deploying an EC system, from pre-deployment testing of sensors to the logistics of deploying the sensitive lander from a vessel. This chapter breaks down, step by step, the deployment and analysis methods needed to obtain a benthic oxygen flux timeseries.

2.1.1 Oxygen flux across the SWI

Solutes diffuse from regions of high to low concentration. The flux of solute (J) is defined as mass of solute that passes through a known area (Boudreau and Jorgensen, 2001), (Figure 2.1). The flux of oxygen across the SWI, JO_2, is quantified by a balance between the rate at which oxygen is supplied to the sediment and the rate at which oxygen is consumed in the sediment. This balance is controlled by biogeochemical processes within the sediment and the controlling hydrodynamics of the overlying water column.

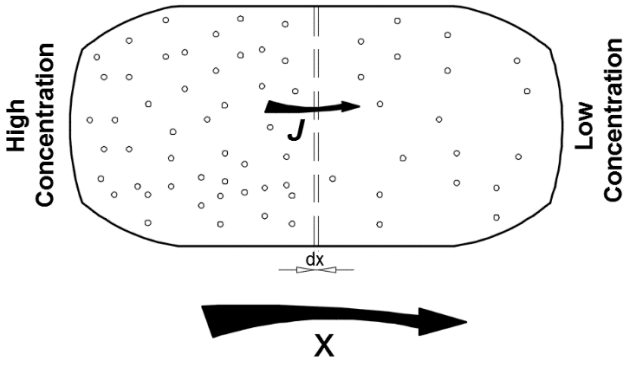

Figure 2.1: Schematic characterisation of the flux of a substance from left to right.

2.1.2 The structure of the bottom boundary layer

The BBL is the region above the sediment where viscous effects control the flow (Figure 2.1) and is of great importance to the biology, chemistry, physics, and geology of water bodies. The BBL is the primary region for dissipation of waves, currents and other turbulent energies (Boudreau and Jorgensen, 2001). These turbulent energies allow for the exchange of heat, particles and solutes which link the water column and sediment (Murray et al., 2017). The region of the benthic water column near the bed allows for relatively strong gradients in physicochemical properties such as sediment oxygen penetration, permeability and solubility (Boudreau and Jorgensen, 2001).

Across the BBL, the flux is driven by either the production and/or consumption of oxygen within the underlying sediment as well as suspended solids being moved between the BBL and bed by biological or physical suspension (Boudreau and Jorgensen, 2001). To fully comprehend the BBL, it is vital to understand the diagenetic processes (change or movement of sediment) which can be divided into two broad categories, reactions and transport, as well as the supply and consumption of particulates and solutes by abiotic or biologically mediated means (Boudreau and Jorgensen, 2001). In addition to controlling fluxes within the BBL, turbulent mixing in this region also governs the thickness of the Diffusive Boundary Layer (DBL) which is a key limitation on fluxes at the SWI (Lorrai et al., 2010).

2.1.3 Determining the thickness of the diffusive boundary layer

DBL thickness and corresponding oxygen transport are controlled by the turbulent mixing in the BBL. As oxygen enters the sediment, it is used for various biogeochemical processes in the

sediment oxic zone. These processes include benthic organic matter mineralization and oxidation of reduced compounds (Boudreau and Jørgensen, 2001). Revsbech et al., (1980) and Revsbech, (1985), established the existence of the DBL with significance to benthic oxygen exchange, using the first ever oxygen microelectrodes. This discovery permitted research into understanding the structure and the dynamics of the DBL (Jørgensen & Revsbech, 1989). The intersection between the constant oxygen concentration in the overlying well-mixed water phase and the extrapolated linear concentration gradient within the DBL defines the upper boundary of the DBL (Glud, 2008).

Lorke et al., (2003) and Brand et al., (2009) have focused on the variability of the DBL thickness with respect to turbulence and the influence on oxygen transport in the BBL. Their lake experiments demonstrated that within less active systems, the DBL thickness increases due to decreased dissipation rates at low velocities (Lorke et al., 2003). The result of an increase in the DBL thickness has implications for oxygen availability within the sediment and corresponding fluxes at the SWI, as an increased DBL thickness reduces diffusive oxygen transport to the sediment and subsequently decreases the oxygen penetration depth into the sediment (Jørgensen & Des Marais 1990; Glud 2008).

2.2 Calculating oxygen flux

Within this study we assess oxygen flux and specifically, oxygen flux into/out (i.e. consumption /production) of sediment through the sediment water interface (SWI) (Boudreau and Jorgensen, 2001). Determination of diffusive oxygen flux of a solute depends on the direction, concentration gradient and size of the sediment surface area it passes through. Solutes diffuse from regions of high to low concentration, driven by concentration gradient as defined by Fick's first law of diffusion (Equation 2.1), (Kamaruddin and Koros, 1997; Bryant et al., 2010).

$$JO_2 = -\varphi D \frac{\partial c}{\partial z} = -\varphi D \frac{C_{bulk} - C_{SWI}}{\delta_{DBL}} \; [mmol\ m^{-2}\ d^{-1}] \qquad [2.1]$$

Where JO_2 is oxygen flux, D is the molecular diffusion coefficient for oxygen in water, φ is sediment porosity, c is the oxygen concentration, $\frac{\partial C}{\partial z}$ is the oxygen concentration gradient within

the diffusive boundary layer (DBL) above the SWI, where z is defined in the vertical direction (Equation 2.1).

Mixing regimes in the water that drive oxygen fluxes include benthic turbulence within the BBL and laminar flow above the sediment within the DBL (Figure 2.2). The SWI is defined as the interface between the benthic water and the sediment (Figure 2.2) (Boudreau and Jorgensen, 2001; Bryant et al., 2010). Many of the key processes influencing oxygen dynamics and resultant water quality occur at the boundary layer (Bryant et al., 2010). The structure of the boundary layer and SWI are affected by biological (i.e., bioturbation/bio-irrigation), chemical (i.e., oxidation and reduction) and physical (i.e., tides, currents) processes (Sanschi et al., 1990).

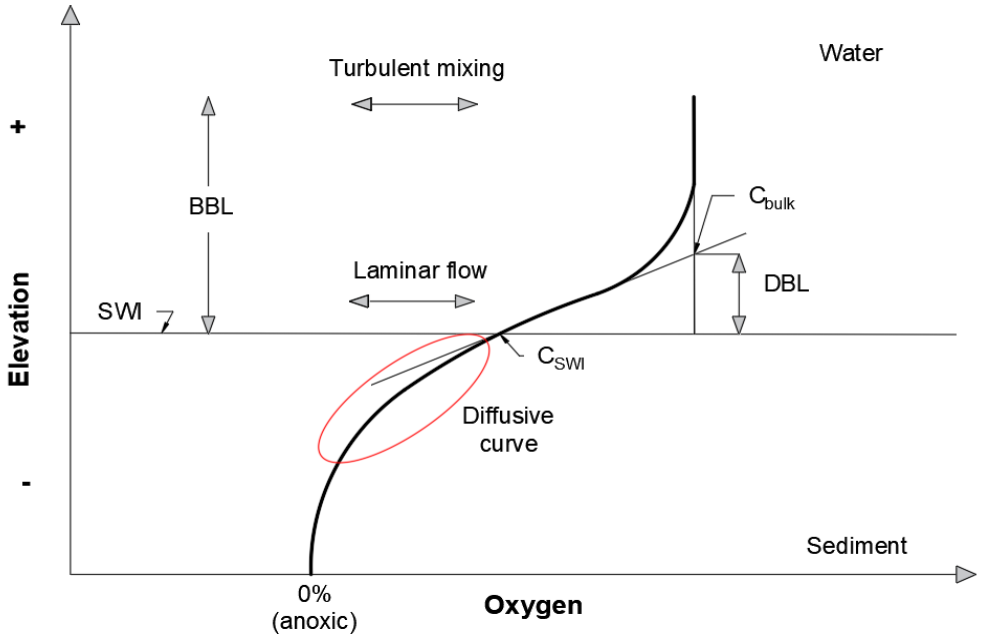

Figure 2.2: Illustrating locations of DBL where laminar flow occurs, BBL where turbulent mixing occurs and SWI using an oxygen profile from the water to the sediment. Red circle is the direct method further described below.

2.3 Methods for quantifying oxygen flux

The methods used to quantify oxygen flux have in general been discussed in Chapter 1 however, Chapter 2 provides a greater level of detail. There are several established methods for quantifying JO_2 in situ, including DBL-focused microprofiling and BBL-focused eddy correlation (EC) as well as benthic chambers. However, the use of benthic chambers to measure flux can be controversial as turbulent mixing within the chambers is often controlled, thereby

creating a false measurement of flux (Ribaudo et al., 2017). Conversely, more non-invasive, in situ measurements such as the EC technique can provide flux estimates based on a larger footprint whereas microprofile measurements facilitate single-point-based flux analyses.

While each method of oxygen flux measurement has its strengths and limitations, they all provide some insight into the transfer of oxygen across the sediment-water interface. Measurements of oxygen fluxes via microprofiles (diffusive uptake) and EC (total uptake) will be a foundation of this thesis supported by Acoustic Doppler Current Profiler (ADCP) data, nutrient analysis and conductivity, temperature and depth (CTD) measurements. With each technique having advantages and disadvantages, using all three techniques can complement each other in providing insight into the oxygen dynamics within a benthic ecosystem.

2.3.1 Microprofiler

One of the more established methods used to measure oxygen dynamics is in situ microprofiling. The microprofiler technique uses single-point-based flux analysis to measure diffusive flux based on Equation 2.1, (Figure 2.2), (Boudreau and Jorgensen, 2001; Bryant et al., 2010). The method quantifies the sediment oxygen uptake flux, by observing the vertical distribution of oxygen at the SWI.

A study conducted by Fabricius et al. (2016) described that the microprofiler technique was used to develop a greater and deeper knowledge of how multiple processes dictate the structure of the SWI. A high spatial resolution of several sediment parameters was implemented, at a sub-millimetre scale, with numerous sensor types available to measure oxygen, pH value, redox potential, hydrogen sulphide and nitrous oxide (Fabricius et al., 2016).

A study investigated the vertical oxygen distribution at the SWI in a hypolimnetic system using a micro-profiler (Bryant et al., 2011). This study characterized the oxygen distribution across the SWI and evaluated the sediment response time for vertical oxic distribution at the SWI (Bryant et al., 2011). This measurement allowed for the characterization of the oxygen dynamics from the water to the sediment in an aquatic system (Wetzel, 2001). Bryant et al., (2010) explored both the water and sediment side factors that control sediment oxygen uptake (Bouldin, 1968; Revsbech and Jørgensen, 1985). Within the study presented in this thesis the direct method was used to quantify oxygen flux using the miroprofiler technique (Figure 2.3).

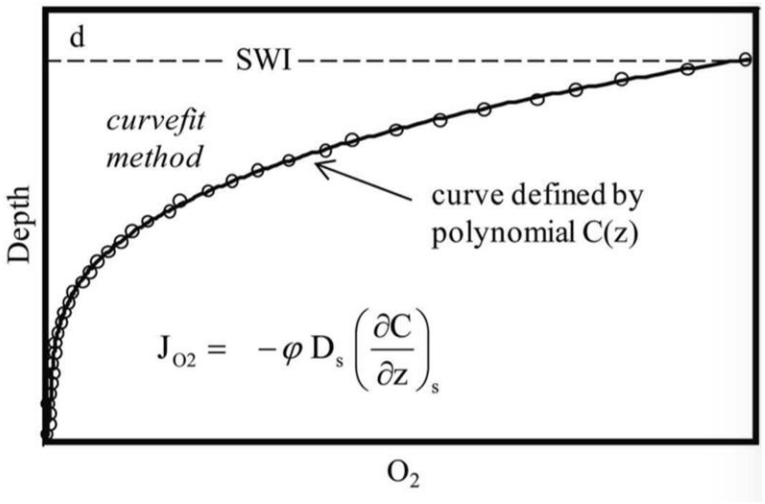

Figure 2.3: Diagram taken from Bryant et al. (2010), illustrating the direct method, where the JO2 is evaluated from the linear slope of the DBL when measured from the oxygen microprofiler, refer to the area circled in (Figure 2.2).

2.3.2 Eddy Correlation

The aquatic EC method, developed by Peter Berg (Berg et al., 2003), computes the total benthic oxygen flux (JO_2) from measurements of the mean and fluctuating oxygen concentration ($\bar{c}$ and c') measured using an microelectrode, and the mean and fluctuating vertical flow velocity ($\bar{\omega}$ and ω') obtained using a velocimeter (see Figure 2.4 for a typical experimental setup). The calculated total oxygen flux includes, but is not limited to, diffusion, photosynthesis, bioirrigation and respiration processes.

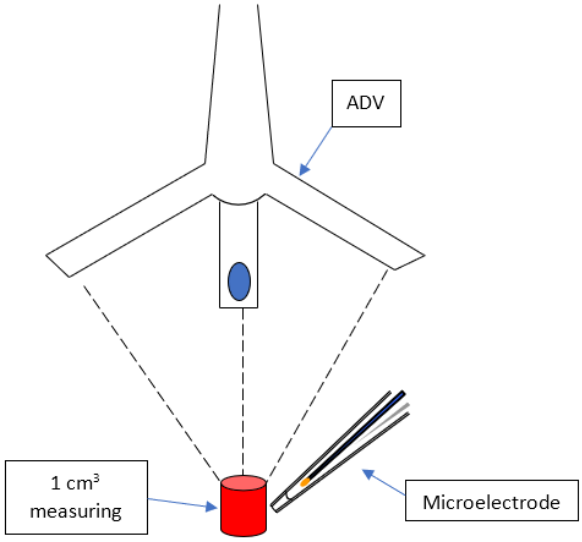

Figure 2.4: Schematic of the ADV (measures velocity) and Microelectrode (measures oxygen) with the red cylinder representing the 1 cm3 measuring volume of the ADV and microelectrode.

EC Basic principals

EC basic principles include turbulent motions carrying oxygen through the water column to the benthos. Berg et al., (2003) describes a chaotic complex turbulent flow where a correlation exists between vertical velocity and oxygen concentration over a sediment surface (Figure 2.5).

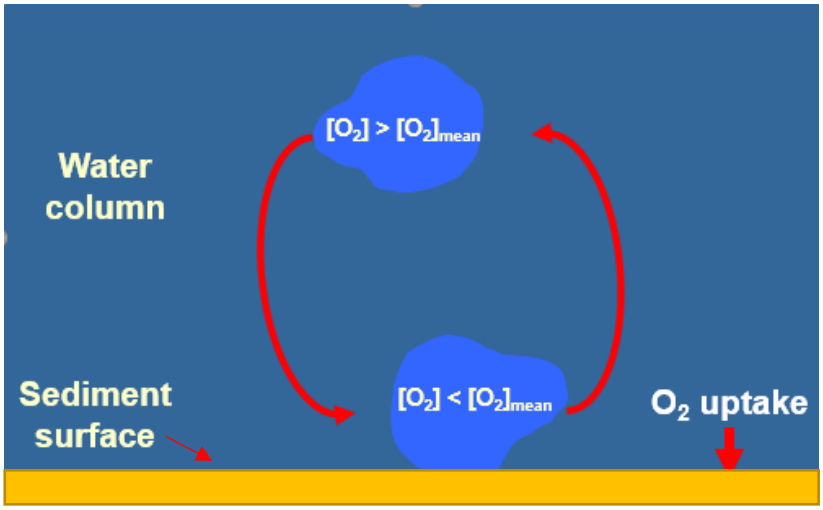

Figure 2.5: Schematic of turbulent motions carrying oxygen through the water column into the sediment modified from Berg et al. (2007).

It has been shown in non-photosynthetic conditions, when velocity points down and the oxygen concentrations are higher than the mean oxygen level, or vice versa when velocity points up and oxygen is lower than mean oxygen level, this creates a net oxygen transport downwards into the sediment (Figures 2.5, 2.6 and 2.7).

Therefore, mean EC oxygen flux is derived using Equation 2.2 (Berg et al., 2003).

$$JO_2 = \overline{\omega' c'} \quad [2.2]$$

Timeseries measurements of vertical velocity (ω) and oxygen (c) are separated into the mean ($\bar{\omega}$ and $\bar{c}$) and fluctuating components through Reynolds decomposition (Reynolds, 1895):

$$\omega = \bar{\omega} + \omega' \text{and } c = \bar{c} + c' \quad [2.3]$$

In this study, oxygen concentrations were obtained using an EC system, consisting of an oxygen microsensor (to measure c) and an acoustic Doppler velocimeter (ADV), (to measure ω).

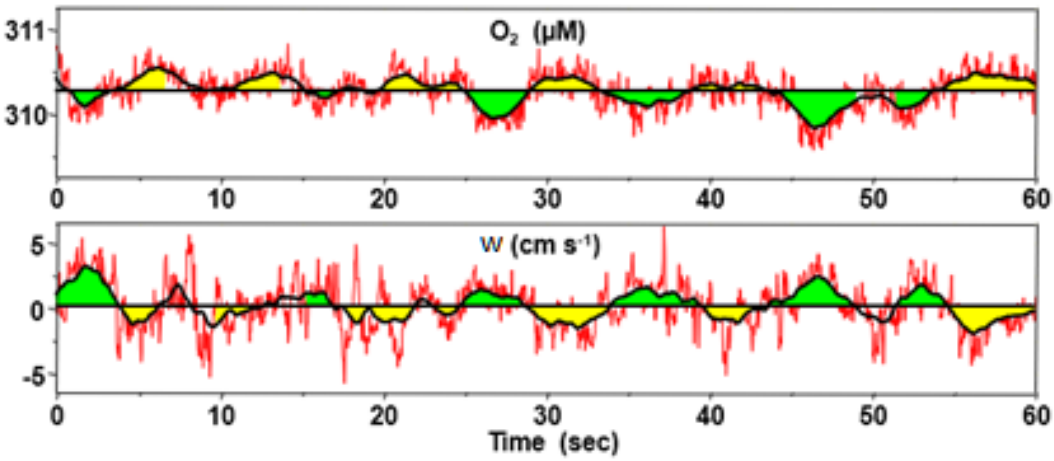

Figure 2.6: Example data modified from Berg et al. (2009) of how EC flux is calculated (green areas represent flow from the sediment and with lower than average oxygen; yellow represents flow entering the sediment with higher oxygen). Red lines represent raw data.

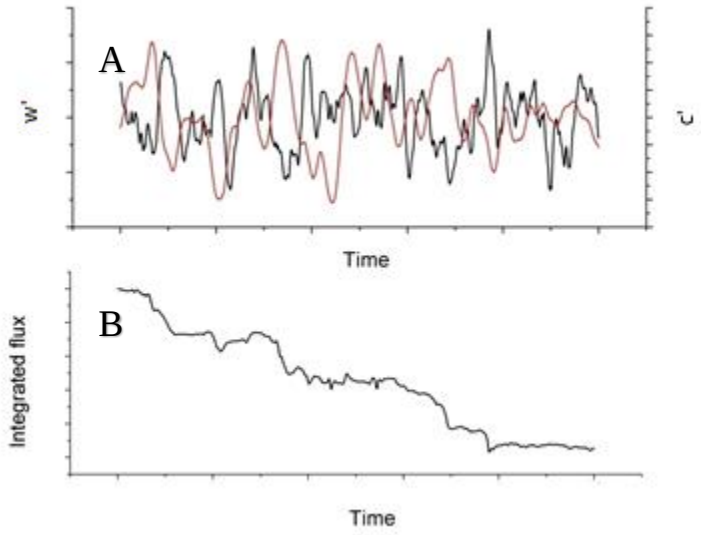

Figure 2.7: A) velocity fluctuations in black (ω') and fluctuating component of oxygen concentration in red (c') over time. B) Integrated flux over time. Example schematic modified from Berg et al. (2009).

2.4 Site description

Initial detail of the sites used in this thesis has already been described in Chapter 1, in Chapter 2 further detail is provided. Two field campaigns were conducted within the Western Channel Observatory (WCO), in semi-permeable sediment. The WCO lies within the South-West of the English Channel and is a reference site for marine biodiversity and oceanographic studies (Smyth et al., 2009). The WCO boasts two monitoring buoys (L4 and E1), several benthic sampling stations as well as atmospheric monitoring stations (Smyth et al., 2009). The first field campaign (2016) took place in Cawsands, over three-days, in a shallow seagrass bed (minimum depth 6 m) close to the shoreline. The second field campaign (2017) occurred over a five-month period at a site named L4 (minimum depth 50 m) (Smyth et al., 2009). The L4 station incorporates a monitoring buoy system and is located 20 miles from the Plymouth, UK shoreline (Refer to Section 1.11.1, Figure 1.6 for site map).

2.4.1 Cawsands

The first field campaign (Cawsands) utilized a microprofiler (MP4, Unisense A/S, see section 2.5.2 methods for details) and EC setup (A/S, Unisense, Denmark, see section 2.5.1 methods for details) which were deployed for 41-hours (from 20:30 on the 5th July to 12:00 on the 7th July 2016) to obtain high-resolution SWI profiles and total oxygen flux data within Cawsands

Bay, Plymouth, UK (N50^0 20.017, W 004^0 11.8523). The EC and microprofiler units were deployed from RV Explorer and placed approximately five meters apart on the seafloor (Figure 2.13). The microprofiler was not autonomous therefore a small vessel was deployed to house the battery and control panel which were connected via a cable, as indicated in Figure 2.13.

2.4.2 L4

The L4 buoy is a monitoring station, established in 2005 and located at 50º 15'N, 4º 13.2'W; 55m depth. This site has many influences including river inflows, topography, semi-diurnal tides and plankton blooms (Tait et al., 2015). L4 is also located within a busy shipping area where trawling is undertaken and is an active naval training area (Smyth et al., 2015). As part of the ongoing data collection at L4, Conductivity Temperature Depth profiler (CTD) data were collected weekly along with hourly surface data from an active automated buoy with a moon-pool at a depth of around 1.5 m (Smyth et al., 2009; Smyth et al., 2015).

This second field campaign was conducted from the 23rd May to the 4th September 2017 at L4. During the study, an EC lander and ADCP (RDI Sentinel V50, Teledyne RDI, USA) were deployed and a CTD profiler (SeaBird SBE 19+) cast was taken as part of the long-term time series at L4. All equipment was deployed within 100 m of each other. Due to unforeseen circumstances, ADCP measurements were only collected in May.

The EC and CTD instrumentation were deployed in the same location every month (May to September): 50'15.095N 004'13.016W and the details of the individual deployments are provided in Table 2.1.

Table 2.1: Dates of deployment and retrieval of equipment at L4.

Instrument	Deployment	Retrieval
EC/ADCP	23rd May 09:15	24th May 12:00
CTD	May: 2nd/ 8th /17th /22nd /31st	
EC	20th June 10:15	21st June 12:00
CTD	June: 12th/19th/26th	
EC	4th July 10:05	5th July 12:15
CTD	July: 3rd/17th/ 24th/31st	
EC	10th August 10:35	10th August 14:25
CTD	August: 7th/14th /21st/29th	
EC	4th September 08:45	5th September 17:15
CTD	September: 4th/15th / 18th /25th	

2.5 Equipment

2.5.1 EC system

The EC system used in both field campaigns were comprised of an ADV (Vector, Nortek, Norway), Clark-type oxygen microelectrode (Unisense A/S, Denmark) and an optode (Aanderaa, Denmark) (Figure 2.8 and Figure 2.9). The ADV and microelectrode sampled at 64 Hz, and the optode sampled at 0.1 Hz. The optode was used to calibrate and validate the microelectrode, and provide independent oxygen concentration data within the BBL. For this reason, it was placed at the same sampling height as the microelectrode, to reduce spatial variability between sensors. Selected equipment settings and setup are further outlined within this chapter.

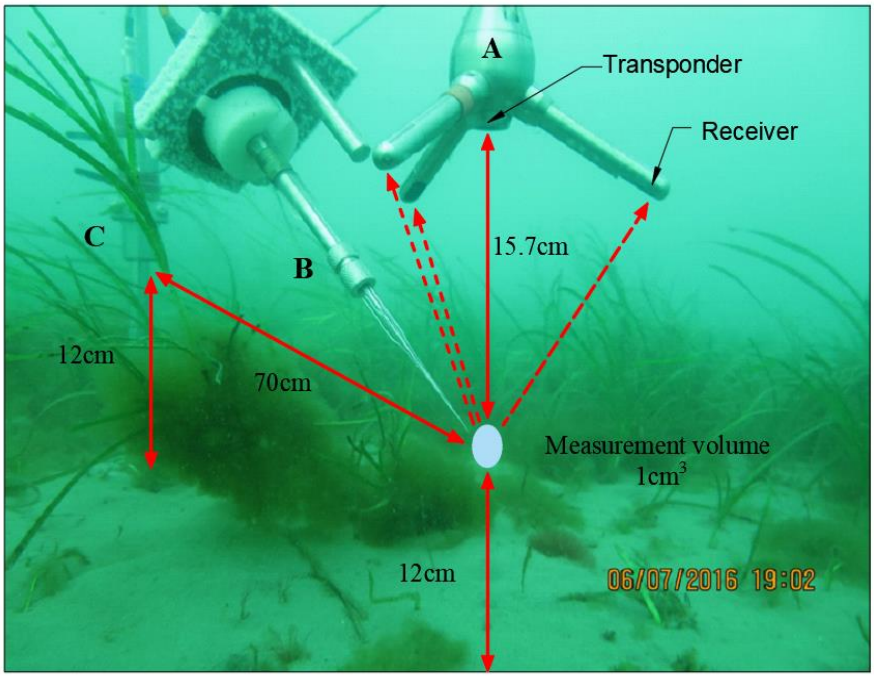

Figure 2.8: EC system comprised of A) ADV, B) an oxygen microelectrode and C) optode. The optode was positioned at the same height as the measurement volume. Position of the measurement volume was 12 cm above the sediment, 15.7 cm from ADV transponder and 70 cm horizontally from the optode.

Figure 2.9: Diver checking the location of the EC instrumentation in-situ at Cawsands. This was not possible at L4 due to the depth and harsh environment therefore, a camera set-up was utilised.

Acoustic Doppler Velocimeter

For the ADV to sample effectively, the settings must be optimised for the specific environment. Test deployments of the ADV were required to ensure the correct environmental settings (velocity range and backscatter level) were made before the delicate and costly microelectrode was added. The ADV would not capture an accurate velocity signal if an incorrect velocity range or backscatter level was selected. Due to the limited number of microelectrodes available within the scope of this study, a deployment with incorrect ADV settings may jeopardise a fragile microelectrode.

A sampling rate of 64 Hz was selected to enable the EC system to capture flux contributions at high frequency. The nominal velocity range of 1 m s^{-1} and the high-power level were selected. Although the high-power setting led to rapid draining of the battery, it was necessary as the levels of backscatter were minimal at both sites. A fixed orthogonal XYZ coordinate system was selected. This setting allowed for the measurement of turbulence levels and the orientation of the ADV.

Identifying the correct height of the ADV above the seabed is essential to avoid the sampling area entering a weak spot. A weak spot is an artefact of the acoustic transmission process where there is some reflection of the signal which creates regions with a decrease in signal quality. Weak spots are related to the spatial separation between pulse pairs which are transmitted by the ADV and occurs near any boundary where there is some reflection in the signal. This reflected signal interferes with the transmission creating poor signal quality. Therefore, distance of the weak spots from the seabed is dependent on the chosen nominal velocity range.

For the deployments conducted within this study, the nominal velocity range was 1 ms^{-1} creating weak spots at 8 cm and 20 cm ± 1 cm. The ADV sampling volume was therefore, set at 12 cm above the seafloor to allow for any sinking of the EC lander (Figure 2.10). Trial deployments in close collaboration with the manufacturer (Nortek) were conducted at various heights of the ADV sampling volume above the seabed and the results were analysed for noise.

Figure 2.10: Photo taken in situ demonstrating the height of the oxygen microelectrode above the seabed. A rule was used to measure the height ensuring no sinkage of the lander occurred which may have led to the ADV entering a weak spot.

Oxygen microelectrode and calibrations

Prepolarization was conducted to ensure no oxygen was present within the microsensor before sampling, as oxygen cannot be measured with a sensor which already contains oxygen. A cathode within the microelectrode removes the oxygen via prepolarization, a standard method outlined in the Unisense manual (Unisense, 2011).

In order to calibrate the microelectrode sensor, zero anoxic solution (sodium ascorbate) and 100% oxygen (aerated water) were used (Unisense, 2019). Once the microelectrode had been calibrated, the sensor was positioned 12 cm above the seabed at the same elevation as the ADV sampling volume. It was also ensured that the sensor tip did not enter the measurement volume, as this would interfere with the receiving of the pulses transmitted from the ADV. Prepolarization and calibration of the microelectrodes were conducted on the vessel prior to departure.

Removing the sensor guard on a moving vessel risks damaging the microelectrode; therefore, the sensor guard was removed from the microelectrode after calibration and prior to the vessel's departure from the harbour.

Stirring effect

Stirring effects must be assessed to ensure artificial flux is not added. The stirring effect is the increase in signal between stagnant and stirred conditions. The stirring sensitivity of the oxygen microelectrode causes a correlation between velocity and recorded oxygen signal. This produces artificial flux calculations which cannot be differentiated from the correlation caused by actual turbulent oxygen transport. Stirring sensitivity issues are evident when examining the correlation between velocity and oxygen microsensors (Holtappels et al., 2015). Therefore, test deployments in the laboratory and in situ were conducted to ensure an appropriate set up of the EC equipment. Various positions of the microelectrode relative to flow direction were trialled as well as ADV power and coordinate settings refer to Figure 2.11. Laboratory testing indicated flux was erratic and unpredictable when the sensor tip was perpendicular from the main flow. In collaboration with the manufacturer 45 degrees to the sampling volume was found be produce the least noise within oxygen data.

2.5.2 Microprofiler system

Data for this study were obtained with the microprofiler equipped with an oxygen microsensor (Clarke type) and a temperature microsensor (Clarke type). The oxygen microsensor (OX100-15785 Unisense A/S) (100-μm tip) featured a negligible stirring sensitivity and a fast response time (90% in <8ms).

The temperature microsensor (TP-100; Unisense A/S) was a thermo-coupled sensor with a tip diameter measurement resolution of `0.1 mV per C with a response time of 90% of <3 m s^{-1}. An oxygen optode was mounted on the EC system to allow for independent oxygen readings within the BBL and for calibration of the oxygen microsensor.

A single sediment-water profile duration was ~50 min. Profiles were measured continuously between the 5th to the 7th of July 2016. The procedure which was followed was developed by Bryant et al. (2010), using 10 mm increments from 10 cm to 1 cm above the SWI, 1 mm increments from 1 cm to 0.5 cm above the SWI, and 0.1 mm increments from 0.5 cm above to 0.5 cm below the SWI. Microsensors were used to create the smallest vertical resolution as well as to ensure robustness (Bryant et al., 2010). A pause was programmed between each measurement to ensure equilibrium was established (Bryant et al, 2010), with three data points collected at each depth within a profile. This study measured 41 oxygen profiles during the

Cawsands experiment. A small craft was deployed alongside the microprofiler lander to store the non-submersible battery and control panel which were connected by cable (Figures 2.13).

2.6 Frame and buoys at Cawsands and L4

Instruments were fixed on a tripod frame forming the EC lander which was deployed from a vessel (RV Plymouth Quest, Cawsand or RV PML Explorer, L4). The frame was braced to prevent any resonance from the surrounding environmental frequencies during deployment. To ensure that the frame rested on the seabed in an upright position after deployment, steel shoes of equal weight were fitted to the legs of the frame, as illustrated in Figure 2.11. The shoes had a large surface area to prevent any sinking of the frame. Additionally, large pins protruded from the shoes to ensure that the frame did not move as a result of large current velocities during spring tides.

As it was important for the tripod not to vibrate, it was equally vital for the arm of the electrode not to move, as this would affect and damage the microelectrode. However, a balance had to be made that the arm of the electrode did not interfere with flow effects measured by the ADV.

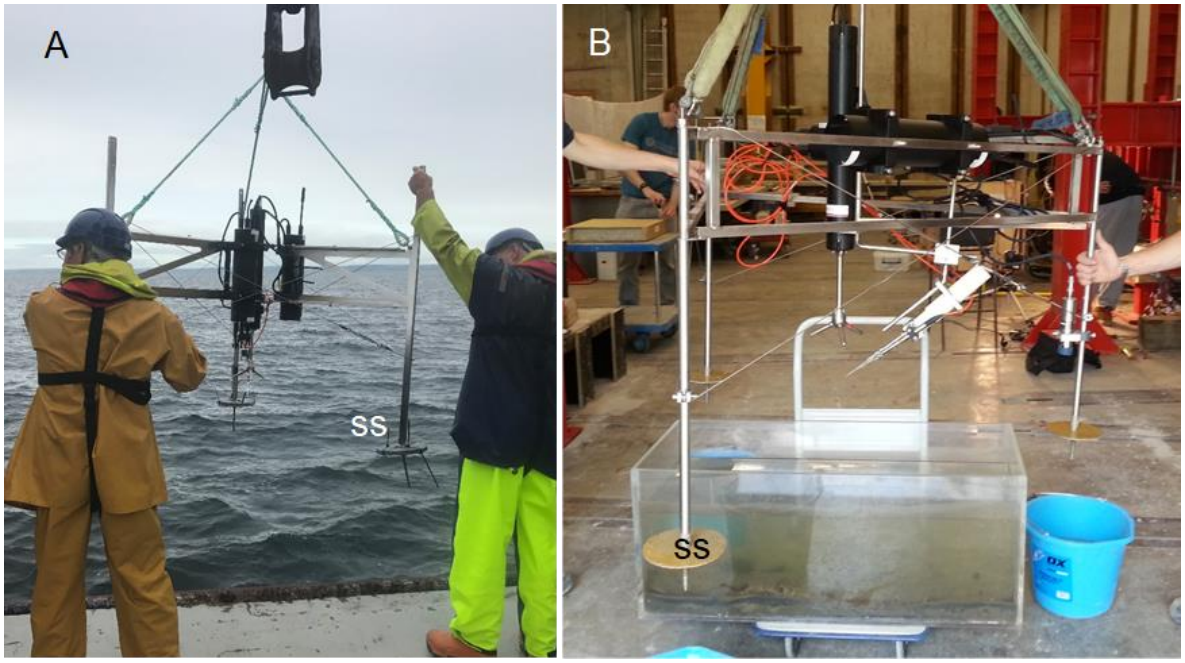

Figure 2.11: EC landers used for the A) L4 site (deeper) and B) Cawsands site (shallower). The steel shoes from both sites are indicated as ss.

The buoy system for the L4 site was designed to indicate the presence of equipment during day and night, as the study site is a hotspot for boating, fishing and trawling. As such, a Kevlar

core sinking line was used to minimise the chance of vessel propeller entanglement. Minimal interference to sensors due to the motion of the buoy system in response to waves, local wind and tides was required. This was achieved by systematic placement of pellet buoys along the line (Figure 2.12 and 2.13).

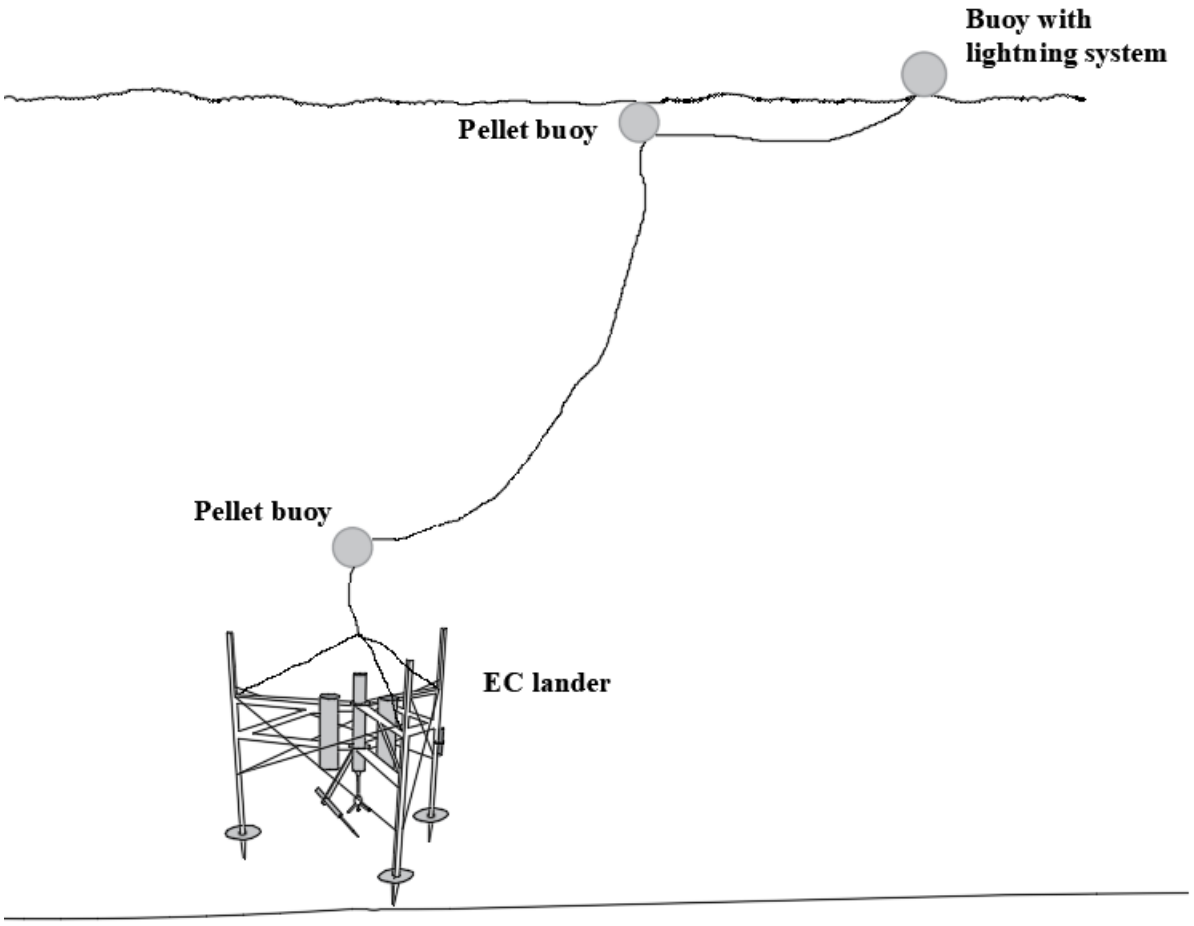

Figure 2.12: Mooring set up of EC lander during the L4 deployment in the summer of 2017.

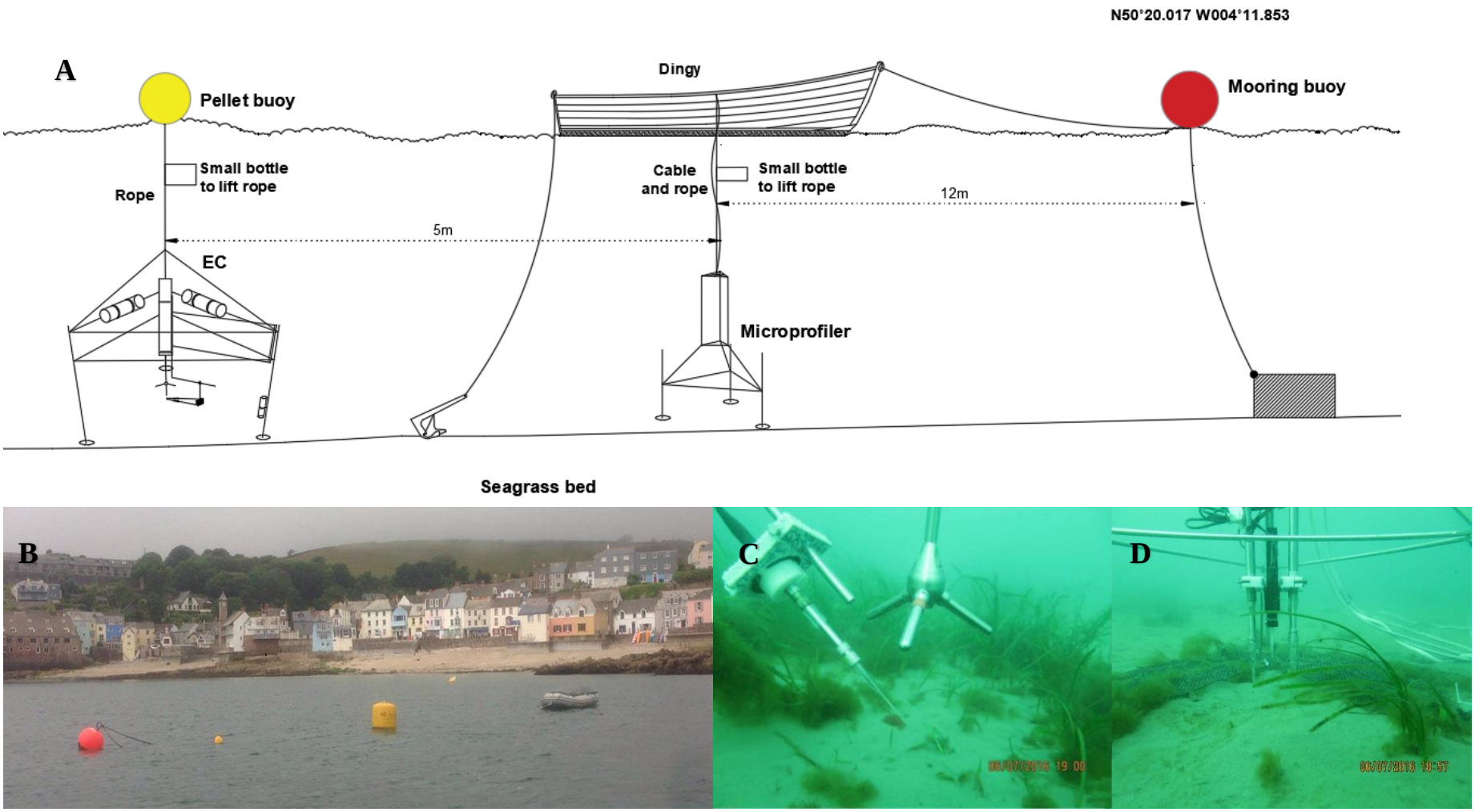

Figure 2.13: Layout of the deployment, A) a schematic of the setup of EC and microprofiler instruments, noting microprofiler is connected via a cable to the dingy which housed the controller and battery (not autonomous). The EC was autonomous (did not require a cable to the dingy). B) The mooring buoy connected to the dingy upon where the control box and battery of the microprofiler lay. C) EC, ADV and oxygen microelectrode surrounded by seagrass. D) Microprofiler oxygen and temperature sensors in situ surrounded by seagrass.

2.7 Deployment of EC lander

At both sites, to ensure the EC lander was deployed in an upright position on the seabed, the equipment was lifted approximately 1 m and lowered again after first reaching the seabed. This method was developed, as the first drop may be uncontrolled, and this method ensured greater control of the deployment of equipment.

2.7.1 L4

To conduct a successful field campaign at L4, careful deployment of the fragile EC lander was crucial. Prior to deployment, the vessel (RV Quest) scanned the seafloor with a fish finder to determine the existence of any obstacles, or features which would obstruct the lander, damage equipment, or lie within the EC footprint. For better control during deployment, the vessel was directed into the current direction.

2.7.2 Cawsands

At Cawsands, a smaller vessel (RV PML Explorer) was used due to the shallow nature of the environment. RV PML Explorer was not equipped with a crane therefore, the equipment was lowered manually and positioned by divers.

2.8 Supporting equipment set-up

A CTD profiler (Seabird SBE 19+), was equipped with a transmissometer, a Chelsea Photosynthetically Active Radiation (PAR) sensor, a fluorometer and an oxygen and temperature optode, as well as a 24-carousel rosette (Smyth, 2019). The CTD was deployed to obtain measurements of oxygen, chlorophyll, nutrients, and temperature throughout the water column. CTD casts were conducted weekly at full depths (~ 60 m) at L4 during the field campaign. An Acoustic Doppler Current Profiler (ADCP) was mounted on a trawl resistant bottom type mount to obtain water column current velocities. The ADCP measured at 1060 pings every 10 minutes with a bin size of 0.6m.

2.8.1 Nutrient sampling

Water samples collected weekly throughout the water column at L4 using a rosette sampler were processed by PML laboratory. Chlorophyll-a data were derived using acetone extracted values measured by a Turner fluorometer (Woodward, 2019). Nutrient samples were kept in cool and dark conditions and filtered using a 0.2 μm Millipore Fluoropore (Woodward, 2019). To determine nutrient levels, a 5-channel Bran and Luebbe segmented flow system was used, and quality control checks were carried out using KANSO certified reference materials, and the Quality Assurance of Information for Marine Environmental Monitoring in Europe programme protocol (this method was conducted by Glen Tarran/PML) (Woodward, 2019).

2.9 Data processing

This section will outline each of the post-processing steps, quantify the influence of different processing methods and suggest the optimal approach for the datasets presented in this thesis. In principle the EC method is straightforward; however, calculated flux values have been shown to be strongly impacted by the specific data processing approach used (Reimers et al., 2016; Reimers et al., 2012; Lorrai et al., 2010). Therefore, in this study a thorough assessment of the different approaches was undertaken considering the chosen study environment. Specific processing routines were developed rather than using a commercially available software package (SOHFEA) (McGinnis et al., 2011; McGinnis et al., 2014). SOHFEA has been used within some previous studies (Attard et al., 2014; Attard et al., 2015; Donis et al., 2015; Rodil et al., 2019).

2.9.1 Microprofiler data analysis

The sediment oxygen uptake rate and the DBL thickness were calculated using the water-side direct method (as described in section 2.3.1, Bryant et al., 2010) applied to oxygen profiles (Figure 2.3). As illustrated in Figure 2.2, the DBL is identified by the linear region, which lies between the inflection points at either end of the oxygen profile (Jørgensen and Revsbech, 1985). Diffusive oxygen uptake was calculated using Fick's first law of diffusion, Equation 2.1, (Rasmussen and Jørgensen 1992). Some microprofiler profiles were lost during the field campaign due to readjustment of the microsensor position above the SWI, which was required

every 12 hours. Additionally, unknown events occurred in the middle of the deployment which eliminated several hours of data.

2.9.2 ADCP tidal analysis

The pressure signal from the ADCP indicates the tidal variation at the site. As the flows in this region are predominantly driven by tides, the full water column velocity profile was depth averaged at each time step to obtain the barotropic (surface) tidal component. This was subtracted from the measured velocity profile (averaged into 5 m bins) to determine the baroclinic (internal) component. As the semidiurnal tide is the dominant tidal force, a harmonic fit with a period of 12.4 hours was fitted to the depth-average and the 5 m binned data. The amplitudes and phases of the harmonic fits were then used to determine the drivers of the eddy fluxes from the seabed (refer to Chapter 4 where this was conducted).

2.9.3 Dissipation rate of turbulent kinetic energy

The dissipation rate of turbulent kinetic energy (ε) is used to indirectly estimate turbulent mixing and fluxes and can be measured in situ through specific devices such as an ADV. To obtain ε a spectrum of velocity fluctuations is calculated from vertical velocity data. Kolmogorov -5/3 slope is subsequently fitted to the inertial subrange of the velocity spectra in log-log space (Bluteau et al., 2011). This identification of the inertial subrange can be challenging as the bounding wavenumbers change with flow condition.

2.9.4 Statistical analysis

Velocity, temperature, nutrient and oxygen flux data were assessed for normality using the Shapiro-Wilk test. All data used for statistically analysis were not normally distributed. Therefore, the Kruskal-Wallis test followed by Dunn's multiple comparison test were used for identifying any significant differences between months for each parameter. PAST statistical software package was used to conduct this analysis (Hammer et al., 2001).

2.9.5 Post-processing of EC data

Post-processing of EC data involves a series of primary processing steps: calibration, filtering, rotation, time-shift and detrending. The exact methods used for each of these steps can influence the final flux estimates. Reimers et al. (2016) has discussed some aspects of this process. This section will discuss each of these steps, quantify the influence of different post-processing methods and suggest the optimal approach for the datasets presented in this thesis.

Assessment of data and Windowing

To assess velocity and oxygen data further, levels of noise and spikes in each timeseries (as in Figure 2.14, large spikes in the data) were screened for unusable data. Unusable data would be subsequently discarded (Figure 2.14, red circles). Noise is common within EC datasets created from a variety of sources however, it was not possible to identify the exact sources within this study. The steps described below further filter out this noise and rendered the data useable for EC data processing.

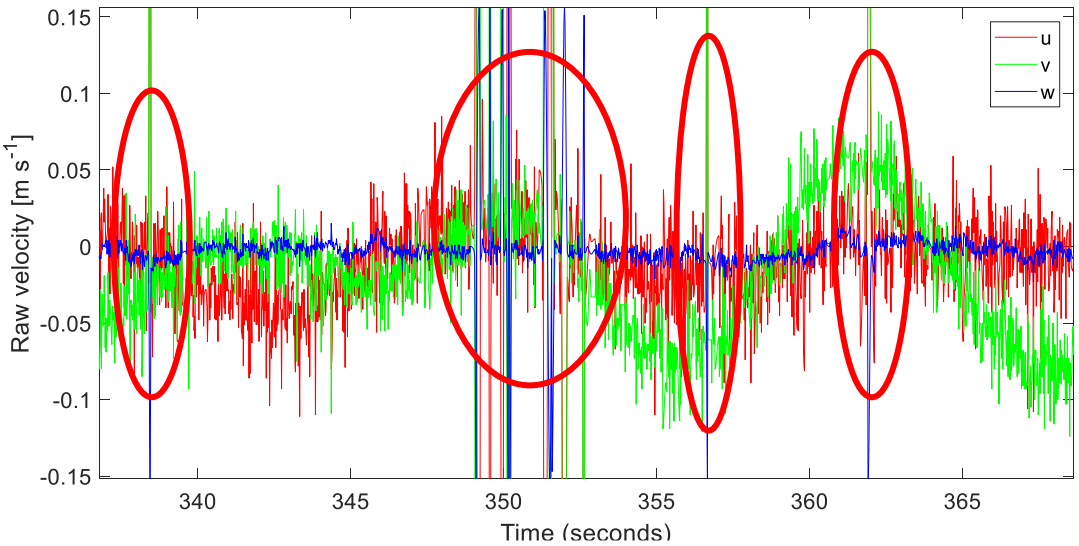

Figure 2.14: A segment of velocity data (u, v and w) prior to removal of unusable data (initial filtering). Levels of noise and spikes were screened for unusable data. Red circles indicate areas of unusable. The data in the red circles would be discarded.

The EC method assumes steady state conditions (Berg et al., 2003), which is a challenge for a coastal shelf sea environment where the tide is constantly varying. To approximate steady state conditions, the data were divided into windows of defined length, within which it was assumed that the tidal variation was negligible. This window size must also be large enough to include

all flux contributing eddy sizes (McGinnis et al., 2008) and small enough not to include changing flow conditions. A variety of window sizes were tested as outlined by McGinnis et al., (2008). Using spectral analysis to identify flux contributions at various frequencies (varying time scales), as further discussed below in section 2.9.4, 15 minutes was determined as the optimal window size for the data from both field campaigns.

Filtering

To remove noise from the ADV and oxygen signals, filtering of data must be conducted. The first step of the analysis removes outliers in both, the velocity and the oxygen data. Anomalies typically exist in the ADV raw data as large, short lived changes in velocity (Lorrai et al., 2010) (Figure 2.15A and B). In the oxygen data, the outliers are large deviations from the raw signal's baseline, which are typically presented as rapid drops in the signal (Figure 2.15 is an example of raw data where deviation from the baseline is seen prior to filtering). If this disturbance in the signal remained constant for a substantial period, this section of data would be removed. For example, the whole section of data would be removed if many rapid drops in signal occurred in a row or the drop-in signal was not rapid. These events can be due to environmental reasons, algae or debris which may have settled on the sensors, rendering this part of the signal unusable. After cleaning of outliers from the data, velocity data which does not exhibit a coherence of more than 70 % is removed.

After data elimination is complete, the velocities are smoothed to remove anomalous peaks by using a filter. The phase space filter, developed by Nikora and Goring (2002), is based on frequency space methods. These processes remove parts of the signal, transforming the signal from the time domain to frequency domain (Neves et al., 2006). This directly acts on the signal values, reducing noise presence. The cubic spline filtering method embodies a curve fitting technique, this method uses curvature minimization to reduce noisy data. A comparison between filtering techniques (cubic spline and space phase filter) demonstrated that flux values were insensitive to the filtering method, and so any of the tested approaches were considered appropriate. The phase space filter was the chosen method in this thesis as it excludes more spikes and noise than the cubic spline.

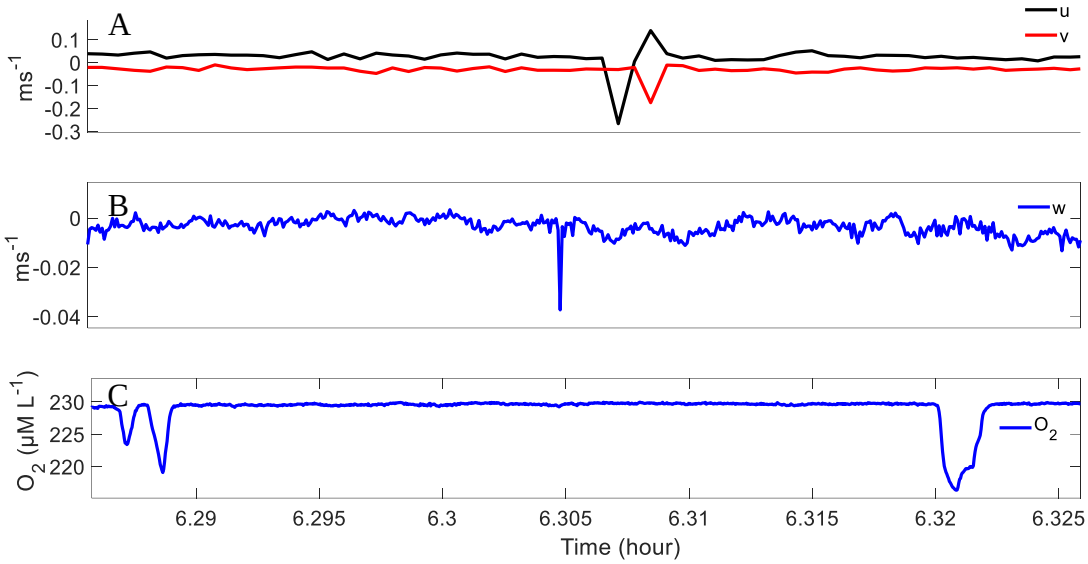

Figure 2.15: Examples of spikes within the raw data (prior to the raw data being processed by the phase space filter) of A) u, v velocity data, B) w velocity data, and C) oxygen data.

Downsampling

The post-processed oxygen microelectrode and ADV were sampled at 64 Hz, therefore measurements made over several days amounted to several gigabytes of data. For ease of management of these large datasets, data were downsampled to 8 Hz by averaging over 8 data points. This downsampling also leads to additional smoothing of the data. The reduced sample frequency of 8 Hz was defined as the point where there is no change in the calculated fluxes, beyond this point a change in calculated flux would occur.

Calibration of microelectrode

Post-deployment calibration of the microelectrode oxygen data is required to correct for any drift or instabilities. The optode is used for post-deployment calibration and quality checking of the microelectrode data, as the optode is more stable and exbibits no drift. This method is currently the most widely used post-deployment calibration method in this field. To examine whether microelectrode data are valid, the optode and microelectrode data should show similar trends and values (Figure 2.16). If the microelectrode does not follow the correct mean trend, as displayed by the optode, it is unlikely that the microelectrode will accurately capture smaller fluctuations. The absolute concentration is not required to measure flux as it is removed from data in the detrending process. However, confidence in the flux measurement increases when a microelectrode signal follows the overall oxygen trend well, as turbulent fluctuations are correctly recorded. This is based on the assumption, that if a microelectrode can detect large

changes in oxygen levels it will record smaller fluctuations and vice versa, if these larger changes in oxygen are not detected/recorded smaller fluctuations will also not be recorded.

A post calibration of the microelectrode is required to provide accurate oxygen readings. A calibration curve is a function of the milli-volt output of the microelectrode taken during the pre-deployment calibration of 0% and 100% solutions, against the oxygen concentration of the optode. The equation of this calibration curve is used to calibrate the microelectrode data.

The drift in the microelectrode data was corrected by applying a polynomial detrending procedure (see Figure 2.16a). The degree of the polynomial to fit the data presented in this thesis was one. Figure 2.16 panel B displays the corrected electrode data, showing the electrode follows the optode trend well.

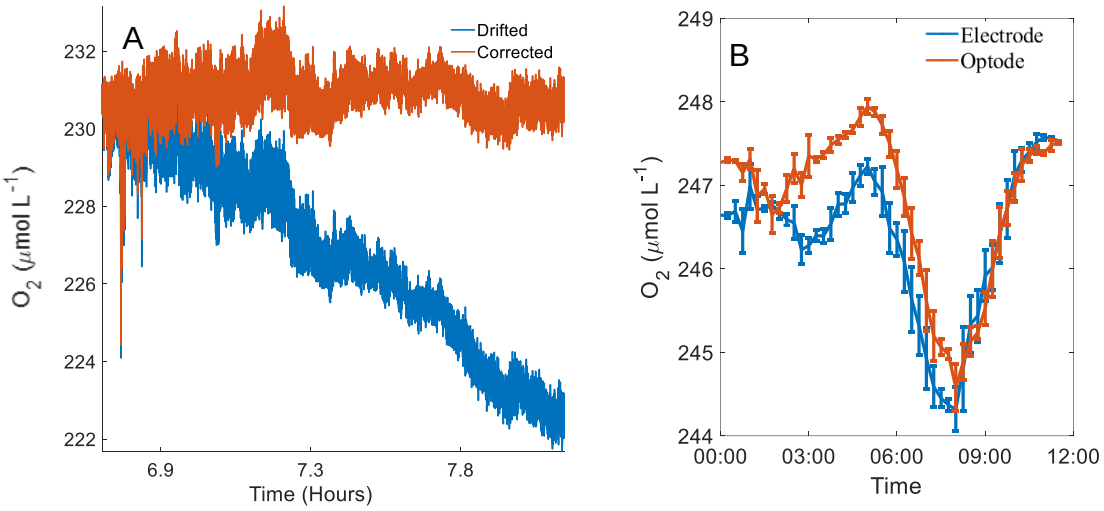

Figure 2.16: A) Drift from microelectrode data corrected using a polynomial fit. B) Final result of the fitted trend between the oxygen microelectrode and optode post calibration. This is a good fitting trend as the electrode follows the general peaks and troughs of the optode. O_2 refers to oxygen.

ADV alignment

Assessing any issues with the ADV is essential to create confidence within any flux calculations. When placed close to the SWI, the mean vertical velocity measured by the ADV should be zero, however, this is not always the case (Figure 2.17). Two reasons could cause the negative mean vertical velocity depicted in Figure 2.17; 1. The ADV could be out of alignment, which could also be creating the spikes in the data or, 2. The flow may be influenced by the frame. In order to identify the cause of the negative mean vertical velocity, trial deployments were required with changes to the frame and configuration of the ADV by the manufacture Nortek.

Further to frame changes, interference from the frame was ruled out by applying the method of McGinnis et al. (2014). Interference from the frame was further not detected within any deployment in the 2016 and 2017 field campaigns.

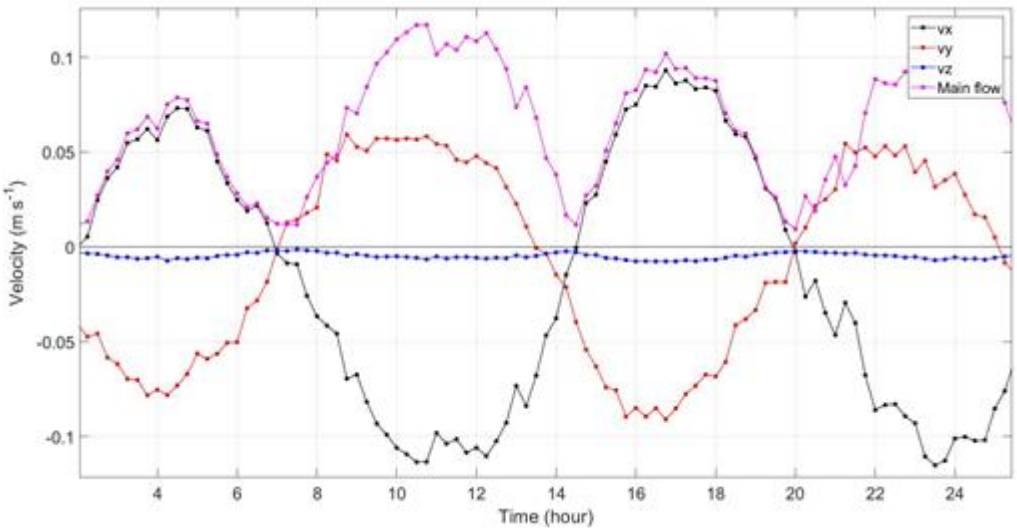

Figure 2.17 15 min averages of XYZ velocities and main flow velocities.

Rotation

For ease of data processing, it is common to align the ADV with the dominant flow direction such that $\bar{v} = \bar{w} = 0\ ms^{-1}$ and $\bar{u} \neq 0\ ms^{-1}$. As the orientation of the EC lander is not known after deployment, a rotation is generally applied to ADV data to adjust for pitch and roll of the instrument with respect to the flow (Finnigan et al., 2003). It is assumed that during a measurement duration of 15 minutes, the mean vertical and crossflow velocities are zero ($\bar{v} = \bar{w} = 0\ ms^{-1}$). If this assumption is not fulfilled, a rotation is applied to the measured velocity field such that only $\bar{u}$ is non-zero (Reimers et al., 2012). If the flow direction is consistent, it is possible to apply a single rotation matrix to the ADV data collected during a deployment. However, more commonly the mean horizontal flow direction varies, and it is necessary to apply a separate rotation to each sampling window. A variety of rotation techniques were trialled on this dataset discussed in this thesis however, $\bar{w}$ was consistently no bigger than -0.01 ms^{-1} and as such no rotation was applied to avoid introducing artefacts of u and v into the vertical velocity signal (Figure 2.17).

Detrending

Linear detrending applies a linear regression to a dataset and then subtracts this from the original data to remove any underlying linear trend. A linear detrend of ADV and oxygen data was conducted within each 15-minute time window to obtain the fluctuating components, as required by Equation 2.2. Alternative detrending methods such as frequency filters and running means have been used by studies such as Attard et al. (2014) and Attard et al. (2015). However, the studies presented in this thesis found a running mean/frequency filter to be unsuitable for the environments in which the EC was deployed. Detrending methods are further discussed in Section 2.10.

Spectral analysis

Spectral analysis determines how the variance distributes over frequency. The Fast Fourier Transform (FFT) method was used within this example dataset (Figure 2.18). Within this study spectral analysis was used to determine fluctuations of velocity and oxygen at different time scales (breaking the fluctuations into different periods).

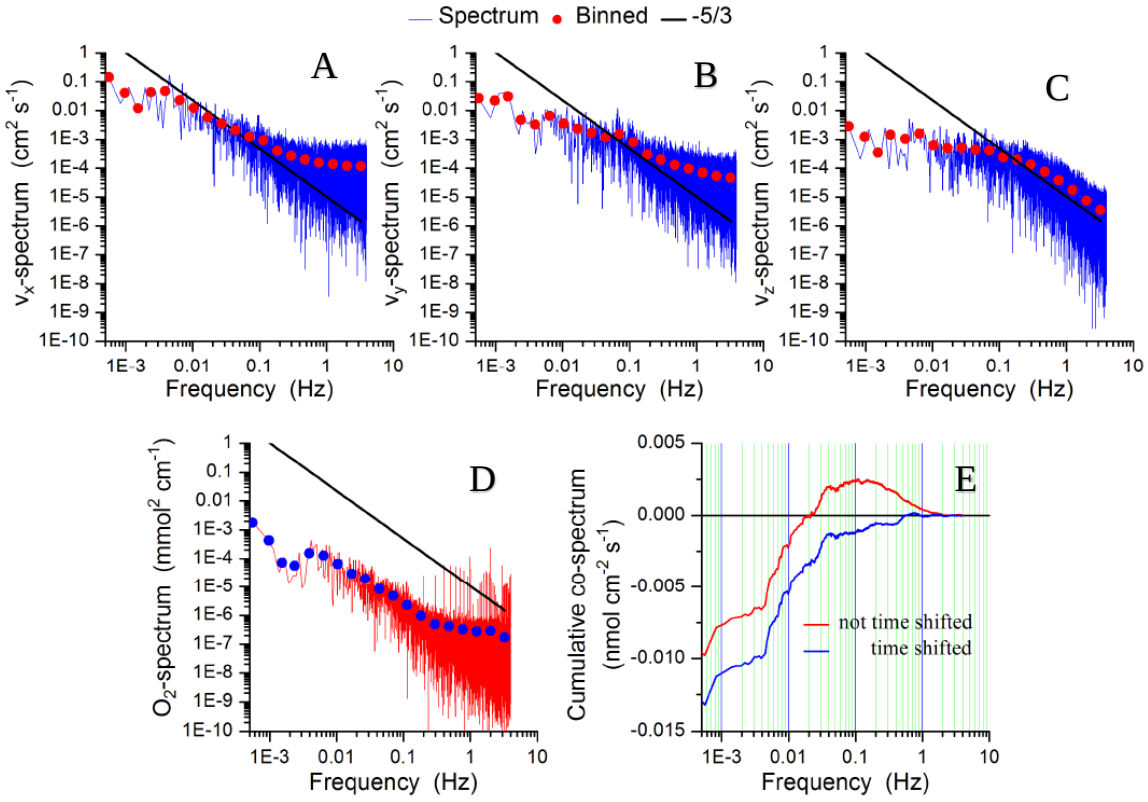

Figure 2.18 A-D) Spectral plots which include XYZ velocities, as well as the oxygen spectrum. Red and blue dots are binned data, the black line indicate the line of -5/3 and the blue and red lines indicates the spectral data. E) Cumulative co-spectrum of w' and c' of a 15-minute segment of data which had a timeshift correction (blue line) and no timeshift correction (red line).

Time synchronisation of ADV and microelectrode

The spatial separation between the measuring tip of the microelectrode and the ADV measurement volume, as well as differing instrument response times leads to a time-offset between the oxygen and velocity timeseries (Berg et al., 2015). This must be corrected by applying a timeshift to one of the datasets (Figure 2.19).

The cumulative co-spectrum provides the integral of an energy spectrum, which starts with the transformation from a time series to spectral space using FFT. The cumulative co-spectrum is the sum of the spectrum across all frequencies. The cumulative co-spectrum of w' and c' indicates the flux starting to accumulate from the right-hand side (Figure 2.18E). If a time offset exists, the flux is bidirectional (accumulate both positive and negative fluxes, red line, Figure 2.18E), which has no physical meaning therefore, the flux should be unidirectional within the same spectrum (blue line, Figure 2.18E). This indicates that this data requires a timeshift between the oxygen and velocity data.

The timeshift is applied to the all timeseries 15-minute windows and not at each frequency however, to provide a simplified illustration of this timeshift Figure 2.19 displays the need for a timeshift for oxygen and velocity within one frequency domain.

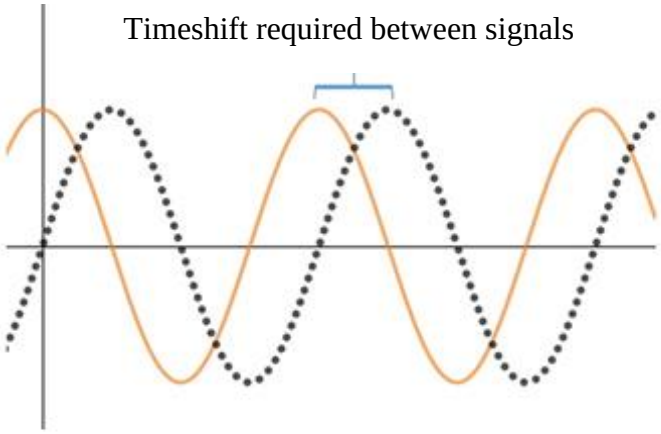

Figure 2.19: Oxygen and velocity signals at one indicating a need for a signal timeshift.

The timeshift required for each 15-minute window was assessed by applying a series of timeshifts in the range from -4 s to 4 s in steps of 0.075s to the oxygen data and calculating the resulting flux value. The optimal timeshift value was chosen as that which produced the highest flux value.

Once optimal timeshifts had been calculated for each window, they were further quality controlled. The timeshift magnitude depends on flow velocity and increases as flow velocity reduces. The calculated optimal timeshifts are shown in Figure 2.24. A large optimal timeshift change (greater than 2 seconds) from one time window to the next, or an abrupt change from positive to negative (or vice versa) is considered non-physical or indicates no correlation between oxygen and velocity data, therefore, that window was eliminated (Figure 2.20, red bars are eliminated sections).

This particular timeshift method (optimal timeshift) was chosen due to tidal conditions at the selected study sites. It allows for the varying flow directions which occur at L4 and Cawsands. However, another timeshift method (average timeshift) was trialled within the analysis of the datasets presented in this thesis. Both methods are further discussed within Section 2.10.

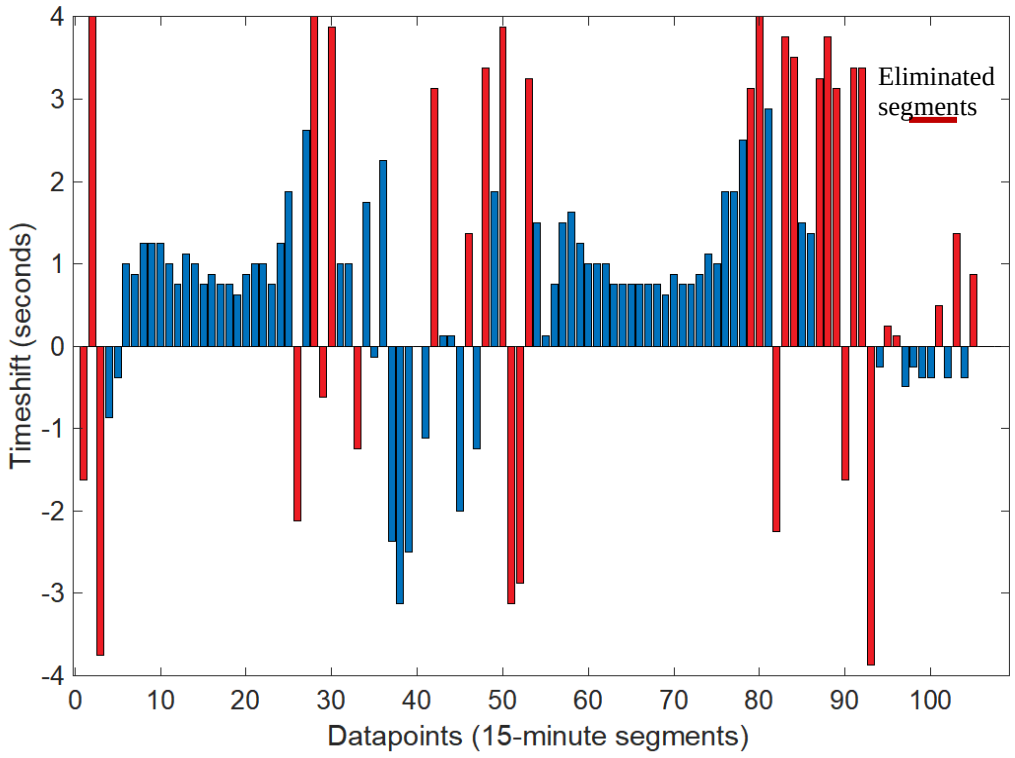

Figure 2.20: Cumulative co-spectrum of w' and c' of a 15-minute segment of data which had a timeshift correction (blue line) and no timeshift correction (red line).

Quality control of flux data

Once flux values had been calculated for each 15-minute time window, further quality control was undertaken by assessing each window individually. Criteria were used to determine whether a window was eliminated or not. These criteria consisted of removing a window if any spikes or distortions remained within the oxygen or velocity data, and the assessment of cumulative co-spectrum (*w'* and *c'*) shape for distortions. Spectra in the z direction (vertical spectra) were quality controlled to check for evidence of energy at the incident surface wave or gravity wave frequencies, however, this was not observed.

Footprint

For flux analysis it is useful to quantify the size of the footprint in order to establish the area in which the EC technique measures oxygen flux for ecological interpretation of the survey area. This footprint is the sediment surface area upstream that contributes to the flux determined by the EC technique, otherwise known as the source-weight function (Prajapati et al., 2018).

The EC system measures oxygen flux over an elliptical footprint which extends from the EC system upstream. The orientation of the major axes of the elliptical footprint is always in the primary flow direction (Figure 2.21 and 2.22). The size of this footprint is dependent on sediment surface roughness (z_0), friction velocity and the height of the measurement volume over the sediment (Berg et al., 2007). The study from Berg et al. (2007) based on detailed modelling, assumed uniform conditions and steady flow whilst calculating the size of the EC footprint. The EC footprint does not alter size or direction with the current velocity magnitude, however, is dependent on current flow direction.

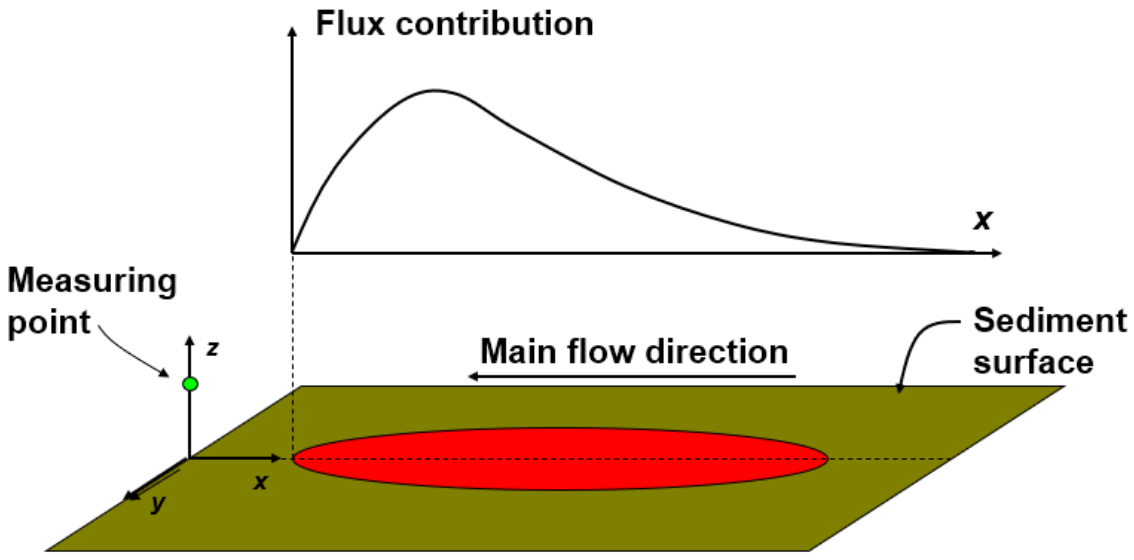

Figure 2.21: Schematic amended from Berg et al. (2007) of the sediment surface, direction of current, and measuring point. Area on sediment surface that gives flux is located upstream from measuring point.

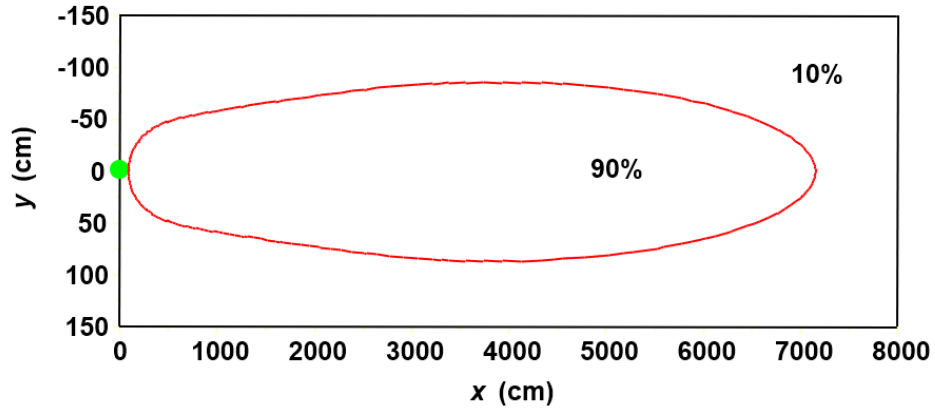

Figure 2.22: Modelling results from Berg et al. (2007) depicts 90% of the bottom flux occurs within the elliptical shape, with 10% outside this area. The figure is an example of a modelled footprint. Berg et al. (2007) presents a footprint of 70 m long and 1.5 m wide with a relatively smooth surface of sediment surface roughness (z_0) = 0.1 cm and measuring height of the ADV from the seabed h = 30 cm. The green dot marks the measuring point. The study explains that the multi-variable non-linear regressions demonstrate that only two variables matter for the size of footprint: measuring height and z_0. Therefore, the footprint becomes smaller when measuring height is reduced.

2.10 Optimisation of data processing methodology for a shelf sea environment

The processing methods described above were specifically selected to accommodate for the study sites. This was essential as previous studies (Lorrai et al., 2010; Reimers et al., 2012) have shown that the selection of the correct processing approaches for detrending and time synchronisation is vital for creating an accurate representation of oxygen flux within the chosen environment. Lorrai et al. (2010) stated that a variety of filtering methods could be used for different study conditions without affecting flux values. However, the method chosen for detrending the oxygen concentration data should be carefully chosen as it can lead to dramatic underestimation of oxygen flux (Lorrai et al., 2010; Reimers et al., 2012).

When using the EC method in a tidal environment where changing flow conditions occur (causing frequency contributions to change), it is important to choose the appropriate detrending option. A common filtering approach is to use a running mean or low pass filter, however Volaric et al (2018) noted that using a running mean or frequency filters with a fixed averaging window/cut off frequency is inappropriate (Volaric et al., 2018). For example, as the flow velocity increases during a deployment, the running mean averaging window (frequency filter cut off) must be made smaller (larger), and vice versa. Studies have shown that when using a running average, variations in the data are filtered out erroneously (Lorrai et al., 2010; Reimers et al., 2012). When using a running mean or frequency filter, larger eddies are filtered

out and the flux is underestimated if a selected window size is too short/ cutoff frequency is too large (Figure 2.23). It has also been noted in previous studies that the frequency filter detrending method has advantages over a running mean as it does not have bias with computational edge effects at the start and end of each 15-minute averaging window (Reimers et al., 2012).

In this study, a variety of running mean and frequency filters as well as a linear detrending method were assessed to determine the influence on the calculated oxygen flux (Figure 2.23 shows results from best performing running mean and frequency filter approaches compared to the linear detrend). Similar results were found between a three-minute running mean and a 0.002 Hz frequency filter. However, the linear detrending method was chosen as the most suitable tool to process datasets as all flux contributions would be incorporated and not removed by a selected window size or cut-off frequency. The higher fluxes obtained using the linear detrend in the current study are consistent with systems where lower frequencies contribute to flux, as a single eddy can be as large as the height of the density boundary (Reimers et al., 2012; Reimers et al., 2016). The study site L4 has a depth of 50 m and a thermocline of ~20 m therefore, relatively large eddies (large frequencies) would contribute to benthic flux. Cawsands also has an average depth of 10 m meaning that eddy contributions of this size are not unreasonable.

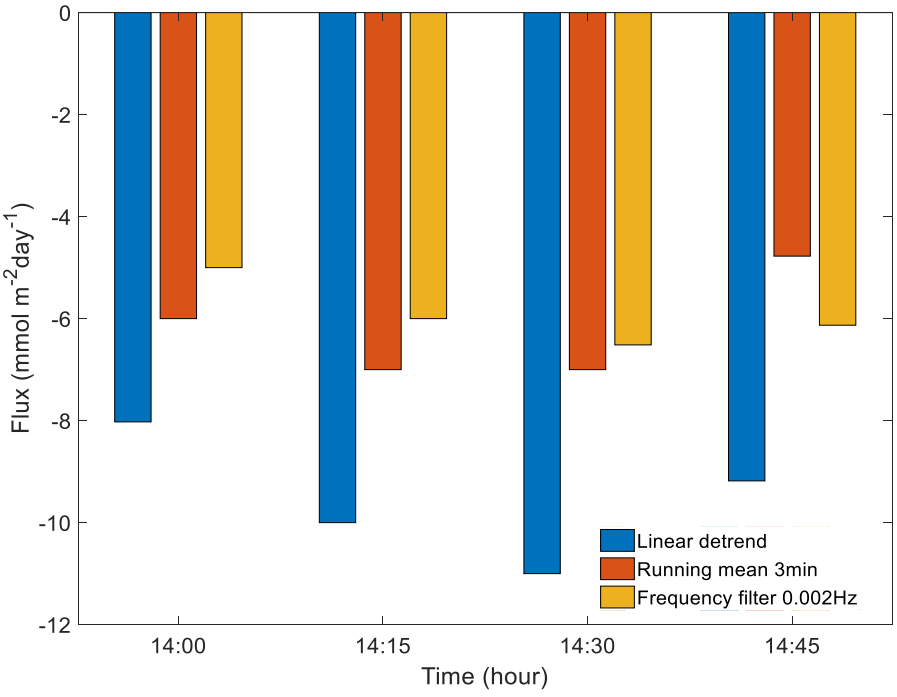

Figure 2.23: One hour of flux detrended using three different methods, linear, running mean (3 minute) and frequency filter (0.002 Hz).

Similar to the detrending method options, the choice of timeshift method can underestimate the flux. As previously discussed, a timeshift is used to correct for delays between the microelectrode and ADV caused by spatial separation and differences in response time. A further step in the timeshift method can be taken. This involves taking an average of the calculated timeshifts from the entire timeseries. This averaged timeshift is then applied to the entire dataset as a fixed timeshift number (Figure 2.24) (Donis et al., 2015). However, this can only be conducted once the 'bad' segments are eliminated, as those 'bad' segments would skew the average result (Donis et al., 2015).

The validity of the chosen processing tool was assessed by comparing the optimal, averaged and no timeshift method in relation to the resulting flux value. When a timeshift was not applied, the lowest flux numbers were obtained (Figure 2.24). The optimal method allowed for slightly increased flux values compared to the application of a fixed timeshift value (Figure 2.24). Therefore, by not implementing an optimal timeshift or using a fixed timeshift the flux would be underestimated (Figure 2.24).

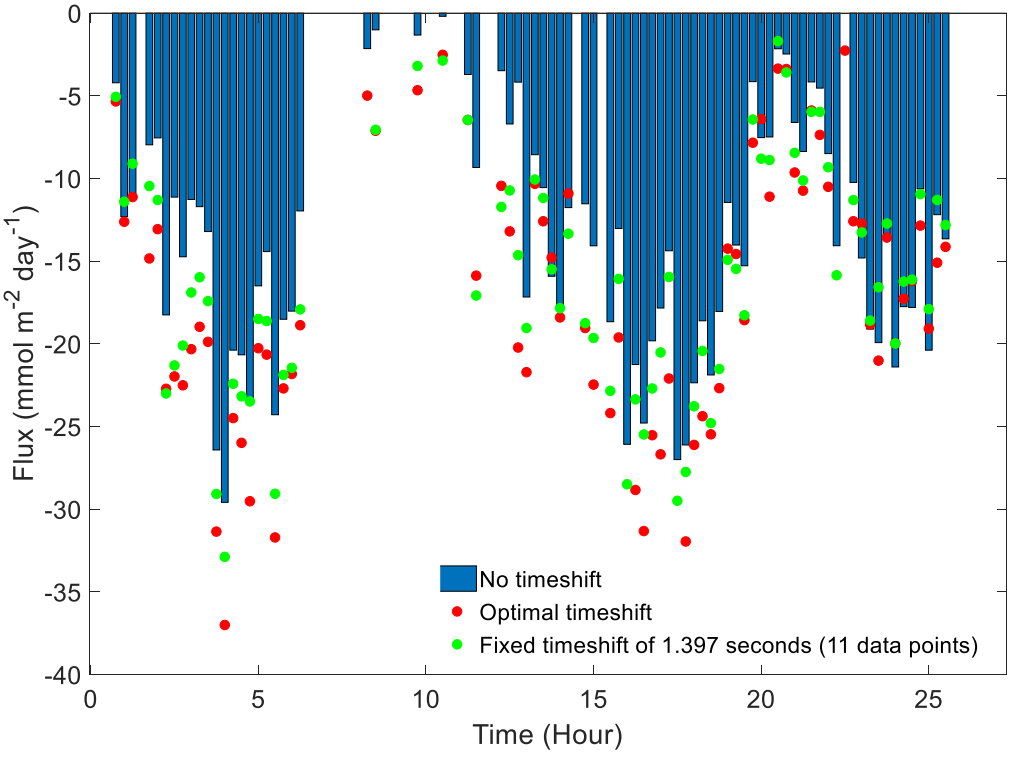

Figure 2.24: 25 hours of flux data calculated using no timeshift (blue bars), the optimal timeshift (red dots), and a fixed timeshift of 11 points (green dots). This EC dataset was obtained from the L4 site.

The similar results for both optimal and averaged timeshift methods provides confidence for either approach and consequently for the whole dataset. However, for data refining reasons, the optimal timeshift is preferred, as this method adjusts for changing tidal direction and magnitudes.

An analysis of processing approaches has confirmed that the choice has implications for the calculated flux values. Specific environmental conditions such as lower frequencies and changing tidal directions/magnitudes have led to the implementation of optimal timeshift and linear detrending processing tools. Based on the above considerations optimal timeshift and a linear detrend are the processing options selected for the EC datasets in this thesis.

The next Chapter (3) will utilise the EC technique outlined in Chapter 2 and the traditional technique microprofiler to assess benthic oxygen flux drivers within a seagrass bed. Results from Chapter 3 will also validate the EC methodology and processing tools which will be further used in Chapter 5.

Chapter 3

3. Cawsands study

The relatively new eddy covariance (EC) technique requires validation to increase confidence in the results obtained. This was achieved in the current study by comparing the EC data with microprofiler data. A seagrass bed is a dynamic site representing a complex oxygen environment. Seagrass beds are vital for carbon storage as well as providing an important ecological habitat. As such, assessment and monitoring of these habitats is of ever-increasing importance. Validation of the EC, within seagrass beds has been under-studied. Combining the EC which measures total turbulent flux, with a traditional technique (microprofiler) which measures diffusive point flux, allows for validation of the newer EC technique. A total of 44 hours of simultaneous EC and microprofiler data were collected at a shallow seagrass meadow (Cawsands, UK). By calculating the size and direction of the EC footprint, co-location of instrument flux readings was determined. However, flux results were the same regardless of co-location, concluding this factor was not important within this study. During night-time, oxygen uptake measured using the EC technique ranged from -4 to -46 mmol m^{-2} d^{-1}, while -8 to -33 mmol m^{-2} d^{-1} was derived from microprofiler oxygen profiles. Median EC and microprofiler oxygen flux levels were of the same magnitude during dark periods, giving confidence in the EC derived measurements. This study also provided the first insight into flux drivers at this site.

3.1 Chapter summary

Measurement techniques such as microprofiling which measures diffusive oxygen uptake (Jørgensen, and Revsbech, 1985) and benthic chambers/cores which measure oxygen uptake (Macreadie et al., 2006) are established methods used to quantify oxygen flux levels in aquatic environments. However, benthic chambers/cores can be controversial because turbulent mixing within the chambers is often controlled, thereby creating a false measurement of flux (Ribaudo et al., 2017). The eddy covariance (EC) technique which measures total turbulent

oxygen flux (Berg et al., 2003) has still not been widely used in energetic nearshore environments, hence the need for the validation of this technique. In this study we examine oxygen dynamics within a seagrass bed, by using both the microprofiler and EC methods. These methods allow short- and long-term physiological responses to be captured by sampling at high frequencies. The high temporal resolution of these methods enables the investigation of how varying environmental conditions affect benthic oxygen flux within seagrass beds (Long et al., 2015).

To date, only few studies have used a combination of oxygen flux measuring tools (Reimers et al., 2012; Berg et al., 2013; McGinnis et al 2014). Within this study the microprofiler flux readings were primarily used to validate EC oxygen flux readings. In addition to the EC validation, the results obtained give some limited insight into benthic oxygen flux drivers within this marine seagrass bed.

3.2 Site description and methods

Cawsands Bay is situated on the Rame Peninsula (Area of Outstanding Natural Beauty) and incorporates the twin villages of Cawsands and Kingsand which overlook Plymouth Sound. This site is vital for local tourism economy, fishing and ecology (seagrass meadow). The bay is an east-facing sand and shingle beach (Smyth et al., 2015). The study location at Cawsand Bay had a minimum depth of 3 m and a maximum depth of 15 m with a tidal range of 4.6 m. The study site represents a shallow seagrass habitat with permeable sandy sediment which is sheltered from south westerly prevailing winds. Site specific literature is described in Chapter 1 Section 1.11.1, with site specific deployment details in Chapter 2 Section 2.4.1. EC and microprofiler methods are described within Chapter 2.

3.3 Results

Due to the dynamic biogeochemical and hydrodynamic processes that occur within seagrass beds, quantifying the various oxygen flux drivers was not trivial. Therefore, a combination of various oxygen flux measurement tools was required to capture the drivers (photosynthesis, respiration, diffusion and bioirrigation) of the total oxygen flux. Permeable sandy sediment predominates at the Cawsands site; therefore, a negative flux direction (into the sediment) is expected when photosynthesis was not occurring (e.g. during dark periods) (Hume et al., 2011).

Several hours of EC data (~4 hours) were eliminated due to bubbles released from the seagrass which interfered with the glass microelectrode and affected oxygen readings. However, an adequate number of EC (15 minute) and microprofiler (~51 minute) oxygen flux measurement segments were acquired to sufficiently characterise oxygen flux readings for both light and dark periods during the campaign. These oxygen bubbles are released from the seagrass and settle on the tip on the oxygen sensor, this bubble realise is also a sign of oxygen production from the seagrass habitat.

3.3.1 Measurement Footprint

As detailed in Section 2.9, the orientation of the EC measurement footprint varies with flow direction. As a result, the EC and microprofiler where initially compared only when the microprofiler fell within the EC footprint (Figure 3.1). This ensures rigour when comparing oxygen flux measurements between instruments. The long, narrow elliptical footprint of the EC was 21.1 m long and 0.7 m wide (refer to Chapter 2 Section 2.9 for footprint calculation). This footprint was calculated using a friction velocity of 0.0058 ms^{-1} and surface roughness of 0.0059 m based on Berg et al., 2007.

The EC method measures total flux from all drivers, yet the contribution to flux from each driver cannot easily be quantified (Berg et al., 2013). However, the simultaneous use of a co-located microprofiler enables insight into the contribution from the diffusive oxygen flux. During the first and second dark period (Table 3.1) of when the microprofiler was within the EC footprint, non-photoperiod occurs (Figure 3.1, 00:00- 05:15 6th July and 00:35 -06:05, 7th July), EC median flux was JO_2 = -14 mmol m^{-2} d^{-1} and microprofile flux was JO_2 = -15 mmol m^{-2} d^{-1}. EC median flux was JO_2 = 15 mmol m^{-2} d^{-1} and microprofile diffusive flux was JO_2 = -19 mmol m^{-2} d^{-1} during the photoperiod when instruments were within the same flux footprint (Figure 3.1, 11:43- 21:23 6th July). Results compare well with oxygen flux data from literature. Berg et al., (2018) reports EC oxygen flux median values within a seagrass bed during photoperiods of 35 mmol m^{-2} d^{-1} and -15 mmol m^{-2} d^{-1} during non- photoperiods.

Figure 3.1 also provides oxygen flux data when the instruments were not co-located (within the same footprint). The results presented are similar, whether or not the instruments were within the same footprint. Therefore, it appears that oxygen fluxes are approximately spatially homogenous and the consideration of when EC and microprofiler were co-located for comparing EC flux results is not essential at this site.

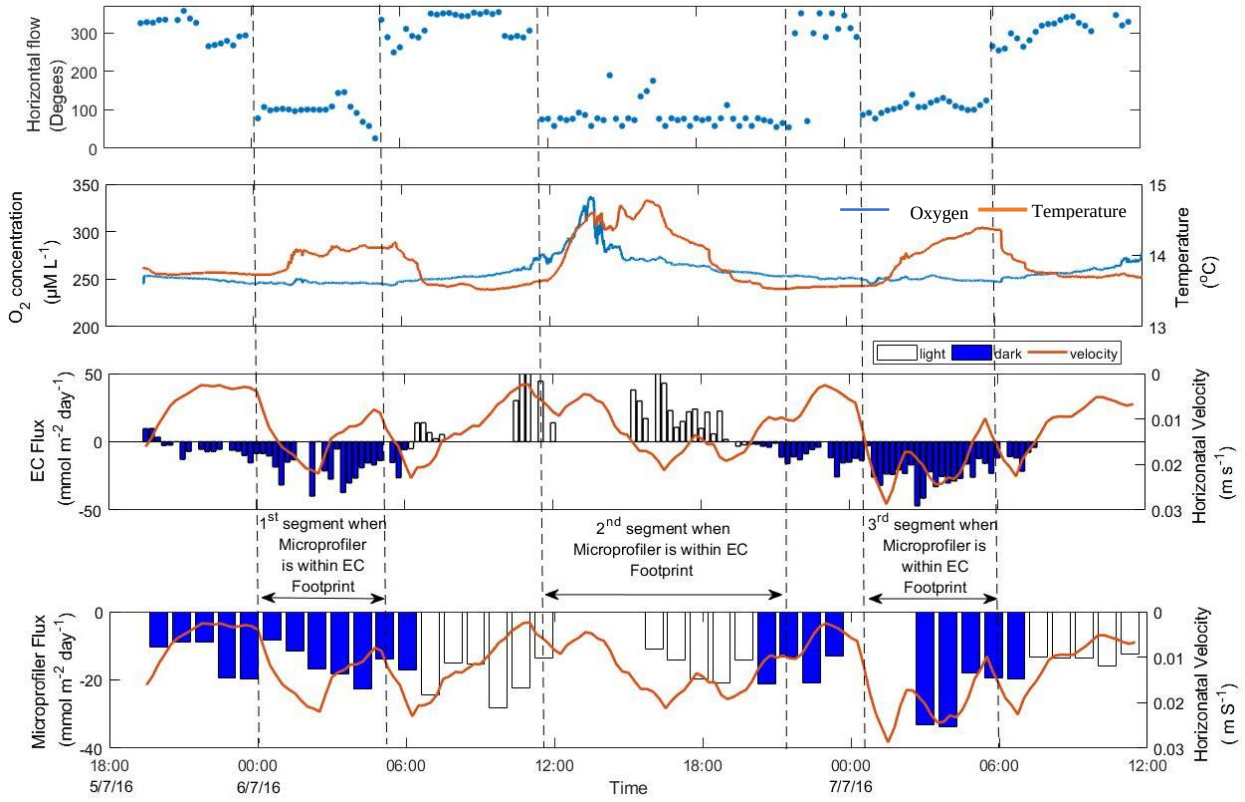

Figure 3.1: A) Direction 15 minute-averaged horizontal flow velocity. B) Oxygen and temperature levels obtained from optode data. C) 15-minute EC oxygen total turbulent flux data overlain with horizontal flow velocity $\sqrt{u^2\,v^2}$, day light (white bars) and dark periods (blue bars). D) 50-minute segments of microprofile oxygen diffusive flux data, daylight (white bars) and dark periods (blue bars) overlain with horizontal flow velocity $\sqrt{u^2\,v^2}$. Three periods of when the microprofiler is within the EC footprint.

Table 3.1: Times and dates of deployment, with reference times of light and dark periods. Refer to Figure 3.1 for EC and microprofiler data within these time periods. Throughout the text in this Chapter times and dates are referred to as correlating light/dark period.

	EC and Microprofiler
Full deployment period	19:34 on the 5th July to 12:00 on the 7th July 2016
Light period	06:15 to 18:33 on the 6th July
Dark period 1	19:34 5th July to 06:15 6th July
Dark period 2	18:33 6th July to 06:45 on the 7th July

3.3.2 Oxygen flux during photosynthetic periods

EC oxygen flux readings were strongly affected by the seagrass bed during daylight hours due to photosynthesis. The release of oxygen from photosynthesis created a median net flux from the sediment/seagrass system (14.9 mmol m^{-2} d^{-1} 06:15 to 18:33 on the 6th July) which was captured by the EC. The microprofiler only measure point diffusive flux, therefore the effect of photosynthesis on oxygen flux was not captured by the microprofiler (median oxygen flux -19.1 mmol m^{-2} d^{-1}, light period) (Table 3.1 and Figure 3.2).

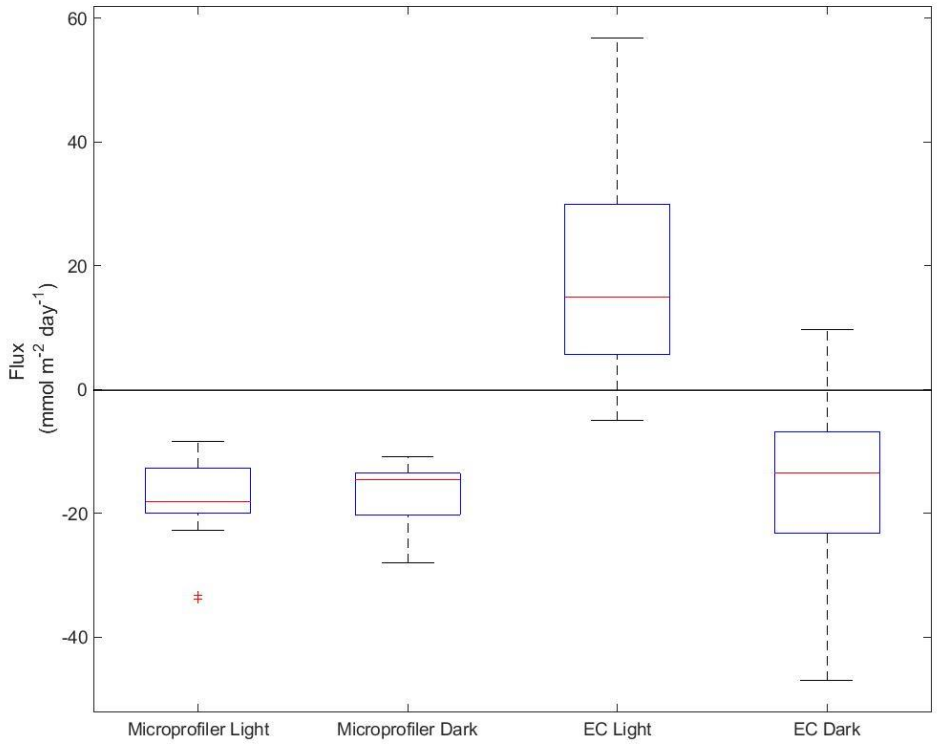

Figure 3.2: Boxplot of EC and microprofiler flux during light (06:15 to 18:33 on the 6th July) and dark (19:34 5th to 06:15 6th July and 18:33 6th to 06:45 on the 7th July) conditions at Cawsands UK. On each box, the central mark indicates the median, and the bottom and top edges of the box indicate the 25th and 75th percentiles, respectively. The whiskers extend to the most extreme data points not considered outliers, and the outliers are plotted individually using the '+' symbol.

Microprofiler oxygen flux measurements were similar during both light and dark periods, this indicates that diffusive flux is similar during photoperiods and non-photoperiods periods (Figure 3.2). EC total median flux was observed into the sediment similar to the diffusive flux during non-photosynthetic periods however, during photosynthetic periods flux is observed from the sediment/seagrass system.

3.3.3 Flux during non-photosynthetic periods

It was expected that the total and diffusive flux would be closer in magnitude when the photosynthesis component was zero. This is observed in Figure 3.1 and 3.2 where EC and microprofiler fluxes were negative and had similar magnitudes during dark periods with no photosynthetic oxygen production (Table 3.1; dark period 1 and 2). The overall median EC flux was JO_2 = -13.5 mmol m^{-2} d^{-1} and median microprofiler flux was JO_2 = -14.6 mmol m^{-2} d^{-1}. These similar median flux levels provide reassurance that both methods capture a consistent representation of flux. The large range of EC fluxes in the non-photic periods illustrates that the EC detected a wide range of drivers. Integrating the seagrass and the sediment fluxes, photosynthesis in the day and respiration of the seagrass at night will lead to differences (phototic and non photoic periods), which was not captured by the microprofiler. This is due is due to the capabilities of both techniques, as the EC measures flux 12 cm above the seabed, capturing total flux from the bottom boundary layer, whereas the microprofiler can only measure diffusive flux within the diffusive boundary layer. The measured oxygen flux values presented within this study also fell in line with other EC seagrass benthic oxygen flux studies (Murray et al 1987; Silva et al., 2009; Rheuban et al., 2014).

3.3.4 Statistical analysis

EC and microprofiler flux data in both light and dark (Figure 3.2) were analysed using PAST statistical software (Hammer et al., 2001). Microprofiler flux data in dark conditions were statistically similar to EC flux data during dark conditions ($H = 2.5$, $df = 2$, $P>0.05$) and microprofiler data in light conditions ($H = 1.93$, $df = 2$, $P>0.05$) and statistically different with EC flux data during light conditions ($H = 82.5$, $df = 2$, $P < 0.001$. EC flux data in light conditions were statistically different to EC flux data in dark conditions ($H = 83.5$, $df = 2$, $P < 0.001$), and microprofiler data in light conditions ($H = 83.5$, $df = 2$, $P < 0.001$). These statistical results demonstrate that EC flux data in dark conditions were comparable to microprofiler data in both dark and light conditions suggesting that diffusive flux was the primary driver detected by the EC when there was no photosynthesis. This was not the case for EC flux data during light conditions where a different driver e.g., photosynthesis was detected by the EC. Microprofiler and EC flux data are therefore only directly comparable when diffusive flux is

the main driver. These results also demonstrate that the microprofiler cannot detect certain flux drivers which are detected by the EC.

3.3.5 Temperature

The optode data showed temperature peaks at 01:45 to 06:42 and 12:00 to 18:42 on the 6th July and 01:24 to 07:22 on the 7th July (Figure 3.1). This may be due to the ebb tide transporting warmer water from shallow waters to the survey area whereas, on a flood tide colder waters are transported from colder, deeper open ocean waters.

3.3.6 Horizontal flow velocity

Figure 3.1 also shows a timeseries of horizontal flow velocity magnitude and direction. This gives further insight into oxygen flux drivers and trends captured by the microprofiler and EC techniques. One of the primary drivers of oxygen flux during dark periods in coastal sea environments are tidal flows (McGinnis et al., 2014). Within this study, EC oxygen flux was generally observed to increase with increasing flow velocity during dark periods 1 and 2 (Table 3.1, Figure 3.1). However, these trends were not clearly observed in the microprofiler oxygen flux data; this is attributed to the time taken for the microprofile profile (~50 minute).

3.3.7 EC Oxygen flux and velocity correlation

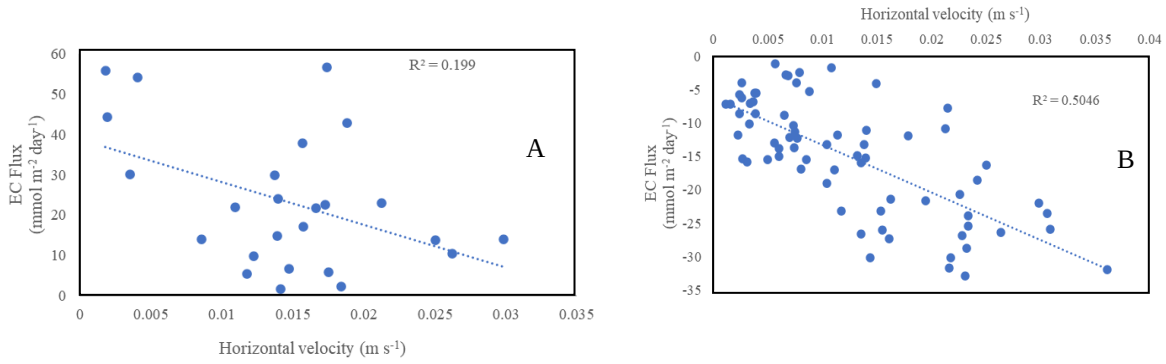

Figure 3.3: Correlations between EC flux and horizontal velocity during light and dark periods (Table 3.1; A) light period and B) dark periods 1 and 2.

Figure 3.3 demonstrates that EC flux correlates with horizontal velocities (R^2= 0.2 y = -1.5x + 8.8) during light conditions and a stronger correlation during dark conditions (R^2= 0.5, y = -

1.9x + 9.8). These statistical results suggest that velocity may be a more important driver of flux during dark periods whereas multiple other drivers (i.e., photosynthesis) dominate during light periods.

3.4 Results discussion

The seagrass habitat at Cawsands was used to validate the EC using the traditional microprofiler method as it represents a dynamic environment with varying tidal influences, primary production and anthropogenic influences e.g. pollution and boating activities. Initially, oxygen fluxes were investigated when the EC and microprofiler were co-located (microprofiler was within the EC footprint). However, further analysis suggested similar oxygen flux was observed when the footprint was not considered, suggesting oxygen flux was relatively homogenous over the seabed at this test site.

The median EC and microprofiler oxygen flux levels were statistically comparable during dark periods, providing confidence in the EC derived measurements. As both techniques detected similar fluxes it can be assumed that diffusive flux is the main driver of EC total oxygen flux during non-photic periods. During photic periods it was likely that photosynthesis was a significant driver of total oxygen flux. This was only detected within EC flux data as the microprofiler can only measure diffusive flux. The large range of EC fluxes in the non-photic periods illustrates the EC detected a wide range of drivers (integrating the seagrass and the sediment fluxes, photosynthesis in the day and respiration of the seagrass at night will lead to differences), which was not captured by microprofiler. This is due is due to the capabilities of both techniques, as the EC measures flux 12 cm above the seabed, capturing total flux from the bottom boundary layer, whereas the microprofiler can only measure diffusive flux with the diffusive boundary layer.

Data from the optode detected the transport of warmer water into the survey area during the ebb tide and colder water from the deeper open ocean on the flood tide. The warmer temperatures associated with the ebb tide could increase microbial activities leading to a corresponding increase in oxygen flux however, this can only be validated using benthic chambers/cores. Furthermore, EC flux data correlated with horizontal flow velocity during dark conditions. This correlation was weak during light conditions, which may be due to the additional drivers (photosynthesis and increased microbial activity). Photosynthesis changed

the direction of flux as more oxygen is available within the BBL due to biochemical reactions from seagrass (release of oxygen).

The results obtained provide the first insight into benthic oxygen flux drivers at this site. This study has also validated EC data processing and resultant flux estimates by comparing the EC with the traditional microprofiler technique during dark periods. Results have also shown that the EC technique can be used to obtain a more complete understanding of benthic oxygen flux within this environment by measuring total flux. Therefore, this method will be used in the upcoming Chapter, as the microprofiler only measures diffusive flux.

Chapter 4

4. L4 study

In continental shelf environments, the drivers dictating benthic oxygen fluxes are poorly documented. This study has investigated the drivers of benthic oxygen flux at a shelf sea site (L4) off the coast of Plymouth, UK. A preliminary hydrodynamic study was conducted which included a combination of 12 hours of benthic eddy covariance (EC) and acoustic Doppler current profiler (ADCP) measurements. The barotropic velocities were twice as high as the baroclinic velocities. EC oxygen fluxes were seen to vary depending on the direction of the tidal current. This was attributed to the varying sediment types in the north/south directions, as well as varying levels of turbulence depending on direction. This assessment will aid future modelling of fluxes at this site.

In addition, the drivers of benthic oxygen uptake over five months during spring and summer were assessed as part of a more comprehensive study using the EC technique at the same site (L4). This site is subject to biannual plankton blooms and dumping of dredged material. Along with the EC system, additional data from a long-term monitoring programme captured chlorophyll, temperature, oxygen, nutrients and sediment composition. Median benthic oxygen uptake differed by 10 mmol m^{-2} d^{-1} over the five-month period. Benthic oxygen flux followed flow velocity trends during the preliminary study using data from May 2017 however, a weak correlation over the five monthly deployments between medium velocity and median flux was observed. Furthermore, it was observed that chlorophyll input into the sediment from the plankton in this area was likely to be extremely low. This study concluded more data such as nutrient composition within the sediment would be required to establish a fuller understanding of drivers at this site.

4.1 Introduction

The open shelves of the ocean are highly dynamic environments, creating challenges for continuous oxygen flux measurements. The aquatic eddy correlation (EC) technique (Berg et al., 2003; Reimers et al., 2016) is relatively new method in measuring oxygen fluxes between the overlying water and benthic sediments. However, minimal work has been conducted in exposed areas such as coastal shelf sea environments (McGinnis et al., 2014).

Historically, the coastal shelf sea waters off the coast of Plymouth, UK have been critical to both the regional and national economy (Seas, 2002.). This coastal area of water has been used for fishing, military, scientific (Western Channel Observatory (WCO)) and tourism industries. The surrounding area has thrived ecologically, as rare corals have been observed; it is also subject to distinct topographical features (e.g. steep shelves creating changes in flow velocities/ internal tides) (Smyth et al., 2009).

The EC method has many advantages over traditional in situ chamber and microprofiler techniques, such as minimal disturbance of natural hydrodynamics, ambient light, and sediment (Berg and Huettel, 2008; Lorrai et al., 2010; Reimers et al., 2012). The EC system is non-invasive, and collects data at high frequency (64 Hz, typically at 10 cm to 30 cm above the sediment). However, disadvantages, such as the cost combined with the fragile nature of the instrument, as well as complicated data analysis (i.e., various assumptions required for data filtering) deters many users from deploying the instrument in challenging and complex environments (Lorrai et al., 2010; Reimers et al., 2012).

To date, EC deployments have been undertaken in a variety of substrate types, including marine and freshwater muddy sediments (Berg et al., 2003; Brand et al., 2008; McGinnis et al., 2008), permeable sands (Berg and Huettel, 2008; Reimers et al., 2012; Berg et al., 2013), deep ocean sediments (Berg et al., 2009), rock surfaces (Glud et al., 2010), oyster beds (Reidenbach et al., 2013), coral reefs (Long et al., 2013; Cathalot et al., 2015; Rovelli et al., 2015), seagrass meadows (Hume et al., 2011; Rheuban et al., 2014; Long et al., 2015; Long et al., 2015a), vertical cliffs (Glud et al., 2010), and down-facing sea-ice surfaces (Long et al., 2012). However, only a few have been performed in sandy, shelf benthic environments (McGinnis et al., 2014, Reimers et al., 2012, Attard et al., 2015). Permeable, sandy sediments are located within areas where there are a combination of processes occurring which influence oxygen

dynamics, including primary production, mixing, influences from land use, leading to strong linkage between the water column and sediment (Huettel et al., 2014).

A combination of hydrodynamics and biology control the temporal and spatial movement of oxygen through sediment, creating an important proxy to quantify carbon mineralisation (Hicks et al., 2016). Understanding the oxygen dynamics in permeable sandy sediment environments and their role in biogeochemical cycling is crucial as these environments constitute up to 70% of the benthic habitats of the world's shelf seas (Glud, 2008). Greenwood et al. (2010) argue oxygen levels within shelf seas are declining, and it is vital to understand why this is occurring.

This results chapter presents field data collected at L4 (study site) over 5 months during the spring and summer of 2017 and focusses on the first month (May 2017) to describe the hydrodynamics of the site and their influence on benthic oxygen flux. This two-part study expands the scope oxygen flux and tidal analysis to nutrient, chlorophyll and temperature analysis over the five-month sampling period, where drivers at L4 are discussed.

4.2 Preliminary study: Tidal dynamics and benthic oxygen flux at L4

The field deployment reported here was conducted from the 23rd to the 24th of May 2017. During the study, an EC lander (A/S, Unisense, Denmark) and ADCP (RDI Sentinel V50, Teledyne RDI, USA) were deployed and a Conductivity Temperature Depth (CTD) profiler (SeaBird SBE 19+) cast was taken as part of the long-term time series at L4. All equipment was deployed within 100 m of each other. In this preliminary study reported here, 30 hours of EC and acoustic Doppler current profiler (ADCP) data from a deployment in May 2017 are presented. These data enable the hydrodynamic contributions from surface and internal tides to benthic oxygen fluxes at L4 to be assessed. EC-derived measurements of benthic oxygen flux in a dynamic and exposed coastal shelf site containing permeable sandy/muddy sediments are almost non-existent and the results presented here enable the first assessment of the contribution of different tidal components to these fluxes.

Tidally driven turbulence has a direct effect on bottom boundary layer dynamics, influencing pore water circulation and biogeochemical processes which affect oxygen dynamics including nutrient exchange (McGinnis et al., 2014) and trace metal cycling (Huettel et al., 2014). Climate change will also impact oceanic currents in the future (Hoegh-Guldberg and Bruno, 2010) and so it is important to understand how hydrodynamic drivers impact benthic oxygen flux. A better understanding of these physical drivers will improve our ability to model benthic

oxygen fluxes and enable robust predictions of the impact of changing conditions on coastal environments (Santos et al. 2012).

4.2.1 CTD results

The density profile from the CTD sensor shows weak stratification, with a pycnocline approximately between 35 m and 40 m height above bottom (HAB) (Figure 4.1). This was also confirmed within the oxygen and temperature profiles (Figure 4.1). The Photosynthetically Active Radiation (PAR) sensor indicated that light did not penetrate to the seabed during this period. The elevation of the pycnocline was calculated from the temperature profile in Figure 4.1A. The buoyancy frequency (a measure of stratification strength) peaks as expected in this same depth range. There is a weak oxygen gradient between 20 m and 40 m HAB (Figure 4.1).

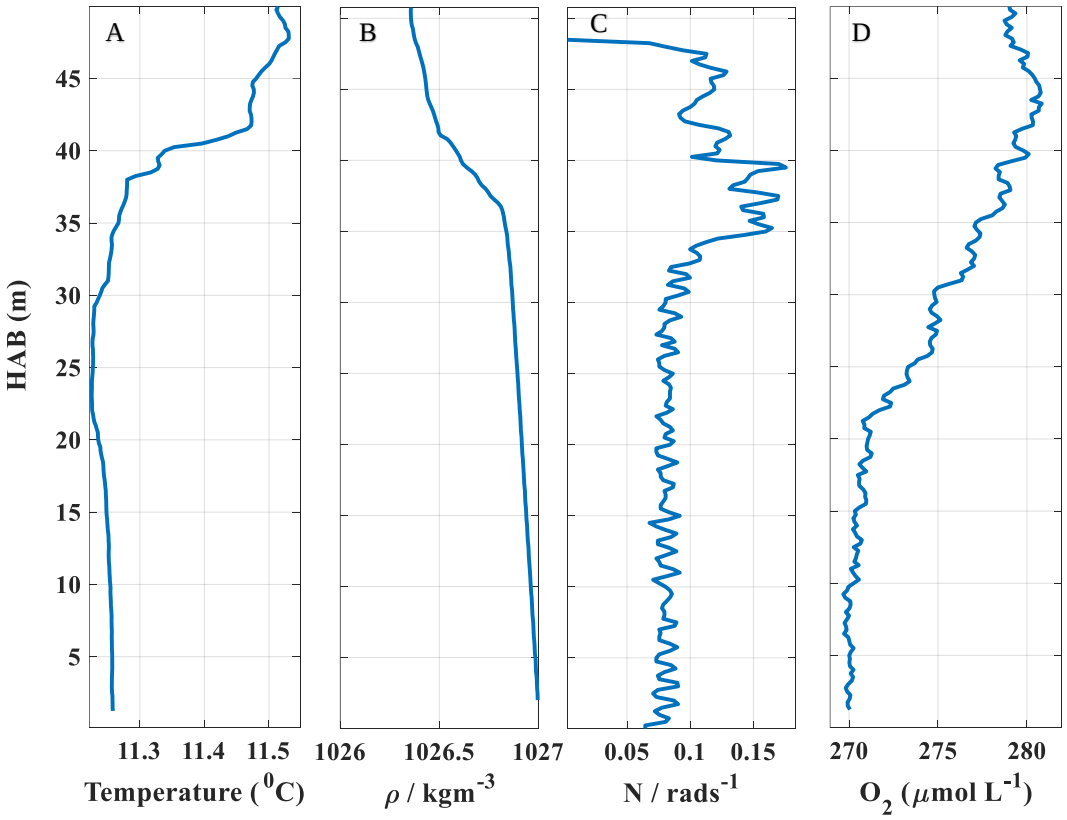

Figure 4.1: CTD data from the cast taken at L4 on the 23rd May 2017. A) Temperature profile B), density profile (ρ) C), buoyancy frequency (N) profile, and D) oxygen data. CTD data has been collected weekly at L4 since 2002. Data courtesy of Tom Bell/PML.

4.2.2 Surface and internal tides

Within this study we are assessing oxygen dynamics in a stratified shelf sea environment. Therefore, it is informative to understand the internal tidal dynamics as this assessment and will potentially aid the prediction (modelling) of oxygen dynamics and inform our understanding of the contribution of internal and surface tides to benthic oxygen transfer.

Oxygen flux JO_2 as measured by the EC system is a function of vertical fluctuating vertical velocity w' (Equation 2.2). This velocity is driven by turbulence which in turn is driven by tidal velocities. These tidal velocities can be decomposed into surface (barotropic) and internal (baroclinic) components.

Barotropic tides (also known as surface tides) are created by a centrifugal force due to rotation of the earth and the gravitational pull of the sun and the moon. The barotropic tidal velocity is the depth averaged velocity of the water column.

Baroclinic tides (also known as internal tides) are created from the tidal energy being transferred at depth into an internal wave with tidal periodicity that oscillates along a density interface. As stratification increases/decreases the strength of the baroclinic tide magnitude will change. Baroclinic velocities change with depth; the vertical velocity structure is computed by subtracting the barotropic from the total observed whole water column velocity.

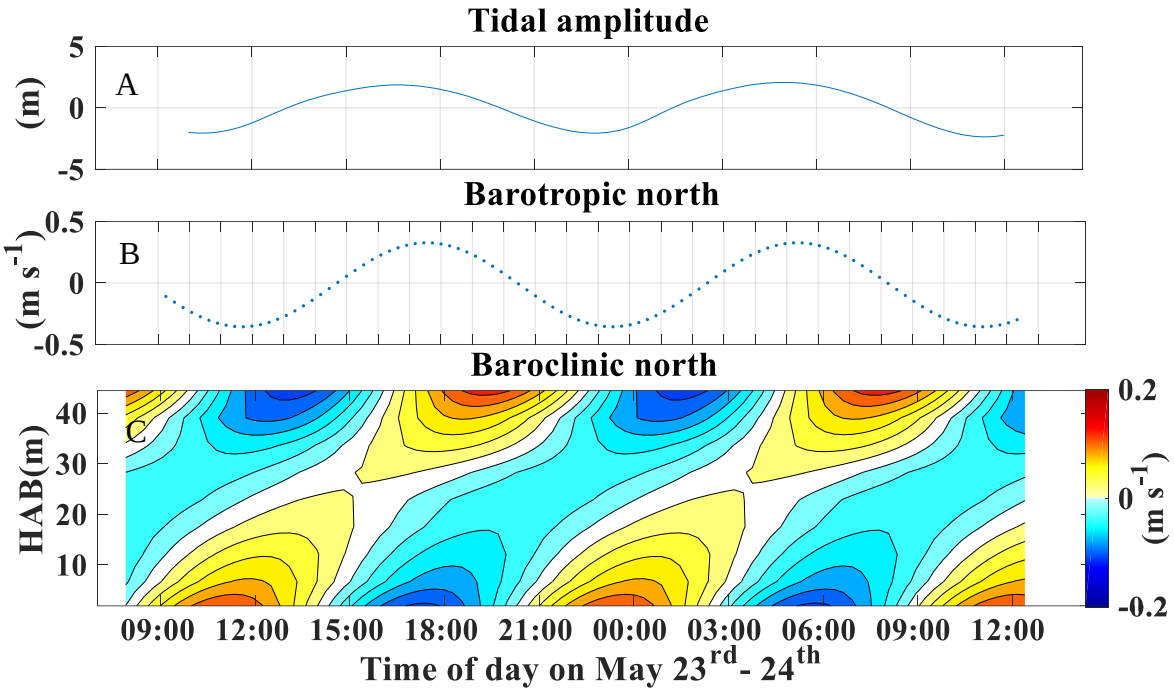

Figure 4.2: A), Tidal amplitude as measured by the ADCP. B), barotropic north velocities C), baroclinic north velocities (2017 year of data collection).

As the campaign was during the month of May, the water column was not as stratified as other months throughout the summer season. It is expected therefore that the baroclinic component would strengthen throughout the summer period. Nonetheless, decomposition of the tidal signals showed baroclinic maximum is 0.15 m s^{-1} which was close to half of the barotropic maximum is 0.35 m s^{-1}. Both the barotropic and baroclinic velocities were predominantly north/south. Results also indicated a partially standing tide rather than a perfectly standing tide (Figure 4.2). A standing tide occurs when there is perfect reflection of the tidal wave from the shoreline (Figure 4.3).

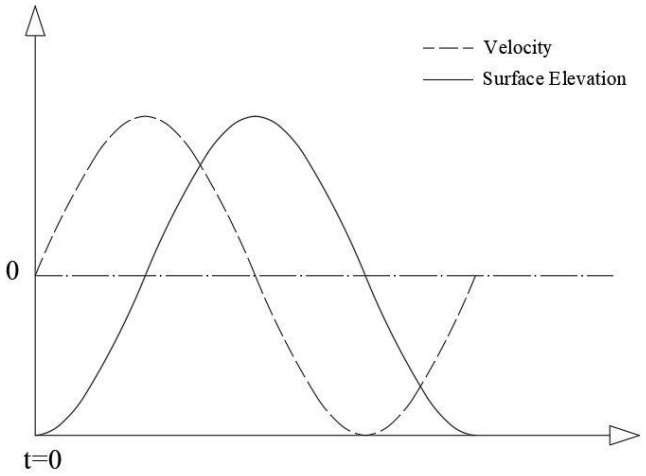

Figure 4.3: Schematic of surface elevation and barotropic velocity for a standing tide, illustrating the phase lag between velocity and surface elevation. A standing tide occurs when there is perfect reflection of the wave from the shoreline.

With a perfectly standing wave the barotropic current would precede the tidal elevation by 3 hours and 6 minutes whereas in this study a lag of 1 hour 13 minutes was observed (Figure 4.2).

Even though oxygen flux is driven by total velocity regardless of how this flow velocity is generated, this insight into the tidal dynamics enables future modelling of oxygen fluxes especially when stratification levels change through a seasonal cycle.

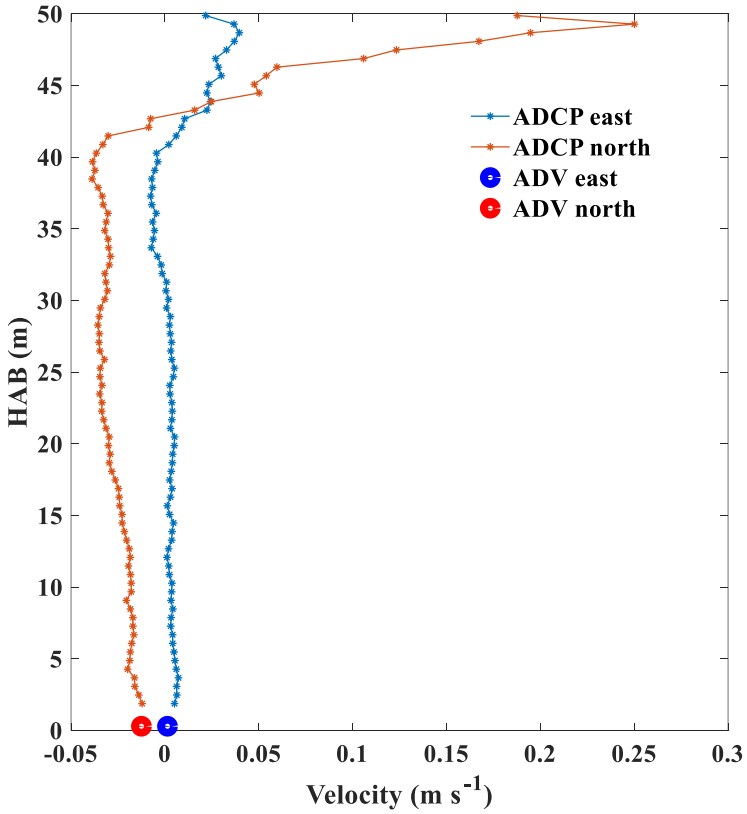

Figure 4.4: Velocity measurements in the east and north directions as measured by the ADV (point measurement at the bed) and ADCP (velocity profile), bin averaged over a tidal phase (12.4hrs).

The ADV velocities match the bottom ADCP velocities at the seabed (Figure 4.4). A weak mean southerly flow throughout the water column and a stronger mean northerly flow at the surface is illustrated in Figure 4.4. The elevated velocities in the upper 10 m of water column may have been due to wind from the south (from South to North at 1 ms^{-1}).

4.2.3 EC fluxes and tides

From CTD casts, the Chelsea PAR sensor revealed minimal light penetration to the seabed (0.5 NTU (turbidity); therefore fluxes of oxygen were expected to be negative (into the sediment). The median benthic oxygen flux was estimated as JO_2 = -14 ± 3 mmol m^{-2} d^{-1} and the largest flux recorded during the deployment was JO_2 = -27 ± 2 mmol m^{-2} d^{-1} (Figure 4.5). Time series of 15 and 60-minute averaged flux throughout the deployment is shown in Figure 4.5F.

As noted above, only a limited number of studies into the magnitude of oxygen uptake have been conducted in situ within shelf sea environments (Queste et al., 2016). Values of oxygen

flux obtained within this study (median JO_2 = -15 mmol m^{-2} d^{-1}) compare well with oxygen flux levels measured in the North Sea (JO_2 = -12 mmol m^{-2} d^{-1}) (McGinnis et al., 2014). A study conducted within the Oregon Shelf, USA obtained mean JO_2 of -6 mmol m^{-2} d^{-1} (Reimers et al., 2012). Both studies observed similar values of oxygen flux to those shown in Figure 4.5F. To understand the drivers causing the measured oxygen flux, the hydrodynamic factors which influence the benthic oxygen dynamics at L4 are described below.

The current measurements obtained oxygen concentrations within a small range between 244 μmol L^{-1} and 248 μmol L^{-1} (Figure 4.5E) therefore changes in flux were primarily driven by changes in the vertical velocity component (Berg et al., 2003; McGinnis et al., 2014), with velocities being almost all tidally driven. In order to determine whether the surface or internal tide is the dominant factor driving the fluxes, the depth-averaged barotropic velocity amplitude and phase is compared with those of the baroclinic velocity field.

The baroclinic tide is influenced by topography and a thermocline in the L4 area (Figures 4.1 and 4.2). A steep slope from 35 m to 50 m in depth in the vicinity of L4 (Chapter 1, Figure 1.6) is thought to contribute to the surface and internal tides being out of phase due to reflection from this shelf. There is a weak southerly mean flow through the water column (Figure 4.4), indicating a net circulation pattern in the region, likely due to the orientation of the shelf topography. At the surface, there is a stronger mean northerly flow, which can be attributed to the wind direction as noted above (Figure 4.4). However, below this surface region, the oscillating flows from the tides dominate the mean flow. Figure 4.5D and E indicate that the velocities measured by the ADV fall to zero and undergo rapid directional changes from south to north on a semidiurnal timescale. The velocity magnitude minima occur over one hour before the comparable minima (indicating flow direction change) in the barotropic component of the tidal current. This lag is attributed to baroclinic component on flow readings taken by the ADV. Both the ADV and barotropic tide velocity magnitudes were smaller in the north direction compared to the south. This led to larger negative fluxes occurring when the ADV and barotropic tidal currents were southerly (Figure 4.5). These dynamics are probably due to the topography of the area (Chapter 1, Figure 1.6), as deflection occurring from the eastern wall of the shelf creates gradual flow reversal, influences the magnitudes and phasing of the tides, and in turn the fluxes. A boxplot of the measured flux data (Figure 4.6) confirms this observed asymmetry; the fluxes are greater when the main tidal flow occurs in the southerly direction.

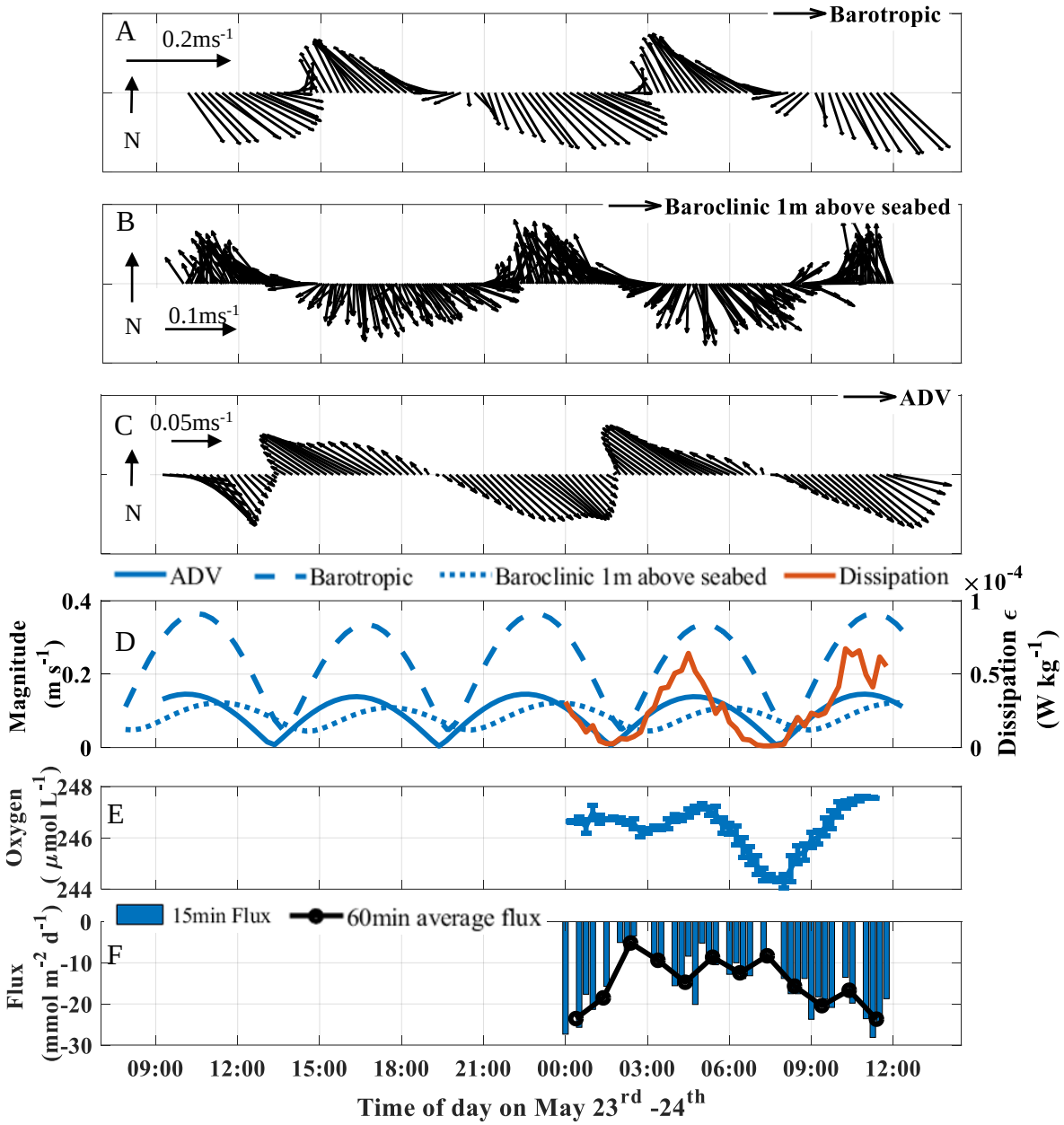

Figure 4.5: Magnitude and direction of the A) barotropic velocity component, B) baroclinic velocity component at 1 m HAB and C) the ADV measured velocities at 12 cm above the bed. D) Magnitude of components (barotropic, baroclinic 1 m HAB and ADV) which have had a tidal harmonic fit added, along with the dissipation rate of turbulent kinetic energy measured by the ADV. E) Oxygen concentration measured by the EC microelectrode. F) Oxygen fluxes computed using 15-minute data windows and 60 min averages of those fluxes. Only 12 hours of EC flux could be measured due to debris on sensor.

As expected, turbulent dissipation rates are forced by the tide (Figure 4.5F). As the bottom water velocities increase and more turbulence is generated, the oxygen gradient between the water column and sediment will increase, allowing for greater benthic oxygen fluxes leading to a tidal signature within the flux values (Figure 4.5F). As assessed within this study, it was

therefore, important to understand which tidal components (barotropic or baroclinic) were driving the oxygen flux into the sediment, or whether it was a combination of both. When considering only the magnitudes, barotropic tides have a greater significance on hourly tidal flux values than baroclinic. Barotropic tides exhibited similar trends, with southerly velocities larger than northerly as seen in the depth average (Figure 4.5A). From Figure 4.5C, it is clear that the barotropic velocity dominates at an amplitude of 0.38 m s^{-1}. However, the baroclinic velocities near the bottom are not insignificant, with an amplitude of 0.14 m s^{-1}.

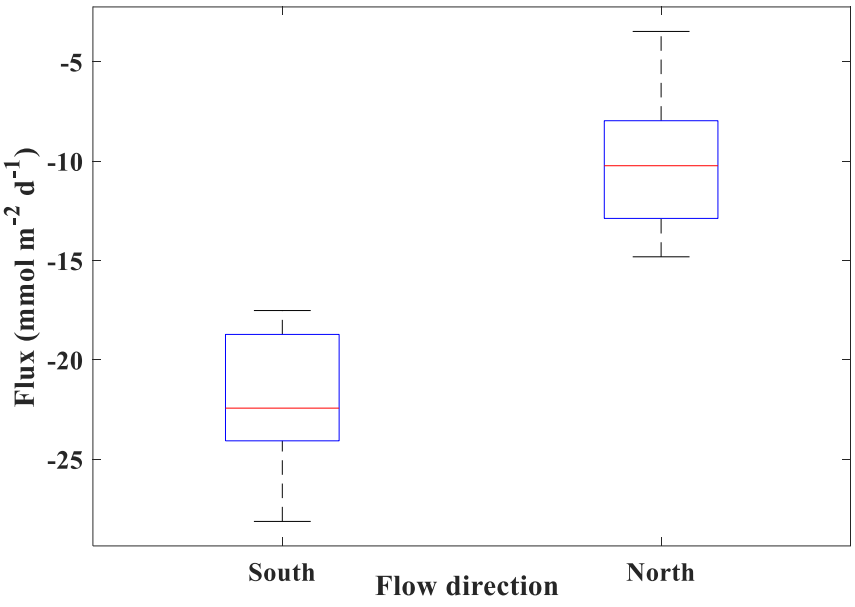

Figure 4.6: Boxplots of EC-derived oxygen flux according to flow direction. On each box, the central mark indicates the median, and the bottom and top edges of the box indicate the 25th and 75th percentiles, respectively. The whiskers extend to the most extreme data points not considered outliers.

Both the baroclinic tidal analysis and CTD data have clearly shown this environment is not homogeneous and is impacted by topography and density gradients. Resultant variations in velocity have significant impact on vertical velocity fluctuation, and in turn oxygen flux values. A substantial range of oxygen flux values were measured but the overall average over a time series is the representative flux of the sediment sink.

This preliminarily study combining flux and hydrographical data provides an understanding of one of the main benthic oxygen flux drivers. Within this complex environment time-series of flux data over several months will provide an indicator of other benthic oxygen drivers at this important and dynamic scientific research site (L4).

4.3 Main study: Investigating the complex drivers of variable benthic oxygen dynamics at a long-term coastal monitoring station.

The L4 site which lies at a depth of 50 m within the WCO was chosen to represent a typical coastal area within southwest British waters (Smyth et al., 2015). This site also benefits from a long-term monitoring timeseries of water column nutrient data, as well as sediment analysis (Smyth et al., 2009). However, no observations of sediment water interface oxygen exchange have been undertaken at this site. As a result, this study was designed to provide new insight into benthic oxygen transfer at a much-studied site.

Assessment of the seasonal variability of benthic oxygen utilization is vital for characterising the biogeochemical dynamics. Benthic oxygen fluctuations can occur due to spatial and temporal effects; drivers include organic matter (OM) influences (affecting chemical and biological demands), bioturbation and hydrodynamics.

In this study, the EC method is used alongside a range of other instrumentation (CTD, nutrient rosset and sediment samples) to evaluate various biogeochemical processes. By applying the EC method at L4, the aim was to enhance understanding of oxygen dynamics during plankton blooms which occur bi-annually (late spring and early autumn), and the effect of dredge spoil dumping in the area which can greatly affect sediment composition. Continual monitoring of sediment oxygen demand will not only extend knowledge of flux drivers to aid future modelling of these fluxes but will also signal changes in the health of nearby ecosystems. This is especially valuable, as these ecological systems are vulnerable to changes in pollution levels, as well as climate change effects, which may alter plankton bloom events and subsequent respiration of exported particulate OM (Whitehead et al., 2009; Macko, S.A., 2018).

A pollution issue investigated within this study is the dumping of dredged refractory spoils. Dredging is undertaken in Plymouth Sound to maintain waterways for shipping and is therefore vital in maintaining local and global economies. However, when dredged material is relocated this creates an addition of material rich in OM within a site. Poor water quality is caused when OM is suspended or resuspended, with potentially devasting implications for ecologically sensitive areas, resulting in poor ecosystem health (Wakeman et al., 1975; Johnston, 1981; Davis, 2017). In this study, EC measurements were conducted before and after the dumping of dredge spoil to examine environmental effects.

This study establishes a cohesive picture of oxygen dynamics at the designated coastal study site L4, via assessment of turbulent oxygen fluxes along with environmental time series data and historical water column data. This assessment focuses on benthic oxygen drivers and the anthropogenic influences such as dumping of dredged spoils have on benthic oxygen fluxes over multiple deployments during spring and summer. This study aims to demonstrate that the EC technique is a useful in situ tool for the monitoring and assessment of oxygen dynamics at a coastal shelf sea environment. To achieve these aims oxygen flux values, as well as environmental data from the entire 5-month field campaign are presented.

4.3.1 Benthic oxygen flux

The oxygen flux timeseries presented in Figure 4.7 were obtained from more than 150 hours of EC data collected at L4 (summary of key deployment details found in Table 4.3). Some deployments were cut short due to sensor interference or damage, however, on average 20 hours of data were collected per deployment, with a minimum of 12.4 hours which represents a complete tidal cycle. A statistical analysis of oxygen flux data is presented as a box plot in Figure 4.8 which enables a comparison of the month-by-month oxygen flux values.

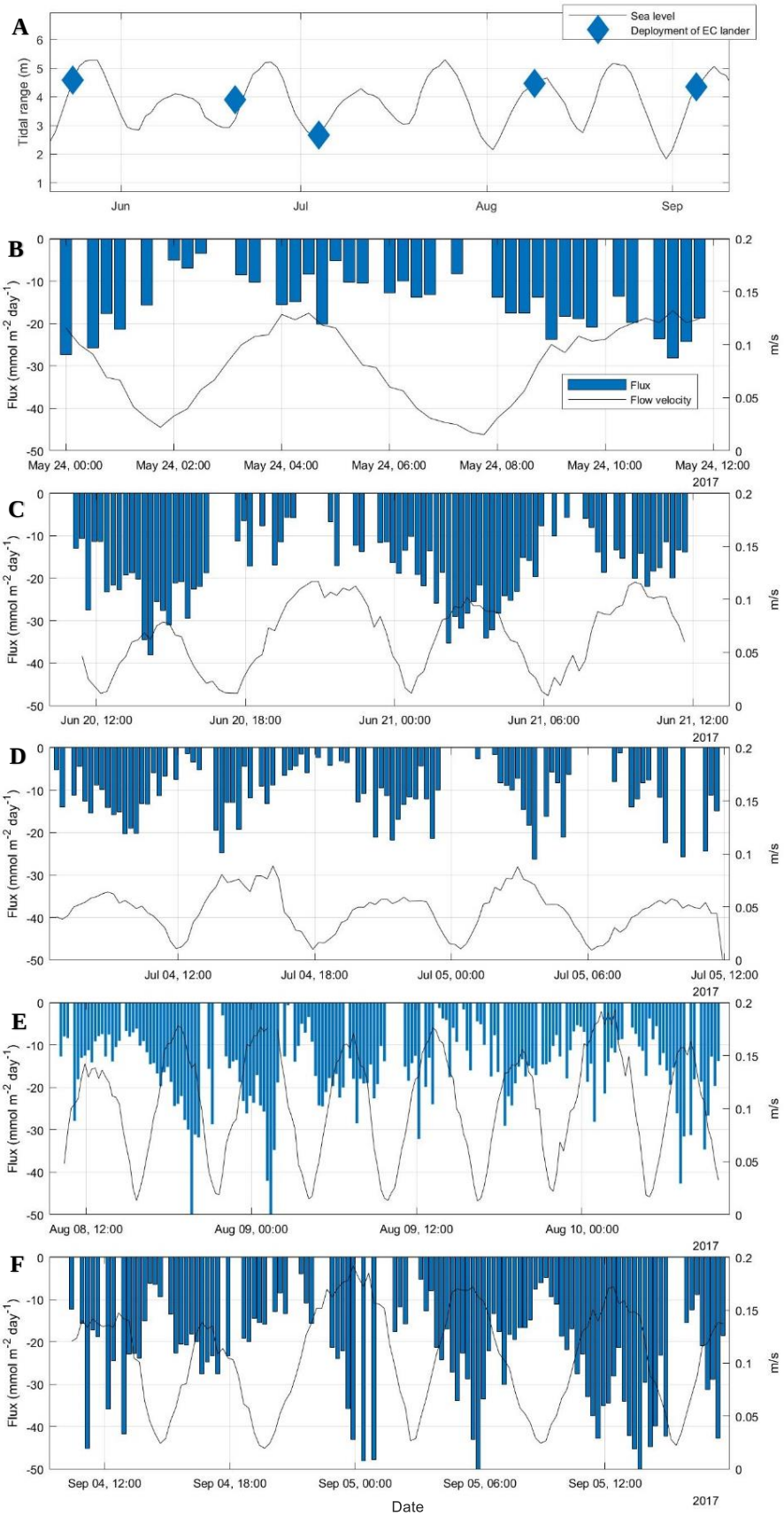

Figure 4.7: A) Tidal range as a function of time during the field campaign. Note that the tide data was taken from Devonport (15 nautical miles from L4) and the sea level differences include residual effects. B, C, D, E and F) Monthly timeseries of EC oxygen flux in 15-minute segments, overlain with mean flow velocity for May 24th to September 5th, 2017.

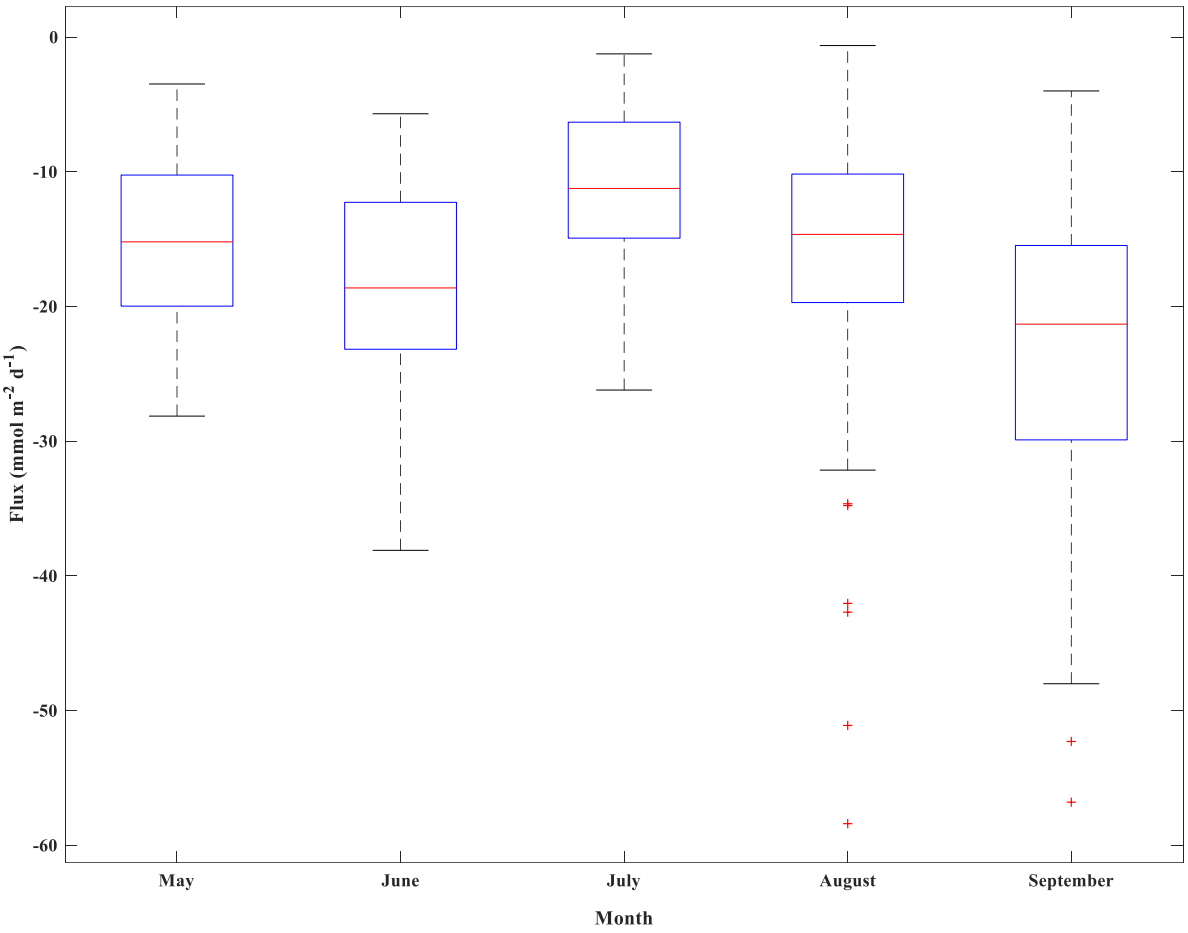

Figure 4.8: Benthic oxygen flux throughout the monthly deployments presented as Boxplots. On each box, the central mark indicates the median, and the bottom and top edges of the box indicate the 25th and 75th percentiles, respectively. The whiskers extend to the most extreme data points not considered outliers, and the outliers are plotted individually using the '+' symbol.

The measured flux data over a 12.4 hr tidal cycle between months was not normally distributed according to the Shapiro-Wilk test, therefore a Kruskal -Wallis with a Dunn's post hoc test was conducted (see summarised results in Table 4.1). The measured oxygen flux values in May were found to be significantly different from July and August ($H = 83.5$, $df = 2$, $P < 0.001$)., and September ($H = 83.5$, $df = 2$, $P < 0.001$).

The oxygen flux values measured in September were significantly different than May, June and July ($H = 83.5$, $df = 2$, $P < 0.001$).. Further examination of flow velocities, chlorophyll, temperature, sediment composition and nutrients on a month-by-month basis presented in Sections 4.3.3, 4.3.4, 4.3.5 and 4.3.6 will aim to elucidate which drivers are contributing to the observed differences in oxygen flux between months.

Table 4.1: Statistical results of median oxygen flux over the five-month field campaign. The contents of the middle and right-hand columns indicate the months in which the median oxygen flux was significantly different to the value recorded in the month in the left-hand column. For example, in the top row, the table indicates that the median oxygen flux measured in September was significantly different to that measured in May ($P < 0.01$).

Month	($H = 83.5$, $df = 2$, $P < 0.05$)	($H = 82.5$, $df = 2$, $P < 0.001$)
May	July and August	September
June		July and September
July	May	June, August and September
August	July	
September		May, June and July

4.3.2 Flow Velocity

As documented in previous studies (McGinnis et al., 2014; Reimers et al., 2016), hydrodynamics is a primary driver of benthic oxygen flux. Figure 4.9 presents a box plot of the horizontal velocity for each of the monthly deployments. Note that these measured velocities are not considered representative of the monthly median flow velocity but capture a range of flow velocities which enable an analysis of the influence of tidal flows on oxygen flux. Figure 4.9 demonstrates that the highest horizontal median flow velocities (12.5 and 13 cm s^{-1}) were measured during the August and September deployments, with both deployments occurring close to spring tides, with tidal ranges of 4.8 m and 4.3 m respectively. The next highest median horizontal velocities were recorded during the May and June deployments (8.5 cm s^{-1} and 6.5 cm s^{-1}), with tidal ranges of 4.6 m and 4 m respectively. The deployment in July occurred during a neap tide (tidal range of 3 m) and the lowest horizontal median flow velocity of 5.5 cm s^{-1} was recorded. Dissipation rates were calculated using the method presented in Section 2.9.3 and followed a similar trend to the velocity data, with the August deployment associated with the highest median dissipation rate ($\varepsilon = -4.5$ W kg^{-1}), and July exhibiting the lowest value ($\varepsilon = -6.2$ W kg^{-1}).

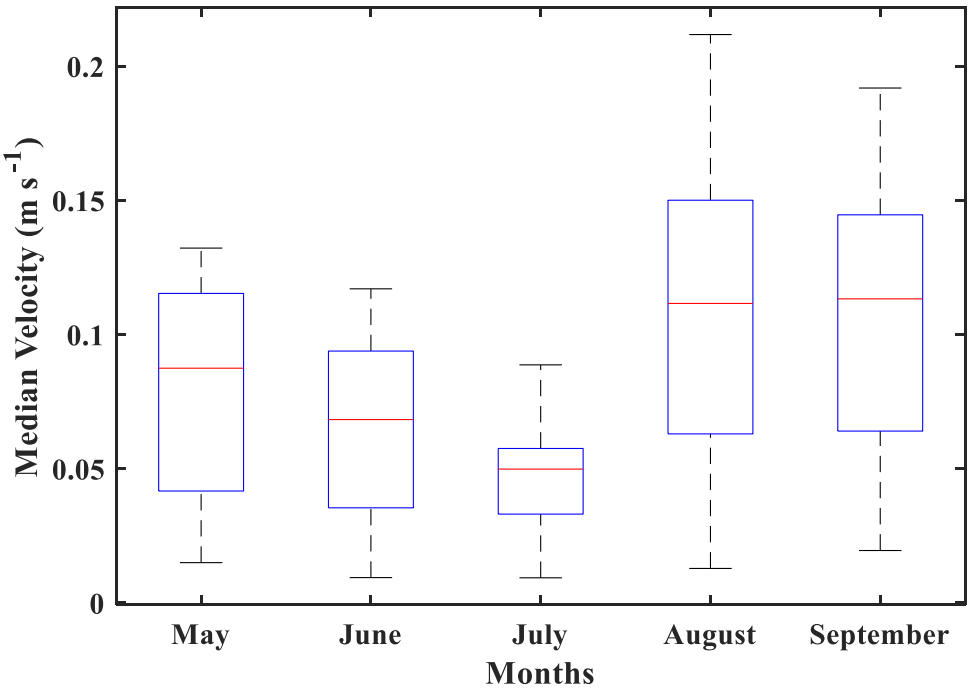

Figure 4.9: Boxplot of horizontal velocity measured during each deployment over an integer number of tidal cycles. On each box, the central mark indicates the median, and the bottom and top edges of the box indicate the 25th and 75th percentiles, respectively. The whiskers extend to the most extreme data points not considered outliers.

Statistical analysis has shown velocity data within each deployment were not normally distributed using the Shapiro-Wilk test therefore, a Kruskal -Wallis with a Dunn's post hoc test was conducted. Data for each month was selected within a 12.4-hour period. May was significantly different to July ($H = 82.5$, $df = 2$, $P < 0.001$). August and September were significantly different to June and July ($H = 82.5$, $df = 2$, $P < 0.001$) (see Table 4.2 for complete results).

Table 4.2: Statistical results of median velocities over the five-month field campaign. The contents of the middle and right-hand columns indicate the months in which the median oxygen flux was significantly different to the value recorded in the month in the left-hand column. For example, in the top row, the table indicates that the median oxygen flux measured in July was significantly different to that measured in May ($P < 0.01$).

Month	($H = 83.5$, $df = 2$, $P < 0.05$)	($H = 82.5$, $df = 2$, $P < 0.001$)
May	June	July
June	May	August and September
July	May	August and September
August		June, July
September		June, July

4.3.3 Comparison of flow velocity and benthic oxygen flux

A weak correlation was observed between median oxygen flux and median velocity for each month (R^2 = 0.43) (Figure 4.10) however, only five data points limit the robustness of this correlation. This analysis indicates that tidal flows may not be the sole nor primary driver of oxygen flux over the five-month field campaign therefore, other drivers such as, sediment composition, chlorophyll and nutrients, will further be examined as a possible driver of flux.

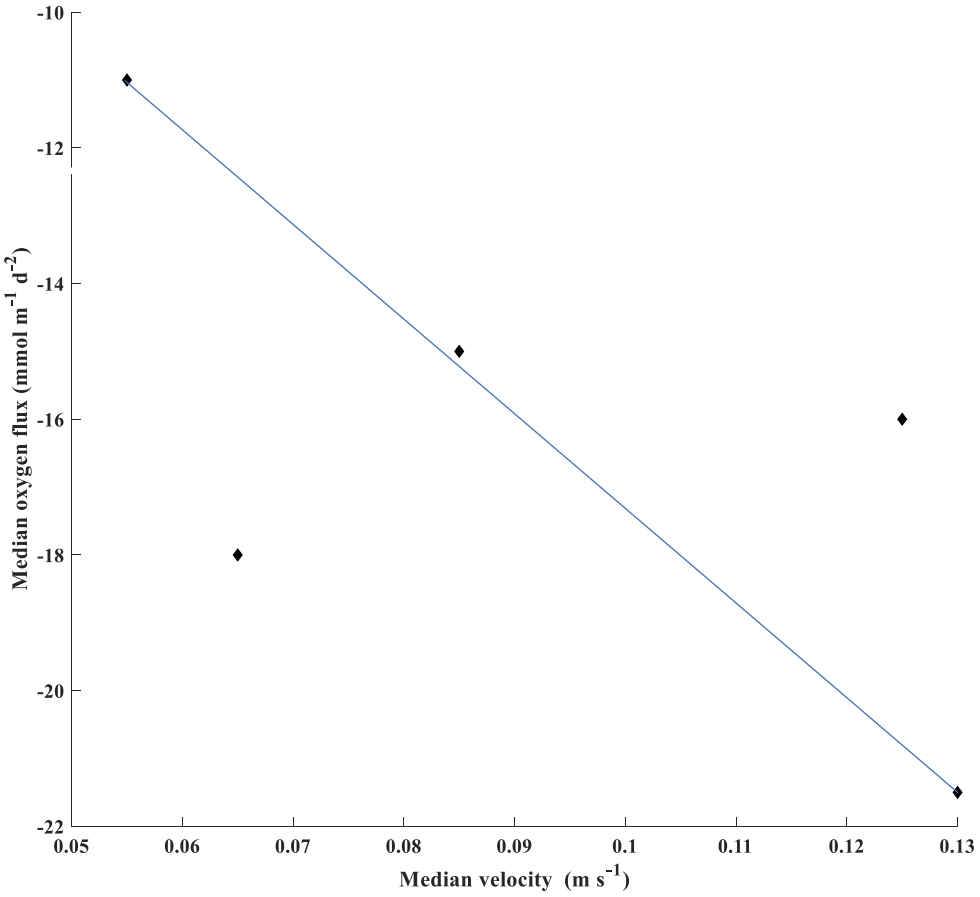

Figure 4.10: Median oxygen flux as a function of median flow velocity for each of the 5 monthly deployments R^2 = 0.43, y = -1.8x + 9.7, n = 5, trendline with a 95% confidence interval.

Table 4.3: Summary of the deployment length, flux, dissipation, tidal range, and temperature for each monthly deployment:

Month	**May**	**June**	**July**	**August**	**September**
Length of deployment (hrs)	13	25.5	30	48	55
Median Flux (mmol m^{-2} d^{-1})	-15	-18	-11	-16	-22
95^{th}percentile Flux (mmol m^{-2} d^{-1})	-27	-35	-25	-53	-53
Flux Standard Deviation (mmol m^{-2} d^{-1})	3	3	3	4	5
Median Velocity (m s^{-1})	0.085	0.09	0.055	0.12	0.13
Median Dissipation log10 (ε) (W kg^{-1})	-4.8	-4.7	-6.2	-4.8	-4.8
Tidal range (m)	4.6	4	2.5	4.8	4.3
Temperature (°C)	12	13	14	14	15

4.3.4 Chlorophyll, phytoplankton and temperature

Chlorophyll-a and temperature data from CTD casts (Figure 4.11) were analysed to examine the variation in benthic flux levels throughout the five-month field campaign. Historically, the highest chlorophyll-a concentration recorded at this site was 10 µmol m^{-2} in 1997, whereas in 2017, chlorophyll-a concentration only reached 2 µmol m^{-2} (surface readings) (Figure 4.11A) (Data courtesy of Tom Bell/PML).

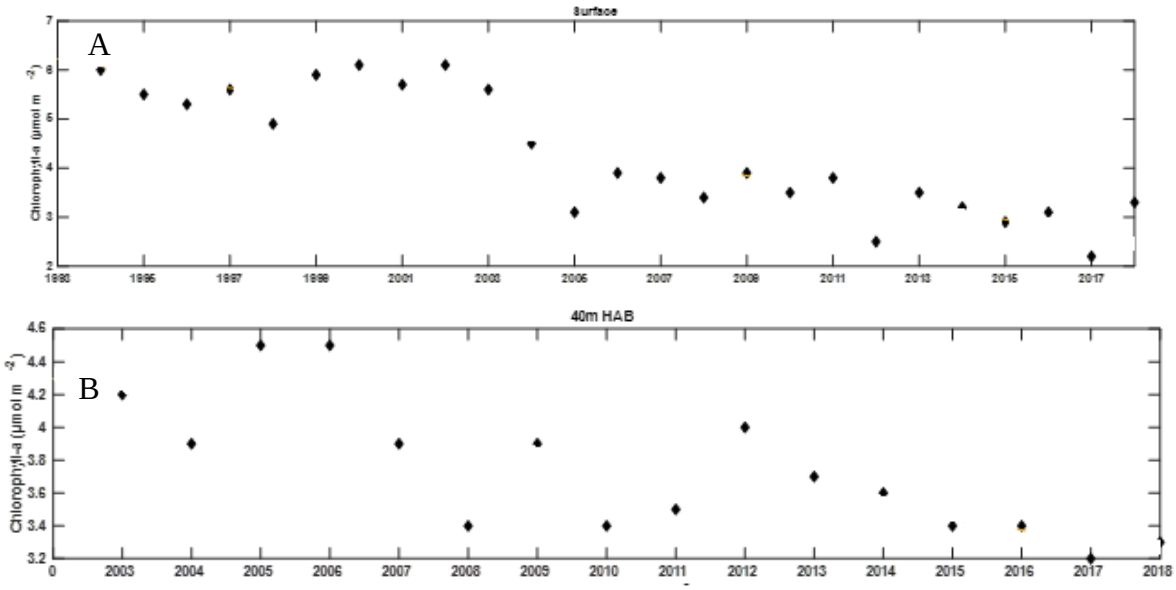

Figure 4.11: Historical peak chlorophyll-a levels from A) 1993 to 2018 at the surface and B) 2003 to 2018 at 40 m

Chlorophyll-a levels on average have reduced from 1.7 µmol m^{-2} in 1992 to 1.5 µmol m^{-2} in 2018 in surface readings.

During the summer of 2017, chlorophyll-a concentrations were measured throughout the water column (Data courtesy of Tom Bell/PML). Chlorophyll-a maximums occurred at different depths throughout the summer (recorded by CTD, Figure 4.12B), indicating varying thermoclines over the various deployments. Chlorophyll-a concentrations are an indicator of phytoplankton abundance and biomass in coastal and estuarine waters and is used as a proxy for plankton levels (Boyer et al., 2009). It is assumed that plankton would eventually sink to the seafloor. Thereafter, it is expected that senescence of this plankton material would have occurred within the sediment (Rontani et al., 2016) however, this can only be validated using settling chambers.

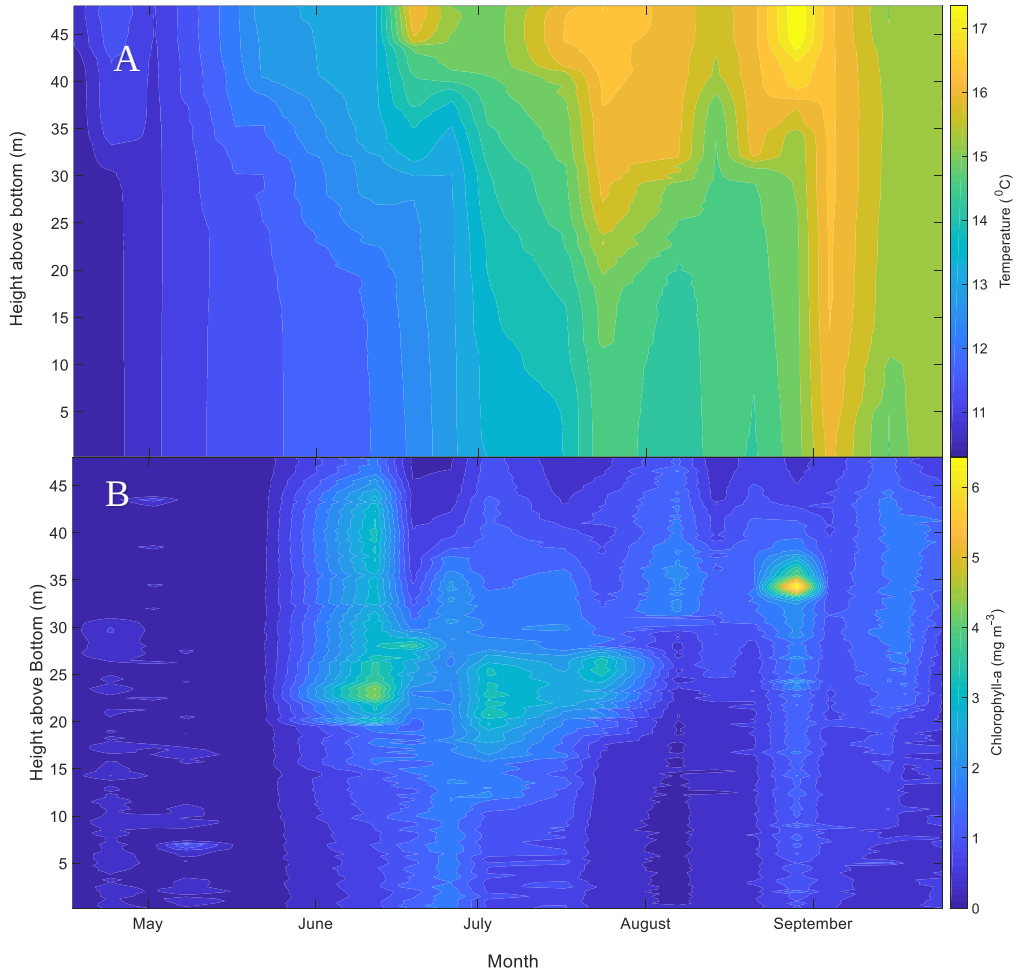

Figure 4.12: A) Contour plot of temperature and B) Chlorophyll-a constructed from CTD data collected weekly during the spring/summer field campaign. Data courtesy of Tom Bell/PML.

It is clear from Figure 4.11 that the weak plankton blooms in 2017 started in June, seen by a chlorophyll-a maximum which occurred from the surface to 25m above the seabed. The chlorophyll-a maximum at 25 m continues into July, until a mixing event occurred in mid-August. These mixing events were also captured in the temperature data (Figure 4.12A). At the beginning of September, another chlorophyll-a maximum occurred at 35 m, shortly followed by another mixing event (seen in Figure 4.12B).

4.3.5 Sediment composition (dumping of spoils)

Dredge spoil has the potential to introduce additional organic matter (and hence nutrients) into the system as well as changing the composition of the surficial sediment. As noted in Section 1.11.1, a volume of dredge spoil from Plymouth Sound was dumped near to the L4 site between 30/5 and 01/06, 2017 and lead to a change in the composition of the surficial sediment (see Figure 4.13). Benthic consumption rates are affected by the amount of OM in the sediment. While OM will degrade over time, material dumped in June could remain for several months (Braeckman et al., 2019). Any recent resuspension from mixing events will also have an impact on the way the OM influences the benthic oxygen flux at the site.

Oxygen has been shown to penetrate up to 25 cm into sand, whereas in silt it is limited to 1 cm (Song et al., 2016). Similarly, sand has a very simple chemical composition (primarily silica), whereas silt contains many chemical compounds, including manganese, iron and phosphorus creating a higher chemical oxygen demand (Lee et al., 2018). It is therefore assumed that the May deployment which occurred prior to the dumping of dredge spoil/ plankton blooms can be considered a control month (Figure 4.13). As oxygen flux values measured in May were significantly different than September ($P<0.01$) and velocity was not significantly different (velocity not as an overriding driver), changes in sediment composition caused by the dumping of dredge spoil may have had an effect on oxygen demand. However, it is important to note that there are additional unknown factors such as patches of debris in the surrounding area, similarly sediment composition in Figure 4.13 was collected 2 nm from the EC.

The dumping event and plankton blooms had possible implications on the sediment composition due to the addition of OM/dredged material which changed the surface roughness, potentially impacting benthic oxygen flux. Sediment surface roughness was estimated using

methods described in Berg et al. (2007) (Section 2.3.2) and was found to be higher by a factor of two during the May deployment compared to all other months (0.0059 m for May and 0.0033 m for June to September). This variation in sediment surface roughness provides further evidence that there were changes in sediment type throughout the deployment period at L4.

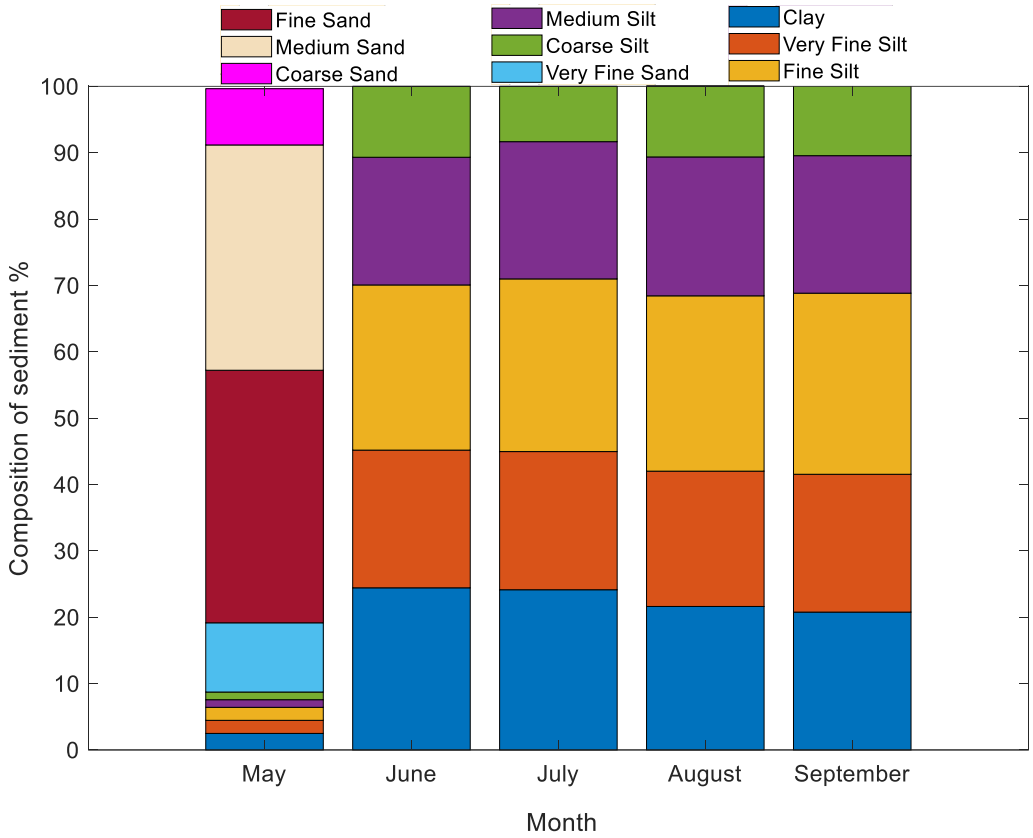

Figure 4.13: Composition of monthly surficial sediment samples over the five-month sampling period at two nautical miles from the EC sampling location, 0-2cm into the sediment (superficial sediment samples). Dredge spoil dumping occurred primarily between 30/5 and 01/06 between the May and June deployments. Data courtesy of PML extended survey.

Without further OM sediment analysis, it is not possible to prove whether plankton blooms or changes in the surficial sediment due to the dumping of dredge spoils is responsible for the change in benthic oxygen consumption during the five-month field campaign.

4.3.6 Nutrients

Figure 4.14 shows a timeseries of nutrient concentrations at multiple water depths throughout 2017. It is notable that in 2016 (data collated from WCO historical records) ammonia levels were observed to increase throughout the water column between May and July whereas in 2017 an increase was only observed at 50 m depth. All nutrients indicated in Figure 4.14 were

compared between 2016 and 2017 however, ammonia was the only nutrient to display different trends within the water column within this comparison. This process thereby potentially generates a higher biological and chemical oxygen demand within the sediment.

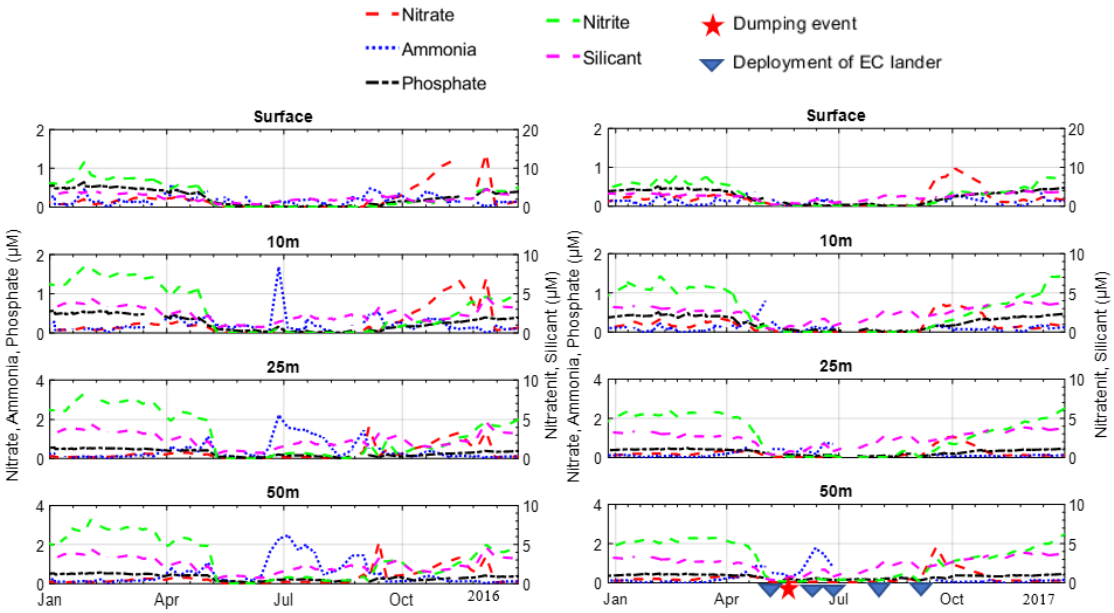

Figure 4.14: Nutrient levels throughout the water column, from the surface to 50 meters depth. Weekly water samples were taken with CTD rosette casts, over the seasonal field campaign. A, 2016 nutrient levels (high Algal bloom and no dumping of OM) B, Weak algal blooms and dumping event. Data courtesy of Tom Bell/PML.

Statistical analysis of the concentrations of the five nutrients shown in Figure 4.14 using data collected weekly at 50 m water depth throughout the five sampling months. All parameters included were found to be not normally distributed using the Shapiro-Wilk test therefore, a Kruskal -Wallis with a Dunn's post hoc test was conducted.

Nitrite

The Nitrite concentrations measured during the May, June and July deployments were significantly different than those measured in August and September ($H = 82.4$, $df = 2$, $P < 0.001$).

Nitrate

The Nitrate concentrations measured during the May were significantly different to those measured in July, August ($H = 83.5$, $df = 2$, $P < 0.001$) and September ($H = 82.4$, $df = 2$, $P < 0.001$). Similarly, the data from September showed a significant difference to May, June and July ($H = 83.5$, $df = 2$, $P < 0.001$).

Ammonia

No data was collected in August due to instrumentation failures. The ammonia concentrations measured in June were significantly different to July ($H = 82.4$, $df = 2$, $P < 0.001$) and September was significantly different to July ($H = 83.5$, $df = 2$, $P < 0.001$).

Silicate

The silicate concentrations measured during May were significantly different to those measured in August and September ($H = 82.4$, $df = 2$, $P < 0.001$), and June/ and July ($P<0.05$). Similarly, silicate concentrations measured during September was significantly different to May ($H = 82.4$, $df = 2$, $P < 0.001$) and June/July ($H = 83.5$, $df = 2$, $P < 0.001$).

Phosphate

Phosphate levels did not show any significant difference between sampling months.

The overall trend of the nutrients throughout the water column is captured in Figure 4.14.

4.4 Chapter summary

The L4 site was chosen for its continual and historical monitoring, as well as the varying environmental dynamics which occurred over a five-month field campaign (May – September). A preliminary study collected 30 hours of ADCP data and 12 hours of EC data in May 2017 to examine the tidal dynamics on oxygen fluxes. Oxygen trend variability had minimal effects on the flux during the deployment in May, results suggested that it was the vertical velocity component driving the fluxes. In this study, it was illustrated that the fluxes at this site were driven tidally. Through closer examination of the tidal dynamics it was discovered that different components/signatures of the tide have varying effects on the flux phasing through their influence on the net flow patterns at the site.

With the further five-month investigation of EC benthic oxygen fluxes at this site, other oxygen drivers were examined. A weak correlation was established between median velocity and oxygen flux over the five-month field campaign. Therefore, other drivers such as nutrients, temperature, the dumping of dredged spoils and chlorophyll concentration were assessed. Inputs of anthropogenic OM (refractory dredged material) had an impact on the sediment type and cannot be ruled out of having some influence on the flux. However, without further sediment analysis at the specific location of where the EC fluxes were measured, the contribution of dredge material or plankton bloom have on OM benthic oxygen flux cannot be conclusively quantified. Statistical analysis was conducted on the nutrient concentrations

within the water column throughout the five-month field campaign. The relationship between nutrients and oxygen flux is further discussed in Chapter 5. The information in the preliminary study with the five-month deployment, contributes to the understanding of how physical oceanic drivers impact benthic oxygen flux, and will also aid any future modelling of oxygen fluxes in their respective environments.

Chapter 5

5. Discussion

5.1 Introduction

The open shelves of the ocean are highly dynamic environments, creating challenges and limitations for continuous oxygen flux measurements. The aquatic EC technique measures total oxygen flux between the overlaying water and benthic sediments. Minimal work has been conducted in exposed areas such as coastal shelf sea environments (McGinnis et al., 2014). The EC method has many advantages over traditional in situ chamber and microprofiler techniques, such as minimal disturbance of natural hydrodynamics, ambient light, and sediment (Berg and Huettel, 2008; Lorrai et al., 2010; Reimers et al., 2012). The EC system also samples at high frequency (64 Hz) however, disadvantages such as the cost combined with the fragile nature of the instrument, as well as complicated data analysis deters many users from deploying the instrument in challenging and complex environments (Lorrai et al., 2010; Reimers et al., 2012).

Within this thesis two shelf sea sites were selected within the scientifically and historically important WCO; Cawsands and L4. For the first field campaign the EC and microprofiler techniques were deployed within a seagrass bed over three tidal cycles which incorporated two dark periods and one light period. The second field campaign at L4 was conducted over a 5-month period (May – September). In addition to the EC, CTD and nutrient data were collected during the 5-month campaign on a weekly basis. An ADCP was utilised for only the initial deployment in May to determine a detailed description of tidal velocities at L4.

5.2 EC data processing methods

As the EC is a relatively new technique, and little is known about how best to process the data collected by the instrument in a complex shelf sea environment, a sensitivity analysis to understand the effect of different processing approaches was completed, to ensure that benthic

oxygen flux was calculated correctly. Particular focus was given to the timeshift (to account for the physical separation of the microelectrode and ADV) and detrending options (to remove underlying trends in the velocity and oxygen readings in order to estimate the fluctuating component) as these steps in the processing of the data are heavily dependent on the environmental conditions (tidal currents, temperature, nutrients and chlorophyll levels). By undertaking this optimisation process it is possible to have greater confidence in the processing methods and hence EC flux datasets for this site. The analysis completed will also be beneficial to researchers undertaking similar deployments at other sites.

Following completion of initial despiking of the dataset to remove obvious anomalies, filtering of the EC dataset is necessary in order to smooth and remove noise. Multiple filtering options, including space-phase and cubic spline filters have been used by previous authors to process ADV and oxygen microelectrode raw data (Lorrai et al., 2010; Long et al., 2013; Volaric et al., 2018). The phase space filter developed by Nikora and Goring (2002) excludes spikes and noise. A cubic spline allows for an interpolating polynomial that is smoother and has a smaller error than other interpolating polynomials. A comparison between filtering techniques described in Section 2.9.5, demonstrated that flux values were insensitive to the filtering method, and so any of the tested approaches were considered appropriate. The phase space filter method was chosen due to the removal of spikes and noise, and the comparison provided confidence, that the flux values presented were not influenced by the filtering method.

A common method used when processing ADV data is to align the results with the dominant flow direction such that $\bar{v} = \bar{w} = 0\ ms^{-1}$ and $\bar{u} \neq 0\ ms^{-1}$. A slight misalignment between the ADV and dominant flow direction is demonstrated in Figure 2.17. For the dataset presented in this thesis, applying a correction to account for this misalignment was not found to improve the accuracy of the flux estimates. Results demonstrated that rotating the ADV data, introduced artefacts of u and v into the vertical velocity signal, producing flux values which were several orders of magnitude different from expected levels stated within literature for a similar environment (Reimers et al., 2012; McGinnis et al., 2014). As a result, the ADV data were not rotated when calculating the flux values presented in this thesis.

Selection of an inappropriate detrending method can result in an underestimation of flux within a tidal environment. As a result, it was necessary to conduct a comparison between multiple detrending methods (including linear detrending, running mean and frequency filter) in order to ensure that value flux data was obtained from the measurements. This comparison

demonstrated that the use of an inappropriate detrending option for a specific environment, could result in a 50% oxygen flux underestimation (Figure 2.23). Figure 2.23 demonstrates an example dataset where using a linear trend produced a median flux value of JO_2 = 10 mmol m^{-2} day^{-1} whereas the running mean produced JO_2 = 7 mmol m^{-2} day^{-1} and frequency filter JO_2 = 5 mmol m^{-2} day^{-1} respectively. Careful analysis of detrending options is vital to ensure that all frequency contribution is captured within the resultant flux value and should be considered for all EC deployments.

The spatial separation between the measuring tip of the microelectrode and the ADV measurement volume, as well as differing instrument response times leads to a time-offset between the oxygen and velocity timeseries. Resultant flux values can be undercalculated up to 25% if a timeshift is not applied. As discussed in Section 2.10 an optimal timeshift was chosen for the studies within this thesis. An optimal timeshift is when a timeshift is calculated for each window by selecting the timeshift for when the flux is the largest, whereas an average timeshift is the application of the average of the optimal timeshift windows over the timeseries to each window. It was found that the application of a fixed average timeshift led to underestimates of flux, it was more appropriate to calculate an optimum timeshift for each 15-minute window which led to the maximum flux calculation. This was necessary due to the constantly changing conditions in this tidal environment which affected whether the water flow hit the ADV or the micro-electrode measuring volume first (Figure 2.4, Schematic of equipment set-up).

Selection of the correct processing tools can have substantial implications on the resultant flux value, and as a result a thorough sensitivity analysis was taken for the data presented in this thesis. This analysis demonstrated that environmental factors, such as a tidal environment can have implications on which tool is selected (detrending and timeshift). Application of site-specific processing methods, selected using appropriate sensitivity analysis, combined with trial deployments, careful and appropriate design of the frame, cleaning of datasets, and quality control of each 15-minute segment of ADV and oxygen data, such as the assessment of each 15-minute segment via spectral analysis, provides confidence in the values of flux obtained using the EC method (Figure 2.18). Even though software such as SOFEA (McGinnis et al., 2008) is available commercially, this analysis of various processing tools has demonstrated that manual processing of data is still required to understand certain processing effects within complex environments, such as coastal shelf sea areas. Application of standard tools without

site-specific sensitivity analysis could lead to substantial errors in the flux data obtained, potentially invalidating the research.

5.3 Cawsands study

Microprofiling (measuring diffusive oxygen uptake) (Jørgensen, and Revsbech, 1985) and benthic chambers/cores (measuring oxygen uptake) (Macreadie et al., 2006) are established measuring techniques used to quantify oxygen flux levels in aquatic environments, whereas the EC (measuring total turbulent oxygen flux) (Berg et al., 2003) is a relatively understudied technique, especially in shelf sea environments. This study compared EC and microprofiler flux during varying environmental conditions (light/dark and flow tidal) within a dynamic seagrass habitat (Cawsands). Seagrass beds contain a variety of benthic oxygen flux drivers, including photosynthesis/respiration, generation of turbulence/mixing as well as seagrass mortality which affects oxygen and carbon cycling (Hume et al., 2011). These ecologically important carbon stores are becoming increasingly under threat due to climate change and rising pollution levels (Erwin, 2009). Therefore, steps to understand and monitor the drivers that effect these sensitive ecosystems of environmental importance is vital.

The location and size of the EC footprint was assessed to determine when the EC and microprofiler were co-located however, the results indicated that flux trends were similar regardless of the co-location of the instruments (Figure 3.1). This may be due to the close proximity of the instruments (<5 meters) and the relatively small quantity of data available for assessment (three tidal cycles with one light period). Statistical comparison of both EC and Microprofiler datasets validated the EC technique during dark periods (Figure 3.2). These flux values were in the same direction and order of magnitude. This result also provided confidence in the EC processing methodology developed within this thesis. EC fluxes were not statistically similar to microprofiler fluxes during light periods (Section 3.3.4). These results suggest that the EC can detect additional flux contributions within light periods which is not possible using a microprofiler.

Within this study it is suggested that oxygen diffusion is the main driver of flux during dark periods as identified by correlating EC and microprofiler flux values. During photic conditions it is suggested that the positive flux values measured by the EC relate to photosynthesis being a contributing driver during this period, with other processes such as diffusion (indicated by the microprofiler), bioirrigation and microbial respiration are also likely to be present. As the

microprofiler can only detect the diffusive flux component, it did not capture photosynthesis during the light period and respiration in non-photic periods.

The large range of EC fluxes in the non-photic periods illustrates the EC detected a wide range of drivers (integrating the seagrass and the sediment fluxes, photosynthesis in the day and respiration of the seagrass at night will lead to differences), which was not captured by microprofiler. This is due is due to the capabilities of both techniques, as the EC measures flux 12 cm above the seabed, capturing total flux from the bottom boundary layer, whereas the microprofiler can only measure diffusive flux with the diffusive boundary layer.

The use of the EC technique which measures total flux is a valuable tool for complex and inhomogeneous environments such as seagrass beds with multiple flux drivers. A combination of oxygen flux measuring tools (i.e., EC and microprofiler) is advantageous as it allows some assessment of the different drivers within the total flux measured by the EC.

An examination of horizontal flow velocities in correlation with oxygen flux values provides further insight in determining benthic flux drivers within this seagrass habitat using the EC technique. Figure 3.3 demonstrates higher flow velocities cause larger values of negative flux during dark periods. This result suggests that diffusion is the main driver during dark periods observed by the EC. As horizontal flow velocity increases, the bottom boundary layer thins, increasing the rate of diffusion. Whereas, during light conditions there was a weaker correlation between horizontal flow velocity and oxygen flux observed, indicating multiple other drivers may be present within this habitat (i.e., photosynthesis, bioirrigation, and increased microbial activity due to higher temperatures seen in optode data Figure 3.1).

Querios et al. (2015) is the only other study conducted in the vicinity of the Cawsands study site; however, their measurements were obtained outside of the seagrass bed. This study by Querios et al. (2015) focused on bioirrigators using sediment cores to identify the main species which contributed to seasonal patterns of bioturbation at this site, but it did not quantify oxygen flux. Quantifying the bioturbation rate during photosynthesis was not within the scope of this thesis therefore, a benthic chamber study was not used. Benthic analysis of bioturbation/bioirrigation during our field campaign would have added to the understanding of flux drivers at this site during light and dark conditions (Topping et al., 2016).

5.4 L4 study

A combination of oxygen flux measuring techniques in a shallow environment as discussed in Chapter 3, provided confidence for the use of the EC instrumentation at the L4 study site and indicated flow velocities (diffusion) as the main driver during dark conditions. A study presented in Chapter 4 utilises the study site L4 which has a minimum depth of 50 m. Chapter 4 outlines the need to assess the tidal components as well as other drivers of benthic oxygen flux within shelf sea environments.

The aim of the L4 study was to establish a cohesive picture of oxygen dynamics at the designated coastal study site, via assessment of oxygen fluxes along with environmental time series data, and historical water column data. Data were collected over a 5-month sampling period (May – September) using an EC, CTD and ADCP. ADCP data was only collected during the May field campaign providing a detailed insight into the flow velocity profiles on the shelf for that month. This enabled an investigation of the contribution of flow velocity to oxygen flux at L4 after flow velocity was identified as the primary driver during dark periods, during the field campaign at Cawsands. CTD and nutrient analysis were conducted to identify additional drivers. Furthermore, this study aimed to demonstrate that the EC technique and processing techniques developed is a useful in situ monitoring and assessment tool for oxygen dynamics in a coastal shelf sea environment.

As indicated in Figure 4.12 and 4.14 environmental changes (temperature, chlorophyll and nutrients) occurred throughout the five-month sampling period. This environmental change may have led to variations in the drivers of these fluxes (Figure 4.8) and is further discussed throughout this section.

Benthic oxygen flux exhibited a strong tidal signature, with significant velocity contributions from the surface tide, as well as some minor contributions from the internal tide. As local topographical features create internal tides, the assessment of these tidal dynamics on benthic oxygen flux measurements is key for understanding biogeochemical cycling. As shown in Figure 4.12, the May deployment occurred during the least stratified period. The magnitude of the internal tide is partially driven by the strength of the density gradient (stratification of the water column). Therefore, as stratification increases throughout the sampling months the potential change of magnitude of the tide may impact flux values.

Examination of median fluxes throughout the five-month sampling campaign found median velocities correlated weakly with median fluxes (R= 0.43). However, it is important to note that only five data points were used to obtain this correlation. This result demonstrated that drivers other than velocity such as nutrient and temperature may contribute to flux throughout the sampling period.

As discussed in Section 1.9, Reimers et al. (2012) and McGinnis et al., (2014) state that velocity is the primary driver of oxygen flux within selected shelf sea environments. Through closer examination of the tidal dynamics at L4, it was discovered that different components/signatures of the tide have varying effects on the flux phasing through their influence on the net flow patterns at the site. This assessment of the tidal components in relation to flux magnitudes is novel as it has not yet been addressed within literature.

In the preliminary study conducted in May dissipation trends demonstrate that at certain times of the tidal cycle changes in turbulence occur, directly impacting flux values (Figure 4.5). When considering the influence of flow direction on the flux values, it can be seen that both the oxygen flux (JO_2 = -11 mmol m^{-2} d^{-1}) and median dissipation rate of turbulent kinetic energy ($\varepsilon = 2.15x10^{-5} \pm 0.01\ x10^{-5}$ W kg^{-1}) were smaller when flow is in the north direction than when the flow was to the south (JO_2 = 18 mmol m^{-2} d^{-1} and $\varepsilon = 2.69x10^{-5} \pm 0.01\ x10^{-5}$ W kg^{-1}). The asymmetry of the tidal velocities and turbulence (Figure 4.5) was due to topographical features at this site (Figure 1.6). However, other factors such as sediment type and biological drivers can also influence patterns in oxygen fluxes (Attard et al., 2016).

Although the EC method assumes oxygen and velocity homogeneity, it can still be used over inhomogeneous substrates. EC footprints are calculated using the height of EC microelectrode and the surface roughness of the seabed. Within a tidal system, the footprint size and location will change with flow direction on a six-hourly basis due to tidal flow reversal. Changing flow direction, therefore, leads to changes in the surface roughness and sediment types as the footprint changes location (Berg et al., 2007). This factor contributes to small flux variations, e.g. higher oxygen fluxes may be observed in different directions as respiration rates vary across the seafloor due to localised patches of microbial communities (de Beer et al., 2006). When the flow is in the southerly direction, the sediment type within the EC footprint (73 m long, 0.78 m wide with peak readings at 41 m) is sandy. By contrast, when the flow is in the northerly direction, the sediment type within the EC footprint (147 m long, 0.78 m wide with peak readings at 75 m) is coarse: refer to Figure 1.6, noting that the footprint occurs upstream.

Several EC studies (Berg et al., 2009; McGinnis et al 2014; Attard et al., 2014) have examined the importance of sediment composition on bottom flows. McGinnis et al. (2014) describe how varying flow rates affected oxygen stored within the sediment. This study found that ripples increased oxygen consumption by 10%, solely due to the increased surface area of the seabed within the footprint of the EC (McGinnis et al., 2014). During our L4 study, bed ripples were not observed by four camera deployments on the EC frame and a remote operated vehicle with a camera however, depressions formed by bio-irrigation were present on the seabed (Figure 5.1). Flow over worm tubes can also stimulate a secondary flow through the tubes, and thus, enhance oxygen uptake (Kristensen et al., 1992).

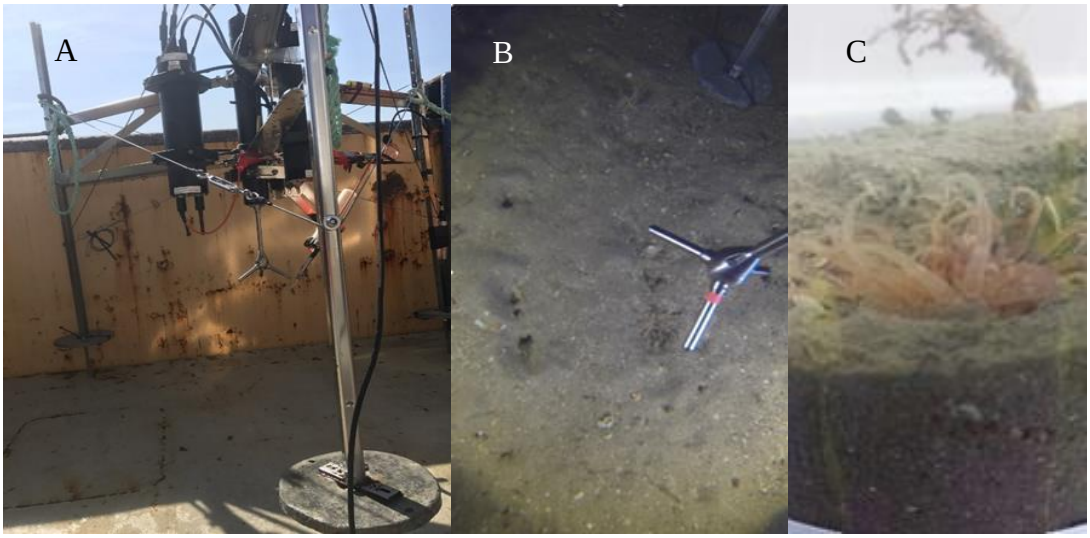

Figure 5.1: A) The EC lander aboard the research vessel prior to deployment. B) The ADV during test deployments, noting sediment type and visible bio-irrigation holes in the seafloor. C) A core taken from the L4 site in May 2017, indicating bioirrigators, Dahlia Anemone (Urticina feline).

Changes to sediment organic matter concentrations can be influenced by multiple factors including dumping of organic material, marine snow from plankton blooms as well as runoff from the land. As demonstrated in Figure 4.12 chlorophyll levels which can be used to indicate plankton blooms were relatively low at L4 but were highest between June and September. Historical records indicate that chlorophyll concentrations in 2017, when this study was conducted, were below average for the time of year (Figure 4.11). Comparative levels of chlorophyll-a found within literature indicate plankton levels are effectively a very low biomass at L4 (Furuya, K., 1990; Gohin et al., 2019; Marañón et al., 2021). The carbon input to the sediment from the plankton in this area is likely to be extremely low due to the hydrology (low chlorophyll concentrations combined with a macrotidal environment) (Cavalcanti et al.,

2018; Abdou et al., 2020; Young et al., 2021). Settling chambers and sediment analysis would be required to further examine the relationship between nutrients, plankton and oxygen flux at this site, which were not within the scope of this thesis.

It was shown that dumping of dredged material led to a substantial change in sediment composition 2 nautical miles from the site and this could potentially be associated with changes in nutrient concentrations (Figure 4.13). However, a comparison between two timeseries of nutrient concentrations, 2016 (no dumping event) and 2017 (dumping event), show no significant differences. Therefore, it is concluded from available data collected during this study that dumping of dredged material does not appear to be a driver of nutrients within the water column or benthic oxygen transfer at L4 during the five-month field campaign. It is important to note that the sediment samples were obtained at a substantial distance (2 nautical miles) from the EC sampling site. The detritus from the dumping may also have settled further from the sampling site when considering the hydrology of the area. Further investigation into plankton and nutrient concentrations within the sediment at L4 is required to provide a more complete understanding of drivers of oxygen flux at L4.

Nitrification (oxidation) of ammonia can lead to increases in nitrite and nitrate concentrations. An ammonia pulse uses oxygen and therefore modifies oxygen levels within that environment. Nutrients within the benthic boundary layer (BBL) and sediment may alter oxygen consumption impacting the oxygen gradient, leading to a variation in oxygen transfer. Furthermore, a change in silicate concentration recorded in June at 50 m depth may be due a release from diatom decomposition with bottom waters (Figure 4.14). Silicate is produced by biological activity. Diatoms extract dissolved silicic acid as they grow, and return it when they die (Puppe, D., 2020; Govindan et al., 2021). However, nutrient analysis within the BBL and sediment analysis at the measurement site is required to relate these nutrient levels definitively to the oxygen flux recorded.

Monthly median flux values throughout the 5-month sampling campaign varied by JO_2 = 11 mmol m^{-2} d^{-1}, from JO_2 = -11 mmol m^{-2} d^{-1} to JO_2 = -22 mmol m^{-2} d^{-1}. The smallest flux value was observed in July (Figure 4.8) coinciding with a pulse in ammonia in June and July (Figure 4.14). Furthermore, lower median turbulence and median flow velocities in July resulted in less oxygen driven into the sediment (lower median flux); the median flow velocity measured in July was $\overline{U}$=5.5 cm s^{-1} less than that recorded in September, when the highest median velocity of $\overline{U}$=13 cm s^{-1} was measured (Figure 4.9). Even though low levels of chlorophyll were

observed, internal loading of phytoplankton could have increased organic matter decomposition leading to mineralisation and release of ammonia. This process takes oxygen out of the water due to mineralisation increasing nutrient release, leading to an increase in oxygen demand e.g., nitrification increasing median flux levels. However, as previously stated, further analysis of nutrients within the sediment is required to definitively correlate flux with nutrient processes outlined in this section.

Changes in temperature were observed through the five-month sampling period (Figure 4.12) with ANOVA tests showing a statistical difference between the temperature in May and September. Previous studies (Bourgeois et al., 2017; Tasnim et al., 2021) have demonstrated that sediment oxygen demand can increase significantly with an increase in temperature. The addition of a microprofiler at the L4 site would have provided insight into changes in temperature gradient throughout the five deployments and benthic chambers would provide further insight into oxygen drivers described within Chapter 5. Without this information, further interpretation of drivers at this site is not possible. Nonetheless, this study has made advances in quantifying the drivers of oxygen flux at L4 and Cawsands, in particular the contribution of tidal dynamics, and photosynthetic conditions.

5.5 Conclusions

This study successfully deployed microprofiler and EC equipment using optimised processing tools to obtain some of the first oxygen flux measurements at two coastal shelf sea sites. This study has validated EC data processing and resultant flux estimates by comparing the EC with the traditional microprofiler technique during dark periods. Results showed that the EC technique can be used to obtain a more complete understanding of benthic oxygen flux within this environment by measuring total flux. This study also provided the first insight into drivers of oxygen flux at Cawsands. Furthermore, at the L4 site the tidal analysis and CTD data have clearly shown this environment is not homogeneous and is impacted by topography and density gradients. It is clear that the surface tidal flows dominate at the site however, the internal tidal velocities near the bottom are not insignificant. As the density gradients increase throughout the summer months it is suspected that internal tidal contribution would increase, creating a stronger driver of flux. It is expected that senescence of plankton material within the sediment at the L4 area is extremely low due to the hydrology of the site and low chlorophyll levels. However, a lack of data capturing nutrients within the sediment and ADCP data throughout the

five-month sampling campaign at L4 meant that a complete quantification of the drivers of oxygen flux at this site was not achievable. A more complete picture could be obtained if a microprofiler (measuring diffusive flux) and benthic chambers (measuring sediment oxygen uptake) were deployed alongside the EC as well as settling chambers and sediment nutrient analysis. Nonetheless, this study has made advances in EC processing and has provided a first insight into tidal and oxygen dynamics at a historical research station.

EC technique measures aquatic oxygen flux non-invasively by capturing the vertical turbulent fluxes within aquatic boundary layers (Berg et al., 2015). Chotikarn, (2015) suggests that even though the EC technique has been used in aquatic systems for over a decade, it is still under development for this purpose. Measurement of oxygen flux within coastal shelf seas is difficult to achieve using more traditional methods such as chambers/cores and microprofiling (McGinnis et al, 2008). Despite this, only a small number of authors have undertaken EC measurements in shelf seas due to the significant deployment challenges. Nonetheless, by solving these challenges, this thesis has demonstrated that this method can advance our knowledge of oxygen dynamics in shallow shelf seas.

5.6 Recommendations for future work

This thesis has presented new data which has enabled improved understanding of benthic oxygen dynamic drivers within two coastal shelf sea sites. However, these results have also highlighted new research questions. In this section another method for measuring benthic oxygen flux is addressed, as well as technologies which can be applied to the EC to improve this technique.

5.6.1 Use of benthic chamber

The research reported in Chapter 3 and Chapter 4 would have benefited from benthic sediment chamber analysis to measure bioirrigation/bioturbation rates. This would have assessed the contribution of bioirrigators from total flux. The method of benthic sediment core analysis in the context of this study is outlined:

5.6.2 Eddy covariance technology

EC optic oxygen sensors have been developed which are more robust than the Clark-type glass oxygen microelectrode (Chipman et al., 2012). However, these sensors have known drawbacks due to the larger size of the measurement tip including reduced sample rate and greater fouling risk. To date these sensors have not been tested in a shelf sea environment and are known to perform less well where the flow direction changes due to the measuring tip not being in the flow direction. It is suggested that a comparative study of Clark type microelectrodes used in this thesis with these robust optic sensors in a shelf sea environment would highlight whether the advantages of a robust sensor outweigh the precise and faster response, yet fragile nature, of the glass Clark-type microelectrode.

5.6.3 Comparative study

Flux readings, discussed in Chapter 4, were obtained during an atypical plankton year (low plankton levels). It is recommended that a similar field campaign is undertaken over a number

of years to capture a year with high plankton levels to categorise the full extent plankton blooms have on benthic oxygen flux at L4. The use of a microprofiler and benthic sediment cores at the site would also enable the quantification of the various benthic drivers from the EC which assesses total turbulent flux. In combination with these techniques, the use of an acoustic Doppler current profiler, throughout a seasonal cycle, would also provide an insight into the hydrodynamic variability throughout the water column. This comparative study could aid future modelling of fluxes at the study location. The combination of a comparative study with the use of a variety of measuring techniques would provide further insight into the annual changes in benthic oxygen dynamics at L4 and can be applied to a variety of shelf sea sites.

References

Abdou, M., Gil-Diaz, T., Schäfer, J., Catrouillet, C., Bossy, C., Dutruch, L., Blanc, G., Cobelo-Garcia, A., Massa, F., Castellano, M. and Magi, E., 2020. Short-term variations of platinum concentrations in contrasting coastal environments: The role of primary producers. *Marine Chemistry*, *222*, p.103782.

Adams, D.D., Matisoff, G. and Snodgrass, W.J., 1982. Flux of reduced chemical constituents (Fe 2+, Mn 2+, NH inf4 sup+ and CH 4) and sediment oxygen demand in Lake Erie. *Hydrobiologia*, *91*, pp.405-414.

Alberto, M.C., Quilty, J., Wassmann, R., Buresh, R., Correa Jr, T. and Centeno, C.A., 2018. Monitoring GHG emissions (water, CO2, CH4) and energy exchange from rice-based cropping systems. *Integrated Land EcoSystem Atmosphere Processes Study*, p.11.

Aller, R.C. and Aller, J.Y., 1998. The effect of biogenic irrigation intensity and solute exchange on diagenetic reaction rates in marine sediments. *Journal of Marine Research*, *56*(4), pp.905-936.

Altieri, A., 2018. Dead Zones: Low Oxygen in Coastal Waters. *Encyclopedia of Ecology*, *321*, p.22.

Altieri, A.H. and Diaz, R.J., 2019. Dead Zones: Oxygen Depletion in Coastal Ecosystems. In *World Seas: an Environmental Evaluation* (pp. 453-473). Academic Press.

Anderson, L.G., Hall, P.O., Iverfeldt, A., Rutgers van der Loejf, M.M., Sundby, B. and Westerlund, S.F., 1986. Benthic respiration measured by total carbonate production. *Limnology and Oceanography*, *31*(2), pp.319-329.

Arrigo, K.R., 2004. Marine microorganisms and global nutrient cycles. *Nature*, *437*(7057), p.349.

Atkins, W. R. G. 1923 The phosphate content of fresh and salt waters in its relationship to the growth of the algal plankton. Journal of the Marine Biological Association of the U.K. 13, 119–150.

Attard, K.M., Glud, R.N., McGinnis, D.F. and Rysgaard, S., 2014. Seasonal rates of benthic primary production in a Greenland fjord measured by aquatic eddy correlation. *Limnology and Oceanography*, *59*(5), pp.1555-1569.

Attard, K.M., Hancke, K., Sejr, M.K. and Glud, R.N., 2016. Benthic primary production and mineralization in a High Arctic Fjord: in situ assessments by aquatic eddy covariance. *Marine Ecology Progress Series*, *554*, pp.35-50.

Attard, K.M., Rodil, I.F., Berg, P., Norkko, J., Norkko, A. and Glud, R.N., 2019. Seasonal metabolism and carbon export potential of a key coastal habitat: The perennial canopy-forming macroalga Fucus vesiculosus. *Limnology and Oceanography*, *64*(1), pp.149-164.

Attard, K.M., Søgaard, D.H., Piontek, J., Lange, B.A., Katlein, C., Sørensen, H.L., McGinnis, D.F., Rovelli, L., Rysgaard, S., Wenzhöfer, F. and Glud, R.N., 2018. Oxygen fluxes beneath Arctic land-fast ice and pack ice: towards estimates of ice productivity. *Polar Biology*, *41*(10), pp.2119-2134.

Attard, K.M., Stahl, H., Kamenos, N.A., Turner, G., Burdett, H.L. and Glud, R.N., 2015. Benthic oxygen exchange in a live coralline algal bed and an adjacent sandy habitat: an eddy covariance study. *Marine Ecology Progress Series*, *535*, pp.99-115.

Badjeck, M.C., Allison, E.H., Halls, A.S. and Dulvy, N.K., 2010. Impacts of climate variability and change on fishery-based livelihoods. *Marine policy*, *34*(3), pp.375-383.

Baldocchi, D.D., 2003. Assessing the eddy covariance technique for evaluating carbon dioxide exchange rates of ecosystems: past, present and future. *Global change biology*, *9*(4), pp.479-492.

Beman, J.M., Vargas, S.M., Vazquez, S., Wilson, J.M., Yu, A., Cairo, A. and Perez-Coronel, E., 2021. Biogeochemistry and hydrography shape microbial community assembly and activity in the eastern tropical North Pacific Ocean oxygen minimum zone. *Environmental Microbiology*, *23*(6), pp.2765-2781.

Berg (2019). *Eddy Covariance - Peter Berg*. [online] Faculty.virginia.edu. Available at: http://faculty.virginia.edu/berg/ [Accessed 5 Jul. 2019].

Berg, P. and Huettel, M., 2008. Monitoring the seafloor using the noninvasive eddy correlation technique. *Oceanography*, *21*(4), pp.164-167.

Berg, P., Glud, R.N., Hume, A., Stahl, H., Oguri, K., Meyer, V. and Kitazato, H., 2009. Eddy correlation measurements of oxygen uptake in deep ocean sediments. *Limnology and Oceanography: Methods*, *7*(8), pp.576-584.

Berg, P., Koopmans, D.J., Huettel, M., Li, H., Mori, K. and Wüest, A., 2016. A new robust oxygen-temperature sensor for aquatic eddy covariance measurements. *Limnology and Oceanography: Methods*, *14*(3), pp.151-167.

Berg, P., Long, M.H., Huettel, M., Rheuban, J.E., McGlathery, K.J., Howarth, R.W., Foreman, K.H., Giblin, A.E. and Marino, R., 2013. Eddy correlation measurements of oxygen fluxes in permeable sediments exposed to varying current flow and light. *Limnology and Oceanography*, *58*(4), pp.1329-1343.

Berg, P., Reimers, C.E., Rosman, J.H., Huettel, M., Delgard, M.L., Reidenbach, M.A. and Özkan-Haller, H.T., 2015. Time lag correction of aquatic eddy covariance data measured in the presence of waves. *Biogeosciences*, *12*(22), pp.6721-6735.

Berg, P., Røy, H. and Wiberg, P.L., 2007. Eddy correlation flux measurements: The sediment surface area that contributes to the flux. *Limnology and Oceanography*, *52*(4), pp.1672-1684.

Berg, P., Røy, H., Janssen, F., Meyer, V., Jørgensen, B.B., Huettel, M. and de Beer, D., 2003. Oxygen uptake by aquatic sediments measured with a novel non-invasive eddy-correlation technique. *Marine Ecology Progress Series*, *261*, pp.75-83.

Bernard, G., Gammal, J., Järnström, M., Norkko, J. and Norkko, A., 2019. Quantifying bioturbation across coastal seascapes: Habitat characteristics modify effects of macrofaunal communities. *Journal of Sea Research*, *152*, p.101766.

Bertagnolli, A.D. and Stewart, F.J., 2018. Microbial niches in marine oxygen minimum zones. *Nature Reviews Microbiology*, *16*(12), pp.723-729.

Bertin, X., de Bakker, A., Van Dongeren, A., Coco, G., Andre, G., Ardhuin, F., Bonneton, P., Bouchette, F., Castelle, B., Crawford, W.C. and Davidson, M., 2018. Infragravity waves: From driving mechanisms to impacts. *Earth-Science Reviews*, *177*, pp.774-799.

Bierlein, K.A., Rezvani, M., Socolofsky, S.A., Bryant, L.D., Wüest, A. and Little, J.C., 2017. Increased sediment oxygen flux in lakes and reservoirs: The impact of hypolimnetic oxygenation. *Water Resources Research*, *53*(6), pp.4876-4890.

Bluteau, C.E., Jones, N.L. and Ivey, G.N., 2011. Estimating turbulent kinetic energy dissipation using the inertial subrange method in environmental flows. *Limnology and Oceanography: Methods*, *9*(7), pp.302-321.

Bolam, S.G., Mason, C., Curtis, M., Griffith, A., Clare, D., Pettafor, A., Hawes, J., Fernand, L., Beraud, C. (2018). Dredged Material Disposal Site Monitoring Round the Coast of England: Results of Sampling. Cefas.

Bonaglia, S., Rämö, R., Marzocchi, U., Le Bouille, L., Leermakers, M., Nascimento, F.J. and Gunnarsson, J.S., 2019. Capping with activated carbon reduces nutrient fluxes, denitrification and meiofauna in contaminated sediments. *Water research*, *148*, pp.515-525.

Bopp, L., Le Quéré, C., Heimann, M., Manning, A.C. and Monfray, P., 2002. Climate-induced oceanic oxygen fluxes: Implications for the contemporary carbon budget. *Global Biogeochemical Cycles*, *16*(2), pp.6-1.

Boström, B., Andersen, J.M., Fleischer, S. and Jansson, M., 1988. Exchange of phosphorus across the sediment-water interface. In *Phosphorus in freshwater ecosystems*(pp. 229-244). Springer, Dordrecht.

Boudreau, B.P. and Jorgensen, B.B. eds., 2001. *The benthic boundary layer: Transport processes and biogeochemistry*. Oxford University Press.

Boudreau, B.P. and Jørgensen, B.B., 2001. *Diagenesis and sediment-water exchange* (pp. 211-244). Oxford University Press, New York.

Boudreau, B.P. and Marinelli, R.L., 1994. A modelling study of discontinuous biological irrigation. *Journal of Marine Research*, *52*(5), pp.947-968.

Bouldin, D.R., 1968. Models for describing the diffusion of oxygen and other mobile constituents across the mud-water interface. *The Journal of Ecology*, pp.77-87.

Bourgeois, S., Archambault, P. and Witte, U., 2017. Organic matter remineralization in marine sediments: A Pan-Arctic synthesis. *Global Biogeochemical Cycles*, *31*(1), pp.190-213.

Boyer, J.N., Kelble, C.R., Ortner, P.B. and Rudnick, D.T., 2009. Phytoplankton bloom status: Chlorophyll a biomass as an indicator of water quality condition in the southern estuaries of Florida, USA. *Ecological indicators*, *9*(6), pp.S56-S67.

Braeckman, U., Foshtomi, M.Y., Van Gansbeke, D., Meysman, F., Soetaert, K., Vincx, M. and Vanaverbeke, J., 2014. Variable importance of macrofaunal functional biodiversity for biogeochemical cycling in temperate coastal sediments. *Ecosystems*, *17*(4), pp.720-737.

Braeckman, U., Pasotti, F., Vázquez, S., Zacher, K., Hoffmann, R., Elvert, M., Marchant, H., Buckner, C., Quartino, M.L., Mác Cormack, W. and Soetaert, K., 2019. Degradation of macroalgal detritus in shallow coastal Antarctic sediments. *Limnology and Oceanography*.

Brand, A., McGinnis, D.F., Wehrli, B. and Wüest, A., 2008. Intermittent oxygen flux from the interior into the bottom boundary of lakes as observed by eddy correlation. *Limnology and Oceanography*, *53*(5), pp.1997-2006.

Brand, A., McGinnis, D.F., Wehrli, B. and Wüest, A., 2008. Intermittent oxygen flux from the interior into the bottom boundary of lakes as observed by eddy correlation. *Limnology and Oceanography*, *53*(5), pp.1997-2006.

Breitburg, D., Levin, L.A., Oschlies, A., Grégoire, M., Chavez, F.P., Conley, D.J., Garçon, V., Gilbert, D., Gutiérrez, D., Isensee, K. and Jacinto, G.S., 2018. Declining oxygen in the global ocean and coastal waters. *Science*, *359*(6371).

Brodie, J., Lewis, S., Wooldridge, S., Bainbridge, Z., Waterhouse, J. and Honchin, C., 2015. Ecologically relevant targets for pollutant discharge from the drainage basins of the Fitzroy Region, Great Barrier Reef.

Bryant, L.D., Gantzer, P.A. and Little, J.C., 2011. Increased sediment oxygen uptake caused by oxygenation-induced hypolimnetic mixing. *Water research*, *45*(12), pp.3692-3703.

Bryant, L.D., Lorrai, C., McGinnis, D., Brand, A., Wüest, A. and Little, J.C., 2010. Variable sediment oxygen uptake in response to dynamic forcing. *Limnology and Oceanography*, *55*(2), pp.950-964.

Bryant, L.D., McGinnis, D.F., Lorrai, C., Brand, A., Little, J.C. and Wüest, A., 2010. Evaluating oxygen fluxes using microprofiles from both sides of the sediment-water interface. Limnology and Oceanography: Methods, 8(11), pp.610-627.

Bryant, L.D., McGinnis, D.F., Lorrai, C., Brand, A., Little, J.C. and Wüest, A., 2010. Evaluating oxygen fluxes using microprofiles from both sides of the sediment-water interface. *Limnology and Oceanography: Methods*, *8*(11), pp.610-627.

Burba, G., 2013. Eddy covariance method for scientific, industrial, agricultural and regulatory applications: A field book on measuring ecosystem gas exchange and areal emission rates. LI-Cor Biosciences.

Calhoun, S.K., Haas, A.F., Takeshita, Y., Johnson, M.D., Fox, M.D., Kelly, E.L., Mueller, B., Vermeij, M.J., Kelly, L.W., Nelson, C.E. and Price, N.N., 2017. Exploring the occurrence of and explanations for nighttime spikes in dissolved oxygen across coral reef environments. *PeerJ Preprints*, *5*, p.e2935v2.

Camargo, J.A. and Alonso, Á., 2006. Ecological and toxicological effects of inorganic nitrogen pollution in aquatic ecosystems: a global assessment. *Environment international*, *32*(6), pp.831-849.

Canal-Vergés, P., Vedel, M., Valdemarsen, T., Kristensen, E. and Flindt, M.R., 2010. Resuspension created by bedload transport of macroalgae: implications for ecosystem functioning. *Hydrobiologia*, *649*(1), pp.69-76.

Cathalot, C., Van Oevelen, D., Cox, T.J., Kutti, T., Lavaleye, M., Duineveld, G. and Meysman, F.J., 2015. Cold-water coral reefs and adjacent sponge grounds: Hotspots of benthic respiration and organic carbon cycling in the deep sea. *Frontiers in Marine Science*, *2*, p.37.

Cavalcanti, L.F., Azevedo-Cutrim, A.C.G., Oliveira, A.L.L., Furtado, J.A., Araújo, B.D.O., Sá, A.K.D.D.S., Ferreira, F.S., Santos, N.G.R., Dias, F.J.S. and Cutrim, M.V.J., 2018. Structure of microphytoplankton community and environmental variables in a macrotidal estuarine complex, São Marcos Bay, Maranhão-Brazil. *Brazilian Journal of Oceanography*, *66*, pp.283-300.

Chan, F., Barth, J.A., Lubchenco, J., Kirincich, A., Weeks, H., Peterson, W.T. and Menge, B.A., 2008. Emergence of anoxia in the California current large marine ecosystem. *Science*, *319*(5865), pp.920-920.

Chang, J.H., 2017. *Climate and agriculture: an ecological survey*. Routledge.

Chipman, L., Berg, P. and Huettel, M., 2016. Benthic oxygen fluxes measured by eddy covariance in permeable Gulf of Mexico shallow-water sands. *Aquatic geochemistry*, *22*(5-6), pp.529-554.

Chipman, L., Huettel, M., Berg, P., Meyer, V., Klimant, I., Glud, R. and Wenzhoefer, F., 2012. Oxygen optodes as fast sensors for eddy correlation measurements in aquatic systems. *Limnology and Oceanography: Methods*, *10*(2012), pp.304-316.

Chotikarn, P., 2015. *An assessment of Eddy Correlation technique in marine habitats* (Doctoral dissertation).

Cloud, P. and Gibor, A., 1970. The oxygen cycle. *Scientific American*, *223*(3), pp.110-123.

Connell, D.W., 2005. *Basic concepts of environmental chemistry*. CRC Press.

Copper, P., 1992. PALEOSCENE 14. Organisms and Carbonate Substrates in Marine Environments. *Geoscience Canada*, *19*(3).

Davies, C.M., Long, J.A., Donald, M. and Ashbolt, N.J., 1995. Survival of fecal microorganisms in marine and freshwater sediments. *Appl. Environ. Microbiol.*, *61*(5), pp.1888-1896.

Davis, J.E., 2017. Booms, Blooms, and Doom: The Life of the Gulf of Mexico Dead Zone. Alabama Review, 70(2), pp.156-170.

de Arellano, J.V.G., Van Heerwaarden, C.C. and Lelieveld, J., 2012. Modelled suppression of boundary-layer clouds by plants in a CO 2-rich atmosphere. *Nature geoscience*, *5*(10), p.701.

de Beer, D., Sauter, E., Niemann, H., Kaul, N., Foucher, J.P., Witte, U., Schlüter, M. and Boetius, A., 2006. In situ fluxes and zonation of microbial activity in surface sediments of the Håkon Mosby Mud Volcano. *Limnology and Oceanography*, *51*(3), pp.1315-1331.

De Leo, F.C., Gauthier, M., Nephin, J., Mihaly, S. and Juniper, S.K., 2017. Bottom trawling and oxygen minimum zone influences on continental slope benthic community structure off Vancouver Island (NE Pacific). *Deep Sea Research Part II: Topical Studies in Oceanography*, *137*, pp.404-419.

Delefosse, M., Kristensen, E., Crunelle, D., Braad, P.E., Dam, J.H., Thisgaard, H., Thomassen, A. and Høilund-Carlsen, P.F., 2015. Seeing the unseen—bioturbation in 4D: tracing bioirrigation in marine sediment using positron emission tomography and computed tomography. *PloS one*, *10*(4), p.e0122201.

Diaz, R.J. and Breitburg, D.L., 2009. The hypoxic environment. In *Fish physiology* (Vol. 27, pp. 1-23). Academic Press.

Diaz, R.J. and Rosenberg, R., 1995. Marine benthic hypoxia: a review of its ecological effects and the behavioural responses of benthic macrofauna. *Oceanography and marine biology. An annual review*, *33*, pp.245-03.

Diaz, R.J. and Rosenberg, R., 2008. Spreading dead zones and consequences for marine ecosystems. *science*, *321*(5891), pp.926-929.

Directive, S.F., 2015, The Western Channel Observatory.

Doney, S.C., Ruckelshaus, M., Emmett Duffy, J., Barry, J.P., Chan, F., English, C.A., Galindo, H.M., Grebmeier, J.M., Hollowed, A.B., Knowlton, N. and Polovina, J., 2012. Climate change impacts on marine ecosystems. *Annual review of marine science*, *4*, pp.11-37.

Donis, D., Holtappels, M., Noss, C., Cathalot, C., Hancke, K., Polsenaere, P., Wenzhöfer, F., Lorke, A., Meysman, F.J., Glud, R.N. and McGinnis, D.F., 2015. An assessment of the precision and confidence of aquatic eddy correlation measurements. *Journal of Atmospheric and Oceanic Technology*, *32*(3), pp.642-655.

Duarte, B., Martins, I., Rosa, R., Matos, A.R., Roleda, M.Y., Reusch, T.B., Engelen, A.H., Serrão, E.A., Pearson, G.A., Marques, J.C. and Caçador, I., 2018. Climate change impacts on seagrass meadows and macroalgal forests: an integrative perspective on acclimation and adaptation potential.

Edwards, W.J., Conroy, J.D. and Culver, D.A., 2005. Hypolimnetic oxygen depletion dynamics in the central basin of Lake Erie. *Journal of Great Lakes Research*, *31*, pp.262-271.

Emery, K.O., 1968. Relict sediments on continental shelves of world. *AAPG Bulletin*, *52*(3), pp.445-464.

Erdem, Z., 2016. *Reconstruction of past bottom water conditions of the Peruvian Oxygen Minimum Zone (OMZ) for the last 22,000 years and the benthic foraminiferal response to (de) oxygenation* (Doctoral dissertation, Christian-Albrechts-Universität).

Erisman, J.W., Galloway, J., Seitzinger, S., Bleeker, A. and Butterbach-Bahl, K., 2011. Reactive nitrogen in the environment and its effect on climate change. *Current Opinion in Environmental Sustainability*, *3*(5), pp.281-290.

Erwin, K.L., 2009. Wetlands and global climate change: the role of wetland restoration in a changing world. *Wetlands Ecology and management*, *17*(1), p.71.

Fabricius, K.E., De'ath, G., Noonan, S. and Uthicke, S., 2014. Ecological effects of ocean acidification and habitat complexity on reef-associated macroinvertebrate communities. *Proceedings of the Royal Society B: Biological Sciences*, *281*(1775), p.20132479.

Fabricius, K.E., Logan, M., Weeks, S.J., Lewis, S.E. and Brodie, J., 2016. Changes in water clarity in response to river discharges on the Great Barrier Reef continental shelf: 2002–2013. *Estuarine, Coastal and Shelf Science*, *173*, pp.A1-A15.

Feuchtmayr, H., Pottinger, T.G., Moore, A., De Ville, M.M., Caillouet, L., Carter, H.T., Pereira, M.G. and Maberly, S.C., 2019. Effects of brownification and warming on algal blooms, metabolism and higher trophic levels in productive shallow lake mesocosms. *Science of the Total Environment*, *678*, pp.227-238.

Flanagan, L.B., Orchard, T.E., Logie, G.S., Coburn, C.A. and Rood, S.B., 2017. Water use in a riparian cottonwood ecosystem: Eddy covariance measurements and scaling along a river corridor. Agricultural and forest meteorology, 232, pp.332-348.

Ford, P.W., Bird, F.L. and Hancock, G.J., 1999. Effect of burrowing macrobenthos on the flux of dissolved substances across the water–sediment interface. *Marine and Freshwater Research*, *50*(6), pp.523-532.

Forster, S., Glud, R.N., Gundersen, J.K. and Huettel, M., 1999. In situ study of bromide tracer and oxygen flux in coastal sediments. *Estuarine, Coastal and Shelf Science*, *49*(6), pp.813-827.

Fourqurean, J.W., Duarte, C.M., Kennedy, H., Marbà, N., Holmer, M., Mateo, M.A., Apostolaki, E.T., Kendrick, G.A., Krause-Jensen, D., McGlathery, K.J. and Serrano, O., 2012. Seagrass ecosystems as a globally significant carbon stock. *Nature geoscience*, *5*(7), p.505.

Furuya, K., 1990. Subsurface chlorophyll maximum in the tropical and subtropical western Pacific Ocean: vertical profiles of phytoplankton biomass and its relationship with chlorophyll a and particulate organic carbon. *Marine Biology*, *107*(3), pp.529-539.

Gedan, K.B., Altieri, A.H., Feller, I., Burrell, R. and Breitburg, D., 2017. Community composition in mangrove ponds with pulsed hypoxic and acidified conditions. *Ecosphere*, *8*(12), p.e02053.

Gilly, W.F., Beman, J.M., Litvin, S.Y. and Robison, B.H., 2013. Oceanographic and biological effects of shoaling of the oxygen minimum zone. *Annual review of marine science*, *5*, pp.393-420.

Gleick, P.H., 2003. Global freshwater resources: soft-path solutions for the 21st century. *Science*, *302*(5650), pp.1524-1528.

Glen Tarran, Standard operating method, analysis and quantification of nano- and picoplankton from station L4 by flow cytometry (bd accuri c6 flow cytometer)

https://www.westernchannelobservatory.org.uk/documents/soml4afc.pdf

Glibert, P.M. and Burkholder, J.M., 2018. Causes of harmful algal blooms. *Harmful Algal Blooms: A Compendium Desk Reference*, pp.1-21.

Glud, M., Klausen, M., Gniadecki, R., Rossing, M., Hastrup, N., Nielsen, F.C. and Drzewiecki, K.T., 2009. MicroRNA expression in melanocytic nevi: the usefulness of formalin-fixed, paraffin-embedded material for miRNA microarray profiling. *Journal of Investigative Dermatology*, *129*(5), pp.1219-1224.

Glud, R.N., 2008. Oxygen dynamics of marine sediments. *Marine Biology Research*, *4*(4), pp.243-289.

Glud, R.N., 2015. Benthic O2 uptake of two cold-water coral communities estimated with the non-invasive eddy correlation technique. *Marine Ecology Progress Series*, *525*, pp.97-104.

Glud, R.N., Berg, P., Hume, A., Batty, P., Blicher, M.E., Lennert, K. and Rysgaard, S., 2010. Benthic O2 exchange across hard-bottom substrates quantified by eddy correlation in a sub-Arctic fjord. *Marine Ecology Progress Series*, *417*, pp.1-12.

Glud, R.N., Gundersen, J.K., Roy, H. and Jorgensen, B.B., 2003. Seasonal dynamics of benthic O~ 2uptake in a semienclosed bay: Importance of diffusion and faunal activity. *Limnology and Oceanography*, *48*(3), pp.1265-1276.

Glud, R.N., Holby, O., Hoffmann, F. and Canfield, D.E., 1998. Benthic mineralization and exchange in Arctic sediments (Svalbard, Norway). *Marine Ecology Progress Series*, *173*, pp.237-251.

Glud, R.N., Kühl, M., Kohls, O. and Ramsing, N.B., 1999. Heterogeneity of oxygen production and consumption in a photosynthetic microbial mat as studied by planar optodes. *Journal of Phycology*, *35*(2), pp.270-279.

Gohin, F., Van der Zande, D., Tilstone, G., Eleveld, M.A., Lefebvre, A., Andrieux-Loyer, F., Blauw, A.N., Bryère, P., Devreker, D., Garnesson, P. and Fariñas, T.H., 2019. Twenty years of satellite and in situ observations of surface chlorophyll-a from the northern Bay of Biscay to the eastern English Channel. Is the water quality improving?. *Remote Sensing of Environment*, *233*, p.111343.

Gonzalez-Rothi, E.J., Lee, K.Z., Dale, E.A., Reier, P.J., Mitchell, G.S. and Fuller, D.D., 2015. Intermittent hypoxia and neurorehabilitation. *Journal of Applied Physiology*, *119*(12), pp.1455-1465.

Govindan, N., Maniam, G.P., Sulaiman, A.Z., Ajit, A., Chatsungnoen, T. and Chisti, Y., 2021. Production of Renewable Lipids by the Diatom Amphora copulata. *Fermentation*, *7*(1), p.37.

Goyet, C., Ito Gonçalves, R. and Touratier, F., 2009. Anthropogenic carbon distribution in the eastern South Pacific Ocean. *Biogeosciences*, *6*(2), pp.149-156.

Green, J.M., Simpson, J.H., Legg, S. and Palmer, M.R., 2008. Internal waves, baroclinic energy fluxes and mixing at the European shelf edge. *Continental Shelf Research*, *28*(7), pp.937-950.

Greenwood, N., Parker, E.R., Fernand, L., Sivyer, D.B., Weston, K., Painting, S.J., Kröger, S., Forster, R.M., Lees, H.E., Mills, D.K. and Laane, R.W.P.M., 2010. Detection of low bottom water oxygen concentrations in the North Sea; implications for monitoring and assessment of ecosystem health. *Biogeosciences*, *7*(4), pp.1357-1373.

Groom, S., Martinez-Vicente, V., Fishwick, J., Tilstone, G., Moore, G., Smyth, T. and Harbour, D., 2009. The western English Channel observatory: Optical characteristics of station L4. *Journal of Marine Systems*, *77*(3), pp.278-295.

Hall, E.K., Neuhauser, C. and Cotner, J.B., 2008. Toward a mechanistic understanding of how natural bacterial communities respond to changes in temperature in aquatic ecosystems. *The ISME journal*, *2*(5), p.471.

Hammer, O., Harper, D.A.T., Ryan, P.D. 2001. PAST: Paleontological statistics software package for education and data analysis. https://palaeo-electronica.org/2001_1/past/past.pdf (Accessed 27 March 2019).

Hansel, C.M., 2017. Manganese in marine microbiology. In *Advances in microbial physiology* (Vol. 70, pp. 37-83). Academic Press.

Hansen, L.S. and Blackburn, T.H., 1992. Effect of algal bloom deposition on sediment respiration and fluxes. Marine Biology, 112(1), pp.147-152.

Harrison, P.L. and Booth, D.J., 2007. Coral reefs: naturally dynamic and increasingly disturbed ecosystems. *Marine ecology*, pp.316-377.

Hartnett, H.E., Keil, R.G., Hedges, J.I. and Devol, A.H., 1998. Influence of oxygen exposure time on organic carbon preservation in continental margin sediments. *Nature*, *391*(6667), p.572.

Hicks, N., Ubbara, G.R., Silburn, B., Smith, H.E., Kröger, S., Parker, E.R., Sivyer, D., Kitidis, V., Hatton, A., Mayor, D.J. and Stahl, H., 2017. Oxygen dynamics in shelf seas sediments incorporating seasonal variability. *Biogeochemistry*, *135*(1-2), pp.35-47.

Hoegh-Guldberg, O. and Bruno, J.F., 2010. The impact of climate change on the world's marine ecosystems. *Science*, *328*(5985), pp.1523-1528.

Holtappels, M., Noss, C., Hancke, K., Cathalot, C., McGinnis, D.F., Lorke, A. and Glud, R.N., 2015. Aquatic eddy correlation: quantifying the artificial flux caused by stirring-sensitive O2 sensors. *PLoS One*, *10*(1), p.e0116564.

Holtappels, M., Noss, C., Hancke, K., Cathalot, C., McGinnis, D.F., Lorke, A. and Glud, R.N., 2015. Aquatic eddy correlation: quantifying the artificial flux caused by stirring-sensitive O2 sensors. *PLoS One*, *10*(1), p.e0116564.

Hondzo, M., Feyaerts, T., Donovan, R. and O'Connor, B.L., 2005. Universal scaling of dissolved oxygen distribution at the sediment-water interface: A power law. *Limnology and Oceanography*, *50*(5), pp.1667-1676.

Huang, C.J., Ma, H., Guo, J., Dai, D. and Qiao, F., 2018. Calculation of turbulent dissipation rate with acoustic Doppler velocimeter. *Limnology and Oceanography: Methods*, *16*(5), pp.265-272.

Huettel, M. and Gust, G., 1992. Solute release mechanisms from confined sediment cores in stirred benthic chambers and flume flows. *Marine ecology progress series. Oldendorf*, *82*(2), pp.187-197.

Huettel, M. and Webster, I.T., 2001. Porewater flow in permeable sediments. *The benthic boundary layer: Transport processes and biogeochemistry*, pp.144-179.

Huettel, M., Berg, P. and Kostka, J.E., 2014. Benthic exchange and biogeochemical cycling in permeable sediments. *Annual Review of Marine Science*, *6*, pp.23-51.

Huettel, M., Cook, P., Janssen, F., Lavik, G., Middelburg, J. and Gust, G., IT Webster. 2000. Porewater flow in permeable sediment.

Hughes, L., McIntyre, S., Lindenmayer, D.B., Parmesan, C., Possingham, H.P. and Thomas, C.D., 2008. Assisted colonization and rapid climate change. *Science (Washington)*, *321*(5887), pp.345-346.

Hume, A.C., Berg, P. and McGlathery, K.J., 2011. Dissolved oxygen fluxes and ecosystem metabolism in an eelgrass (Zostera marina) meadow measured with the eddy correlation technique. *Limnology and Oceanography*, *56*(1), pp.86-96.

Huotari, J., Ojala, A., Peltomaa, E., Nordbo, A., Launiainen, S., Pumpanen, J., Rasilo, T., Hari, P. and Vesala, T., 2011. Long-term direct CO2 flux measurements over a boreal lake: Five years of eddy covariance data. *Geophysical Research Letters*, *38*(18).

Ito, T., Nenes, A., Johnson, M.S., Meskhidze, N. and Deutsch, C., 2016. Acceleration of oxygen decline in the tropical Pacific over the past decades by aerosol pollutants. *Nature Geoscience*, *9*(6), p.443.

Johnston, S.A., 1981. Estuarine dredge and fill activities: a review of impacts. Environmental management, 5(5), pp.427-440.

Jönsson, B., 1991. A 14C-incubation technique for measuring microphytobenthic primary productivity in intact sediment cores. *Limnology and Oceanography*, *36*(7), pp.1485-1492.

Jordan, M.B. and Joint, I., 1998. Seasonal variation in nitrate: phosphate ratios in the English Channel 1923–1987. Estuarine, Coastal and Shelf Science, 46(1), pp.157-164.

Jørgensen, B.B. and Revsbech, N.P., 1985. Diffusive boundary layers and the oxygen uptake of sediments and detritus 1. *Limnology and oceanography*, *30*(1), pp.111-122.

Kamaruddin, H.D. and Koros, W.J., 1997. Some observations about the application of Fick's first law for membrane separation of multicomponent mixtures. *Journal of membrane science*, *135*(2), pp.147-159.

Kanwisher, J., 1963, July. On the exchange of gases between the atmosphere and the sea. In *Deep Sea Research and Oceanographic Abstracts* (Vol. 10, No. 3, pp. 195-207). Elsevier.

Kemp, W.M. and Boynton, W.R., 1980. Influence of biological and physical processes on dissolved oxygen dynamics in an estuarine system: implications for measurement of community metabolism. *Estuarine and Coastal Marine Science*, *11*(4), pp.407-431.

Kennedy, H. and Björk, M., 2009. Seagrass meadows. *The management of natural coastal carbon sinks*, *23*.

Kirchman, D.L., 2018. *Processes in microbial ecology*. Oxford University Press.

Klimant, I., Meyer, V. and Kühl, M., 1995. Fiber-optic oxygen microsensors, a new tool in aquatic biology. *Limnology and Oceanography*, *40*(6), pp.1159-1165.

Knights, A.M., Firth, L.B., Thompson, R.C., Yunnie, A.L., Hiscock, K. and Hawkins, S.J., 2016. Plymouth—a world harbour through the ages. Regional studies in marine science, 8, pp.297-307.

Kondoy, K.I., 2017. Seagrass as carbon holder in Waleo coastal waters, North Sulawesi, Indonesia. *AACL Bioflux*, *10*(5), pp.1342-1350.

Koopmans, D., Holtappels, M., Chennu, A., Weber, M. and de Beer, D., 2018. The response of seagrass (Posidonia oceanica) meadow metabolism to CO2 levels and hydrodynamic exchange determined with aquatic eddy covariance.

Koopmans, D., Holtappels, M., Chennu, A., Weber, M. and de Beer, D., 2018. The response of seagrass (Posidonia oceanica) meadow metabolism to CO2 levels and hydrodynamic exchange determined with aquatic eddy covariance.

Koopmans, D.J. and Berg, P., 2015. Stream oxygen flux and metabolism determined with the open water and aquatic eddy covariance techniques. *Limnology and Oceanography*, *60*(4), pp.1344-1355.

Köstner, N., Scharnreitner, L., Jürgens, K., Labrenz, M., Herndl, G.J. and Winter, C., 2017. High viral abundance as a consequence of low viral decay in the Baltic Sea redoxcline. *PloS one*, *12*(6), p.e0178467.

Koziorowska, K., Kuliński, K. and Pempkowiak, J., 2018. Comparison of the burial rate estimation methods of organic and inorganic carbon and quantification of carbon burial in two high Arctic fjords. *Oceanologia*, *60*(3), pp.405-418.

Kristensen, E., 1988. Factors influencing the distribution of nereid polychaetes in Danish coastal waters. *Ophelia*, *29*(2), pp.127-140.

Kristensen, E., Andersen, F.Ø. and Blackburn, T.H., 1992. Effects of benthic macrofauna and temperature on degradation of macroalgal detritus: the fate of organic carbon. *Limnology and Oceanography*, *37*(7), pp.1404-1419.

Kristensen, E., Delefosse, M., Quintana, C.O., Flindt, M.R. and Valdemarsen, T., 2014. Influence of benthic macrofauna community shifts on ecosystem functioning in shallow estuaries. *Frontiers in Marine Science*, *1*, p.41.

Kristensen, E., Penha-Lopes, G., Delefosse, M., Valdemarsen, T., Quintana, C.O. and Banta, G.T., 2012. What is bioturbation? The need for a precise definition for fauna in aquatic sciences. *Marine Ecology Progress Series*, *446*, pp.285-302.

Kuwae, T., Kamio, K., Inoue, T., Miyoshi, E. and Uchiyama, Y., 2006. Oxygen exchange flux between sediment and water in an intertidal sandflat, measured in situ by the eddy-correlation method. *Marine Ecology Progress Series*, *307*, pp.59-68.

Lam, P. and Kuypers, M.M., 2011. Microbial nitrogen cycling processes in oxygen minimum zones. *Annual review of marine science*, *3*, pp.317-345.

Larsen, S.J., Kilminster, K.L., Mantovanelli, A., Goss, Z.J., Evans, G.C., Bryant, L.D. and McGinnis, D.F., 2019. Artificially oxygenating the Swan River estuary increases dissolved

oxygen concentrations in the water and at the sediment interface. *Ecological engineering*, *128*, pp.112-121.

Lee, M.H., Jung, H.J., Kim, S.H., An, S.U., Choi, J.H., Lee, H.J., Huh, I.A. and Hur, J., 2018. Potential linkage between sediment oxygen demand and pore water chemistry in weir-impounded rivers. Science of The Total Environment, 619, pp.1608-1617.

Lee, X., Massman, W. and Law, B. eds., 2004. *Handbook of micrometeorology: a guide for surface flux measurement and analysis* (Vol. 29). Springer Science & Business Media.

Levin, L.A., Whitcraft, C.R., Mendoza, G.F., Gonzalez, J.P. and Cowie, G., 2009. Oxygen and organic matter thresholds for benthic faunal activity on the Pakistan margin oxygen minimum zone (700–1100 m). *Deep Sea Research Part II: Topical Studies in Oceanography*, *56*(6-7), pp.449-471.

Lindeboom, H., 2002. The coastal zone: an ecosystem under pressure. In *Oceans* (Vol. 2020, pp. 49-84).

Liu, C., Chen, K., Wang, Z., Fan, C., Gu, X. and Huang, W., 2017. Nitrogen exchange across the sediment-water interface after dredging: The influence of contaminated riverine suspended particulate matter. *Environmental Pollution*, *229*, pp.879-886.

Lohrer, A.M., Thrush, S.F. and Gibbs, M.M., 2004. Bioturbators enhance ecosystem function through complex biogeochemical interactions. *Nature*, *431*(7012), p.1092.

Long, M.H., Berg, P. and Falter, J.L., 2015a. Seagrass metabolism across a productivity gradient using the eddy covariance, E ulerian control volume, and biomass addition techniques. *Journal of Geophysical Research: Oceans*, *120*(5), pp.3624-3639.

Long, M.H., Berg, P., de Beer, D. and Zieman, J.C., 2013. In situ coral reef oxygen metabolism: An eddy correlation study. *PLoS One*, *8*(3), p.e58581.

Long, M.H., Berg, P., McGlathery, K.J. and Zieman, J.C., 2015. Sub-tropical seagrass ecosystem metabolism measured by eddy covariance. *Marine Ecology Progress Series*, *529*, pp.75-90.

Long, M.H., Koopmans, D., Berg, P., Rysgaard, S., Glud, R.N. and Søgaard, D.H., 2012. Oxygen exchange and ice melt measured at the ice-water interface by eddy correlation. *Biogeosciences*, *9*(6), pp.1957-1967.

Lorke, A., McGinnis, D.F. and Maeck, A., 2013. Eddy-correlation measurements of benthic fluxes under complex flow conditions: Effects of coordinate transformations and averaging time scales. *Limnology and Oceanography: Methods*, *11*(8), pp.425-437.

Lorke, A., Muller, B., Maerki, M. and Wuest, A., 2003. Breathing sediments: The control of diffusive transport across the sediment-water interface by periodic boundary-layer turbulence. *Limnology and Oceanography*, *48*(6), pp.2077-2085.

Lorrai, C., McGinnis, D.F., Berg, P., Brand, A. and Wüest, A., 2010. Application of oxygen eddy correlation in aquatic systems. *Journal of Atmospheric and Oceanic Technology*, *27*(9), pp.1533-1546.

Lu, Y., Song, S., Wang, R., Liu, Z., Meng, J., Sweetman, A.J., Jenkins, A., Ferrier, R.C., Li, H., Luo, W. and Wang, T., 2015. Impacts of soil and water pollution on food safety and health risks in China. *Environment international*, *77*, pp.5-15.

Macko, S.A., 2018. A Perspective on Marine Pollution. In *The Marine Environment and United Nations Sustainable Development Goal 14* (pp. 291-308). Brill Nijhoff.

Macreadie, P.I., Ross, D.J., Longmore, A.R. and Keough, M.J., 2006. Denitrification measurements of sediments using cores and chambers. *Marine Ecology Progress Series*, *326*, pp.49-59.

Maguire, M.S., 2018. *An Evaluation of Unmanned Aerial System Multispectral and Thermal Infrared Data as Information for Agricultural Crop and Irrigation Management* (Doctoral dissertation, University of Nebraska-Lincoln).

Mann, K.H. and Lazier, J.R., 2013. *Dynamics of marine ecosystems: biological-physical interactions in the oceans*. John Wiley & Sons.

Marañón, E., Van Wambeke, F., Uitz, J., Boss, E.S., Dimier, C., Dinasquet, J., Engel, A., Haëntjens, N., Pérez-Lorenzo, M., Taillandier, V. and Zäncker, B., 2021. Deep maxima of phytoplankton biomass, primary production and bacterial production in the Mediterranean Sea. *Biogeosciences*, *18*(5), pp.1749-1767.

Marchand, A.M., Apps, G., Li, W. and Rotzien, J.R., 2015. Depositional processes and impact on reservoir quality in deepwater Paleogene reservoirs, US Gulf of Mexico. *AAPG Bulletin*, *99*(9), pp.1635-1648.

Mass, T., Genin, A., Shavit, U., Grinstein, M. and Tchernov, D., 2010. Flow enhances photosynthesis in marine benthic autotrophs by increasing the efflux of oxygen from the organism to the water. *Proceedings of the National Academy of Sciences*, *107*(6), pp.2527-2531.

Mateo, M., Cebrián, J., Dunton, K. and Mutchler, T., 2006. Carbon flux in seagrass ecosystems. *Seagrasses: biology, ecology and conservation*, pp.159-192.

Matson, P.A., Parton, W.J., Power, A.G. and Swift, M.J., 1997. Agricultural intensification and ecosystem properties. *Science*, *277*(5325), pp.504-509.

McCann-Grosvenor, K., Reimers, C.E. and Sanders, R.D., 2014. Dynamics of the benthic boundary layer and seafloor contributions to oxygen depletion on the Oregon inner shelf. *Continental Shelf Research*, *84*, pp.93-106.

McGinnis, D.F., Berg, P., Brand, A., Lorrai, C., Edmonds, T.J. and Wüest, A., 2008. Measurements of eddy correlation oxygen fluxes in shallow freshwaters: Towards routine applications and analysis. *Geophysical Research Letters*, *35*(4).

McGinnis, D.F., Cherednichenko, S., Sommer, S., Berg, P., Rovelli, L., Schwarz, R., Glud, R.N. and Linke, P., 2011. Simple, robust eddy correlation amplifier for aquatic dissolved oxygen and hydrogen sulfide flux measurements. *Limnology and Oceanography: Methods*, *9*(8), pp.340-347.

McGinnis, D.F., Sommer, S., Lorke, A., Glud, R.N. and Linke, P., 2014. Quantifying tidally driven benthic oxygen exchange across permeable sediments: An aquatic eddy correlation study. *Journal of Geophysical Research: Oceans*, *119*(10), pp.6918-6932.

McGlathery, K.J., Sundbäck, K. and Anderson, I.C., 2007. Eutrophication in shallow coastal bays and lagoons: the role of plants in the coastal filter. *Marine Ecology Progress Series*, *348*, pp.1-18.

McMahon, R., Taveras, Z., Neubert, P. and Harvey, H.R., 2021. Organic biomarkers and Meiofauna diversity reflect distinct carbon sources to sediments transecting the Mackenzie continental shelf. *Continental Shelf Research*, *220*, p.104406.

Meysman, F.J., Galaktionov, O.S., Gribsholt, B. and Middelburg, J.J., 2006. Bioirrigation in permeable sediments: Advective pore-water transport induced by burrow ventilation. *Limnology and Oceanography*, *51*(1), pp.142-156.

Middelburg, J.J. and Levin, L.A., 2009. Coastal hypoxia and sediment biogeochemistry. *Biogeosciences*, *6*(7), pp.1273-1293.

Middelburg, J.J., 2019. *Marine Carbon Biogeochemistry: A Primer for Earth System Scientists*. Springer.

Murray, L. and Wetzel, R.L., 1987. Oxygen production and consumption associated with the major autotrophic components in two temperate seagrass communities. *Mar Ecol Prog Ser*, *38*, pp.231-239.

Muyzer, G., 2016. Marine microbial systems ecology: microbial networks in the sea. In *The Marine Microbiome* (pp. 335-344). Springer, Cham.

Naik, S.S., Godad, S.P., Naidu, P.D., Tiwari, M. and Paropkari, A.L., 2014. Early-to late-Holocene contrast in productivity, OMZ intensity and calcite dissolution in the eastern Arabian Sea. *The Holocene*, *24*(6), pp.749-755.

Naqvi, S.W.A., Jayakumar, D.A., Narvekar, P.V., Naik, H., Sarma, V.V.S.S., D'souza, W., Joseph, S. and George, M.D., 2000. Increased marine production of N 2 O due to intensifying anoxia on the Indian continental shelf. *Nature*, *408*(6810), p.346.

National Oceanography Centre. 2016. *Shelf seas and coastal processes*. [ONLINE] Available at:http://noc.ac.uk/science-technology/earth-ocean-system/ocean-processes/shelf-seas-coastal-processes. [Accessed 22 September 2016].

Neves, J.A.C., Fernandes, J.A. and Restivo, F., 2006, December. Phase space signal filtering. In *2006 IEEE International Conference on Industrial Technology* (pp. 1805-1809). IEEE.

Nickell, L.A., Black, K.D., Hughes, D.J., Overnell, J., Brand, T., Nickell, T.D., Breuer, E. and Harvey, S.M., 2003. Bioturbation, sediment fluxes and benthic community structure around a salmon cage farm in Loch Creran, Scotland. *Journal of Experimental Marine Biology and Ecology*, *285*, pp.221-233.

Nikora, V.I. and Goring, D.G., 2002. Fluctuations of suspended sediment concentration and turbulent sediment fluxes in an open-channel flow. *Journal of Hydraulic Engineering*, *128*(2), pp.214-224.

Nurse, L.A., Sem, G., Hay, J.E., Suarez, A.G., Wong, P.P., Briguglio, L. and Ragoonaden, S., 2001. Small island states. *Climate change*, pp.843-875.

O'Boyle, S., McDermott, G., Silke, J. and Cusack, C., 2016. Potential impact of an exceptional bloom of Karenia mikimotoi on dissolved oxygen levels in waters off western Ireland. *Harmful Algae*, *53*, pp.77-85.

O'Brien, K.R., Waycott, M., Maxwell, P., Kendrick, G.A., Udy, J.W., Ferguson, A.J., Kilminster, K., Scanes, P., McKenzie, L.J., McMahon, K. and Adams, M.P., 2018. Seagrass ecosystem trajectory depends on the relative timescales of resistance, recovery and disturbance. *Marine pollution bulletin*, *134*, pp.166-176.

Olesen, M. and Lundsgaard, C., 1995. Seasonal sedimentation of autochthonous material from the euphotic zone of a coastal system. *Estuarine, Coastal and Shelf Science*, *41*(4), pp.475-490.

Orth, R.J., Carruthers, T.J., Dennison, W.C., Duarte, C.M., Fourqurean, J.W., Heck, K.L., Hughes, A.R., Kendrick, G.A., Kenworthy, W.J., Olyarnik, S. and Short, F.T., 2006. A global crisis for seagrass ecosystems. *Bioscience*, *56*(12), pp.987-996.

Orth, R.J., Heck, K.L. and van Montfrans, J., 1984. Faunal communities in seagrass beds: a review of the influence of plant structure and prey characteristics on predator-prey relationships. *Estuaries*, *7*(4), pp.339-350.

Paerl, H.W., Gardner, W.S., Havens, K.E., Joyner, A.R., McCarthy, M.J., Newell, S.E., Qin, B. and Scott, J.T., 2016. Mitigating cyanobacterial harmful algal blooms in aquatic ecosystems impacted by climate change and anthropogenic nutrients. *Harmful Algae*, *54*, pp.213-222.

Park, S.S. and Jaffe, P.R., 1999. A numerical model to estimate sediment oxygen levels and demand. *Journal of Environmental Quality*, *28*(4), pp.1219-1226.

Parsons, T.R. and Takahashi, M., 1973. Environmental control of phytoplankton cell size. *Limnology and Oceanography*, *18*(4), pp.511-515.

Pilegaard, K., Hummelshøj, P., Jensen, N.O. and Chen, Z., 2001. Two years of continuous CO 2 eddy-flux measurements over a Danish beech forest. *Agricultural and Forest Meteorology*, *107*(1), pp.29-41.

Pörtner, H.O., Karl, D.M., Boyd, P.W., Cheung, W., Lluch-Cota, S.E., Nojiri, Y., Schmidt, D.N., Zavialov, P.O., Alheit, J., Aristegui, J. and Armstrong, C., 2014. Ocean systems. In *Climate change 2014: impacts, adaptation, and vulnerability. Part A: global and sectoral aspects. contribution of working group II to the fifth assessment report of the intergovernmental panel on climate change*(pp. 411-484). Cambridge University Press.

Prajapati, P. and Santos, E.A., 2018. Estimating methane emissions from beef cattle in a feedlot using the eddy covariance technique and footprint analysis. *Agricultural and Forest Meteorology*, *258*, pp.18-28.

Precht, E., Franke, U., Polerecky, L. and Huettel, M., 2004. Oxygen dynamics in permeable sediments with wave-driven pore water exchange. *Limnology and Oceanography*, *49*(3), pp.693-705.

Puppe, D., 2020. Review on protozoic silica and its role in silicon cycling. *Geoderma*, *365*, p.114224.

Queirós, A.M., Stephens, N., Cook, R., Ravaglioli, C., Nunes, J., Dashfield, S., Harris, C., Tilstone, G.H., Fishwick, J., Braeckman, U. and Somerfield, P.J., 2015. Can benthic community structure be used to predict the process of bioturbation in real ecosystems?. *Progress in Oceanography*, *137*, pp.559-569.

Queirós, A.M., Stephens, N., Widdicombe, S., Tait, K., McCoy, S.J., Ingels, J., Rühl, S., Airs, R., Beesley, A., Carnovale, G. and Cazenave, P., 2019. Connected macroalgal-sediment systems: blue carbon and food webs in the deep coastal ocean. *Ecological Monographs*, p.e01366.

Queirós, Ana M., Nicholas Stephens, Richard Cook, Chiara Ravaglioli, Joana Nunes, Sarah Dashfield, Carolyn Harris et al. "Can benthic community structure be used to predict the process of bioturbation in real ecosystems?." *Progress in Oceanography* 137 (2015): 559-569.

Queste, B.Y., Fernand, L., Jickells, T.D., Heywood, K.J. and Hind, A.J., 2016. Drivers of summer oxygen depletion in the central North Sea. *Biogeosciences*, *13*(4), pp.1209-1222.

Rabalais, N.N., Diaz, R.J., Levin, L.A., Turner, R.E., Gilbert, D. and Zhang, J., 2010. Dynamics and distribution of natural and human-caused hypoxia. *Biogeosciences*, *7*(2), p.585.

Rabouille, C., Caprais, J.C., Lansard, B., Crassous, P., Dedieu, K., Reyss, J.L. and Khripounoff, A., 2009. Organic matter budget in the Southeast Atlantic continental margin close to the Congo Canyon: In situ measurements of sediment oxygen consumption. *Deep Sea Research Part II: Topical Studies in Oceanography*, *56*(23), pp.2223-2238.

Rasmussen, H. and Jørgensen, B.B., 1992. Microelectrode studies of seasonal oxygen uptake in a coastal sediment: role of molecular diffusion. *Marine ecology progress series. Oldendorf*, *81*(3), pp.289-303.

Rehmann, C.R., Wain, D.J. and Soga, C.L., 2004. Estimates of the dissipation of turbulent kinetic energy from temperature microstructure. Proc. ASCE World Water Environ. Resour. Cong.

Reidenbach, M.A., Berg, P., Hume, A., Hansen, J.C. and Whitman, E.R., 2013. Hydrodynamics of intertidal oyster reefs: The influence of boundary layer flow processes on sediment and oxygen exchange. *Limnology and Oceanography: Fluids and Environments*, *3*(1), pp.225-239.

Reimers, C.E., 1987. An in situ microprofiling instrument for measuring interfacial pore water gradients: methods and oxygen profiles from the North Pacific Ocean. *Deep Sea Research Part A. Oceanographic Research Papers*, *34*(12), pp.2019-2035.

Reimers, C.E., Fischer, K.M., Merewether, R., Smith, K.L. and Jahnke, R.A., 1986. Oxygen microprofiles measured in situ in deep ocean sediments. *Nature*, *320*(6064), p.741.

Reimers, C.E., Özkan-Haller, H., Berg, P., Devol, A., McCann-Grosvenor, K. and Sanders, R.D., 2012. Benthic oxygen consumption rates during hypoxic conditions on the Oregon continental shelf: Evaluation of the eddy correlation method. Journal of Geophysical Research: Oceans, 117(C2).

Reimers, C.E., Özkan-Haller, H.T., Albright, A.T. and Berg, P., 2016. Microelectrode velocity effects and aquatic eddy covariance measurements under waves. *Journal of Atmospheric and Oceanic Technology*, *33*(2), pp.263-282.

Reimers, C.E., Özkan-Haller, H.T., Berg, P., Devol, A., McCann-Grosvenor, K. and Sanders, R.D., 2012. Benthic oxygen consumption rates during hypoxic conditions on the Oregon continental shelf: Evaluation of the eddy correlation method. *Journal of Geophysical Research: Oceans*, *117*(C2).

Reimers, C.E., Tender, L.M., Fertig, S. and Wang, W., 2001. Harvesting energy from the marine sediment− water interface. *Environmental science & technology*, *35*(1), pp.192-195.

Resplandy, L., Keeling, R.F., Eddebbar, Y., Brooks, M.K., Wang, R., Bopp, L., Long, M.C., Dunne, J.P., Koeve, W. and Oschlies, A., 2018. Quantification of ocean heat uptake from changes in atmospheric O 2 and CO 2 composition. *Nature*, *563*(7729), p.105.

Revsbech, N.P. and Jørgensen, B.B., 1985. Microprofiles of oxygen in epiphyte communities on submerged macrophytes. *Marine Biology*, *89*(1), pp.55-62.

Revsbech, N.P., JØrgensen, B.B. and Brix, O., 1981. Primary production of microalgae in sediments measured by oxygen microprofile, H14CO3-fixation, and oxygen exchange methods 1. *Limnology and Oceanography*, *26*(4), pp.717-730.

Revsbech, N.P., Jorgensen, B.B., Blackburn, T.H. and Cohen, Y., 1983. Microelectrode studies of the photosynthesis and O2, H2S, and pH profiles of a microbial mat 1. *Limnology and Oceanography*, *28*(6), pp.1062-1074.

Reynolds, O., 1895. IV. On the dynamical theory of incompressible viscous fluids and the determination of the criterion. *Philosophical transactions of the royal society of london.(a.)*, (186), pp.123-164.

Reynolds, O., 1895. IV. On the dynamical theory of incompressible viscous fluids and the determination of the criterion. *Philosophical transactions of the royal society of london.(a.)*, (186), pp.123-164.

Rheuban, J.E., Berg, P. and McGlathery, K.J., 2014. Ecosystem metabolism along a colonization gradient of eelgrass (Zostera marina) measured by eddy correlation. *Limnology and Oceanography*, *59*(4), pp.1376-1387.

Ribaudo, C., Bertrin, V., Jan, G., Anschutz, P. and Abril, G., 2017. Benthic production, respiration and methane oxidation in Lobelia dortmanna lawns. *Hydrobiologia*, *784*(1), pp.21-34.

Riisgard, H.U., 1991. Suspension feeding in the polychaete Nereis diversicolor. *Mar. Ecol. Prog. Ser*, *70*(1), pp.19-37.

Riisgard, H.U., Banta, G.T. and et Milieu, V., 1998. Irrigation and deposit feeding by the lugworm Arenicola marina, characteristics and secondary effects on the environment. A review of current knowledge. *Vie et milieu*, *48*(4), pp.243-258.

Rodil, I.F., Attard, K.M., Norkko, J., Glud, R.N. and Norkko, A., 2019. Towards a sampling design for characterizing habitat-specific benthic biodiversity related to oxygen flux dynamics using Aquatic Eddy Covariance. *PloS one*, *14*(2), p.e0211673.

Rontani, J.F., Belt, S.T., Brown, T.A., Amiraux, R., Gosselin, M., Vaultier, F. and Mundy, C.J., 2016. Monitoring abiotic degradation in sinking versus suspended Arctic sea ice algae during a spring ice melt using specific lipid oxidation tracers. *Organic geochemistry*, *98*, pp.82-97.

Sampou, P. and Oviatt, C.A., 1991. Seasonal patterns of sedimentary carbon and anaerobic respiration along a simulated eutrophication gradient.

Sankey, T.T., McVay, J., Swetnam, T.L., McClaran, M.P., Heilman, P. and Nichols, M., 2018. UAV hyperspectral and lidar data and their fusion for arid and semi-arid land vegetation monitoring. *Remote Sensing in Ecology and Conservation*, *4*(1), pp.20-33.

Santos, I.R., Eyre, B.D. and Huettel, M., 2012. The driving forces of porewater and groundwater flow in permeable coastal sediments: A review. *Estuarine, Coastal and Shelf Science*, *98*, pp.1-15.

Santschi, P., Höhener, P., Benoit, G. and Buchholtz-ten Brink, M., 1990. Chemical processes at the sediment-water interface. *Marine chemistry*, *30*, pp.269-315.

Sarmiento, J.L. and Gruber, N., 2006. *Ocean biogeochemical dynamics*. Princeton university press.

Scalo, C., Piomelli, U. and Boegman, L., 2012. High-Schmidt-number mass transport mechanisms from a turbulent flow to absorbing sediments. *Physics of Fluids*, *24*(8), p.085103.

Schindler, D.W., 2006. Recent advances in the understanding and management of eutrophication. *Limnology and oceanography*, *51*(1part2), pp.356-363.

Schlesinger, W.H. and Bernhardt, E.S., 2013. *Biogeochemistry: an analysis of global change*. Academic press.

Schwefel, R., Hondzo, M., Wüest, A. and Bouffard, D., 2017. Scaling oxygen microprofiles at the sediment interface of deep stratified waters. *Geophysical Research Letters*, *44*(3), pp.1340-1349.

Schwefel, R., Steinsberger, T., Bouffard, D., Bryant, L.D., Müller, B. and Wüest, A., 2018. Using small-scale measurements to estimate hypolimnetic oxygen depletion in a deep lake. *Limnology and Oceanography*, *63*(S1), pp.S54-S67.

Seas, S.O., 2002. A strategy for the conservation and sustainable development of our marine environment.

Seibel BA. Critical oxygen levels and metabolic suppression in oceanic oxygen minimum zones. Journal of Experimental Biology. 2011 Jan 15;214(2):326-36.

Seitaj, D., Sulu-Gambari, F., Burdorf, L.D., Romero-Ramirez, A., Maire, O., Malkin, S.Y., Slomp, C.P. and Meysman, F.J., 2017. Sedimentary oxygen dynamics in a seasonally hypoxic basin. *Limnology and Oceanography*, *62*(2), pp.452-473.

Shmeis, R.M.A., 2018. Water Chemistry and Microbiology. In *Comprehensive Analytical Chemistry* (Vol. 81, pp. 1-56). Elsevier.

Silva, J., Sharon, Y., Santos, R. and Beer, S., 2009. Measuring seagrass photosynthesis: methods and applications. *Aquatic Biology*, *7*(1-2), pp.127-141.

Simmons, H.L., Hallberg, R.W. and Arbic, B.K., 2004. Internal wave generation in a global baroclinic tide model. *Deep Sea Research Part II: Topical Studies in Oceanography*, *51*(25-26), pp.3043-3068.

Smith, S.V. and Hollibaugh, J.T., 1993. Coastal metabolism and the oceanic organic carbon balance. *Reviews of Geophysics*, *31*(1), pp.75-89.

Smith, V.H. and Schindler, D.W., 2009. Eutrophication science: where do we go from here?. *Trends in ecology & evolution*, *24*(4), pp.201-207.

Smyth, T. (2019). *Western Channel Observatory*. [online] Westernchannelobservatory.org.uk. Available at: https://www.westernchannelobservatory.org.uk/l4_ctdf/index.php [Accessed 8 Jul. 2019].

Smyth, T., Atkinson, A., Widdicombe, S., Frost, M., Allen, I., Fishwick, J., Queiros, A., Sims, D. and Barange, M., 2015. The Western channel observatory. *Prog. Oceanogr*, *137*, pp.335-341.

Smyth, T.J., 2017. Plymouth Deep (PL035) Dredge Disposal Monitoring, CEFAS PMA

Smyth, T.J., Fishwick, J.R., Al-Moosawi, L., Cummings, D.G., Harris, C., Kitidis, V., Rees, A., Martinez-Vicente, V. and Woodward, E.M., 2009. A broad spatio-temporal view of the Western English Channel observatory. *Journal of Plankton Research*, *32*(5), pp.585-601.

Smyth, T.J., Fishwick, J.R., Gallienne, C.P., Stephens, J.A. and Bale, A.J., 2010. Technology, design, and operation of an autonomous buoy system in the western English Channel. *Journal of Atmospheric and Oceanic Technology*, *27*(12), pp.2056-2064.

Soeder, C.J., 1965. Some aspects of phytoplankton growth and activity. *Mem. Ist. Ital. Idrobiol*, *18*, pp.47-59.

Song, G., Liu, S., Zhu, Z., Zhai, W., Zhu, C. and Zhang, J., 2016. Sediment oxygen consumption and benthic organic carbon mineralization on the continental shelves of the East China Sea and the Yellow Sea. Deep Sea Research Part II: Topical Studies in Oceanography, 124, pp.53-63.

Stachowitsch, M., Riedel, B., Zuschin, M. and Machan, R., 2007. Oxygen depletion and benthic mortalities: the first in situ experimental approach to documenting an elusive phenomenon. *Limnology and Oceanography: Methods*, *5*(10), pp.344-352.

Stanley, D.W. and Nixon, S.W., 1992. Stratification and bottom-water hypoxia in the Pamlico River estuary. *Estuaries*, *15*(3), pp.270-281.

Stramma, L., Johnson, G.C., Sprintall, J. and Mohrholz, V., 2008. Expanding oxygen-minimum zones in the tropical oceans. *science*, *320*(5876), pp.655-658.

Sulu-Gambari, F., Seitaj, D., Meysman, F.J., Schauer, R., Polerecky, L. and Slomp, C.P., 2016. Cable bacteria control iron–phosphorus dynamics in sediments of a coastal hypoxic basin. *Environmental science & technology*, *50*(3), pp.1227-1233.

Suntharalingam, P., Zamora, L.M., Bange, H.W., Bikkina, S., Buitenhuis, E., Kanakidou, M., Lamarque, J.F., Landolfi, A., Resplandy, L., Sarin, M.M. and Seitzinger, S., 2019. Anthropogenic nitrogen inputs and impacts on oceanic N2O fluxes in the northern Indian Ocean: The need for an integrated observation and modelling approach. *Deep Sea Research Part II: Topical Studies in Oceanography*.

Tait, K., Airs, R.L., Widdicombe, C.E., Tarran, G.A., Jones, M.R. and Widdicombe, S., 2015. Dynamic responses of the benthic bacterial community at the Western English Channel observatory site L4 are driven by deposition of fresh phytodetritus. *Progress in oceanography*, *137*, pp.546-558.

Tappan, H., 1968. Primary production, isotopes, extinctions and the atmosphere. *Palaeogeography, Palaeoclimatology, Palaeoecology*, *4*(3), pp.187-210.

Tarran, G. (2019). Western Channel Observatory. [online] Westernchannelobservatory.org.uk. Available at: https://www.westernchannelobservatory.org.uk/l4_flow_cyto.php [Accessed 26 Apr. 2019].

Tasnim, B., Jamily, J.A., Fang, X., Zhou, Y. and Hayworth, J.S., 2021. Simulating Diurnal Variations of Water Temperature and Dissolved Oxygen in Shallow Minnesota Lakes. *Water*, *13*(14), p.1980.

Topping, B.R., Kuwabara, J.S., Carter, J.L., Garrett, K.K., Mruz, E., Piotter, S. and Takekawa, J.Y., 2016. Effects of salt pond restoration on benthic flux: sediment as a source of nutrients to the water column. *Journal of Environmental Protection*, *7*(07), p.1064.

Torres-Sospedra, J., Jiménez, A., Knauth, S., Moreira, A., Beer, Y., Fetzer, T., Ta, V.C., Montoliu, R., Seco, F., Mendoza-Silva, G. and Belmonte, O., 2017. The smartphone-based offline indoor location competition at IPIN 2016: Analysis and future work. *Sensors*, *17*(3), p.557.

Toussaint, E., De Borger, E., Braeckman, U., De Backer, A., Soetaert, K. and Vanaverbeke, J., 2021. Faunal and environmental drivers of carbon and nitrogen cycling along a permeability gradient in shallow North Sea sediments. *Science of the Total Environment*, *767*, p.144994.

Turner, C.B., 2010. Influence of zebra (Dreissena polymorpha) and quagga (Dreissena rostriformis) mussel invasions on benthic nutrient and oxygen dynamics. *Canadian Journal of Fisheries and Aquatic Sciences*, *67*(12), pp.1899-1908.

Turner, R.E. and Rabalais, N.N., 1994. Coastal eutrophication near the Mississippi river delta. *Nature*, *368*(6472), pp.619-621.

Tyrrell, H.J.V., 1964. The origin and present status of Fick's diffusion law. *Journal of chemical education*, *41*(7), p.397.

Unisense 2011. Unisense MP4 Lander manual. Denmark

Unisense., 2019. Eddy Correlation System2 manual, Unisense A/S.

Valdemarsen, T., Wendelboe, K., Egelund, J.T., Kristensen, E. and Flindt, M.R., 2011. Burial of seeds and seedlings by the lugworm Arenicola marina hampers eelgrass (Zostera marina) recovery. *Journal of Experimental Marine Biology and Ecology*, *410*, pp.45-52.

Van Colen, C., Rossi, F., Montserrat, F., Andersson, M.G., Gribsholt, B., Herman, P.M., Degraer, S., Vincx, M., Ysebaert, T. and Middelburg, J.J., 2012. Organism-sediment interactions govern post-hypoxia recovery of ecosystem functioning. *PLoS One*, *7*(11), p.e49795.

Van Soest, P.J., 2018. *Nutritional ecology of the ruminant*. Cornell university press.

Vilà-Guerau de Arellano, J., Ouwersloot, H.G., Baldocchi, D. and Jacobs, C.M., 2014. Shallow cumulus rooted in photosynthesis. *Geophysical Research Letters*, *41*(5), pp.1796-1802.

Vitousek, P.M., Mooney, H.A., Lubchenco, J. and Melillo, J.M., 1997. Human domination of Earth's ecosystems. *Science*, *277*(5325), pp.494-499.

Volaric, M.P., Berg, P. and Reidenbach, M.A., 2018. Oxygen metabolism of intertidal oyster reefs measured by aquatic eddy covariance. *Marine Ecology Progress Series*, *599*, pp.75-91.

Volkenborn, N., Hedtkamp, S.I.C., Van Beusekom, J.E.E. and Reise, K., 2007. Effects of bioturbation and bioirrigation by lugworms (Arenicola marina) on physical and chemical sediment properties and implications for intertidal habitat succession. Estuarine, Coastal and Shelf Science, 74(1), pp.331-343.

Volkmar, E.C. and Dahlgren, R.A., 2006. Biological oxygen demand dynamics in the lower San Joaquin River, California. *Environmental science & technology*, *40*(18), pp.5653-5660.

Voss, M., Dippner, J.W. and Montoya, J.P., 2001. Nitrogen isotope patterns in the oxygen-deficient waters of the Eastern Tropical North Pacific Ocean. *Deep Sea Research Part I: Oceanographic Research Papers*, *48*(8), pp.1905-1921.

Wakeman, T., Peddicord, R. and Sustar, J., 1975, September. Effects of suspended solids associated with dredging operations on estuarine organisms. In OCEAN 75 Conference(pp. 431-436). IEEE.

WCO paper/report of the Dumping. Dredging disposal monitoring document'PMA 202

Webb, J.E. and Theodor, J., 1968. Irrigation of submerged marine sands through wave action.

Wenzhöfer, F. and Glud, R.N., 2004. Small-scale spatial and temporal variability in coastal benthic O2 dynamics: Effects of fauna activity. *Limnology and Oceanography*, *49*(5), pp.1471-1481.

Western Channel Observatory. 2016. *What is the Western Channel Observatory*. [ONLINE] Available at: http://www.westernchannelobservatory.org.uk/. [Accessed 22 September 2017].

Wetzel, R.G., 2001. *Limnology: lake and river ecosystems*. gulf professional publishing.

White DA, Widdicombe CE, Somerfield PJ, Tarran GA, Maud JL, Atkinson A (2015) The combined effects of seasonal community succession and adaptive algal physiology on lipid profiles of coastal phytoplankton in the Western English Channel. Marine Chemistryi, 177. 638-652. 10.1016/j.marchem.2015.10.005

Whitehead, P.G., Wilby, R.L., Battarbee, R.W., Kernan, M. and Wade, A.J., 2009. A review of the potential impacts of climate change on surface water quality. *Hydrological Sciences Journal*, *54*(1), pp.101-123.

Whitney, F.A., Freeland, H.J. and Robert, M., 2007. Persistently declining oxygen levels in the interior waters of the eastern subarctic Pacific. *Progress in Oceanography*, *75*(2), pp.179-199.

Wiberg, P.L., Drake, D.E. and Cacchione, D.A., 1994. Sediment resuspension and bed armoring during high bottom stress events on the northern California inner continental shelf: measurements and predictions. *Continental Shelf Research*, *14*(10), pp.1191-1219.

Widdicombe, D. Eloire, D. Harbour, R. P. Harris, P. J. Somerfield., 2010. Long-term phytoplankton community dynamics in the Western English Channel, Journal of Plankton Research, Volume 32, Issue 5, 1 May 2010, Pages 643–655

Wilkinson, C. and Salvat, B., 2012. Coastal resource degradation in the tropics: Does the tragedy of the commons apply for coral reefs, mangrove forests and seagrass beds. *Marine Pollution Bulletin*, *64*(6), pp.1096-1105.

Woodall L, Stewart C, Rogers A. Function of the High Seas and Anthropogenic Impacts Science Update 2012–2017. University of Oxford: Oxford, UK. 2017.

Woodward, M. (2019). *Western Channel Observatory*. [online] Westernchannelobservatory.org.uk . Available at: https://www.westernchannelobservatory.org.uk/l4_nutrients.php [Accessed 8 Jul. 2019].

Xie, Y., Tilstone, G.H., Widdicombe, C., Woodward, E.M.S., Harris, C. and Barnes, M.K., 2015. Effect of increases in temperature and nutrients on phytoplankton community structure and photosynthesis in the western English Channel. *Marine Ecology Progress Series*, *519*, pp.61-73.

You, B.S., Zhong, J.C., Fan, C.X., b, T.C., Zhang, L. and Ding, S.M., 2007. Effects of hydrodynamics processes on phosphorus fluxes from sediment in large, shallow Taihu Lake. *Journal of Environmental Sciences*, *19*(9), pp.1055-1060.

Young, M.J., Feyrer, F., Stumpner, P.R., Larwood, V., Patton, O. and Brown, L.R., 2021. Hydrodynamics drive pelagic communities and food web structure in a tidal environment. *International Review of Hydrobiology*, *106*(2), pp.69-85.

Yu, K. and Jones, M.C., 1998. Local linear quantile regression. Journal of the American statistical Association, 93(441), pp.228-237.

Zhang, F., Zhou, G., Wang, Y., Yang, F. and Nilsson, C., 2012. Evapotranspiration and crop coefficient for a temperate desert steppe ecosystem using eddy covariance in Inner Mongolia, China. *Hydrological Processes*, *26*(3), pp.379-386.

Ziebis, W., Huettel, M. and Forster, S., 1996. Impact of biogenic sediment topography on oxygen fluxes in permeable seabeds. *Marine Ecology Progress Series*, *140*, pp.227-237.